A STUDY OF ZONATION AT THE NANISIVIK ZN-PB-AG MINE,

BAFFIN ISLAND, CANADA

By

Dennis C. Arne Ⓒ

Submitted in Partial Fulfillment of the

Requirements for the Degree of

Master of Science

Faculty of Science

LAKEHEAD UNIVERSITY

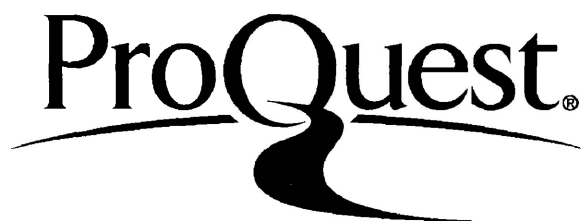Thunder Bay, Ontario, Canada

December, 1985

ProQuest Number: 10611728

![ProQuest logo]

ProQuest 10611728

Permission has been granted to the National Library of Canada to microfilm this thesis and to lend or sell copies of the film.

The author (copyright owner) has reserved other publication rights, and neither the thesis nor extensive extracts from it may be printed or otherwise reproduced without his/her written permission.

L'autorisation a été accordée à la Bibliothèque nationale du Canada de microfilmer cette thèse et de prêter ou de vendre des exemplaires du film.

L'auteur (titulaire du droit d'auteur) se réserve les autres droits de publication; ni la thèse ni de longs extraits de celle-ci ne doivent être imprimés ou autrement reproduits sans son autorisation écrite.

FRONTISPIECE

NANISIVIK MINE SITE. FROM FRONT TO BACK;
TOWN SITE, WEST OPEN PIT WITH ADIT (RIGHT)
AND MILL (LEFT), DOCK FACILITY (FAR LEFT),
AND STRATHCONA SOUND

Lakehead University

THUNDER BAY, ONTARIO, CANADA, POSTAL CODE P7B 5E1

DEPARTMENT OF GEOLOGY

Title of Thesis: A Study Of Zonation At The Nanisivik Zn-Pb-Ag
Mine, Baffin Island, Canada

Name of Candidate: Dennis C. Arne

Degree: Master of Science (Geology) Thesis with Commendation.

Date: May 1986

This thesis has been prepared under my supervision and the candidate has

complied with the regulations for the degree.

Thesis Supervisor.......................

Date....February 24, 1986......

Chairman Geology Department................

TABLE OF CONTENTS

LIST OF FIGURES

LIST OF TABLES

ABSTRACT

Zn-Pb-Ag mineralization at Nanisivik, northwest Baffin Island, is hosted by Proterozoic, laminated dolostone of the Society Cliffs Formation. Mineralization of the Main Orebody is highly variable in terms of texture and mineralogy exhibiting both replacement and open space filling textures. Sulfides are generally coarsely crystalline and banding, consisting of interlayered pyrite, sphalerite, galena and sparry dolomite, is common along the margins of the Upper Lens of the Main Orebody. The eastern and central portions of the Upper Lens are characterized by laterally extensive mine units, which are distinguished on the basis of texture and mineralogy. Contacts between units are generally sharp.

The physical and chemical parameters responsible for the textural and mineralogical variations have been evaluated through a study of fluid inclusions, sulfur isotopes and ore mineralogy. Fluid inclusion homogenization temperatures from simple, two-phase primary and pseudo-secondary inclusions in sphalerite and sparry dolomite gangue indicate initial temperatures of ore formation from 150-210°C in the eastern Upper Lens when the estimated pressure of ore formation is taken into consideration. The temperature of ore formation decreased to 100-150°C in the western portion of the Upper Lens. Freezing studies indicate that the ore-forming fluid

was a brine containing 20-37 equivalent weight percent $CaCl_2$. The sulfur isotopic compositions of late and main stage pyrite crystals range from $\delta^{34}S$ = +27.4‰ to + 28.0‰., suggesting relatively constant temperature, fluid source and dominant sulfur species in the ore fluid during ore formation, providing there has been no subsequent re-equilibriation of sulfur isotopes. The iron content of sphalerite varies from 14 mole % to 0 mole % from crystal centers to rims respectively, corresponding to well developed colour zonation. Sphalerite iron contents constrain the oxygen activity of the ore fluid from 10^{-46} to 10^{-41} at 200°C during sphalerite precipitation. The best developed zoning and, thus, the highest oxygen activities occur within sphalerite adjacent to carbonate wall rock. Under high oxygen activities, conditions were favorable for the generation of sulfanes considered necessary for precipitation of marcasite. X-ray diffraction studies indicate that primary marcasite has inverted completely to pyrite. The stability of the simplest sulfane, H_2S_2, constrains the maximum allowable pH of the ore fluid at the time of marcasite precipitation to 5.0. The presence of interbanded marcasite pseudomorphs and sparry dolomite indicate that the ore fluid fluctuated around pH = 5.0.

Comparison of solid organics extracted from the Society Cliffs dolostone to bitumen associated with minerali-

zation suggests that organics within the host formation have played a role in sulfate reduction. The model of ore forma-tion therefore proposed involves the *in situ* reduction of a hot, saline, metal-bearing ore fluid by hydrocarbons liberated by the replacement and dissolution of wall rock. Sulfate reduction was probably concentrated at the wall rock orebody interface along a replacement front that migrated away from the orebody. Banding was likely the result of repetitive sulfate reduction, metal precipitation and wall rock dissolution in response to the pulsatory influx of ore fluid. Gross textural and mineralogical variations are probably a result of slight variations in the oxidation state of the ore fluid, the availability of H_2S and, to a lesser extent, temperature.

ACKNOWLEDGEMENTS

CHAPTER 1:   INTRODUCTION

1.1   Introductory Statement

Carbonate-hosted Zn-Pb-Ag mineralization in the Nanisivik area occurs in the northern portion of the Churchill Structural Province (Figure 1.1). Massive sulfide occurrences were first reported at Strathcona Sound in 1910-11 by a prospector on board a Canadian government survey vessel. However, it was not until 1958 that the showings were examined in detail by Texas Gulf Inc. Subsequent drilling and geophysical surveys outlined most of the major sulfide bodies presently known in the area. In 1974 a consortium of companies formed Nanisivik Mines Ltd. to develop the property with Strathcona Mineral Services Ltd. as operators. Published ore grade reserves are estimated at 6.5 million tonnes at 12.0% Zn, 1.5% Pb and 50 g/tonne Ag (Clayton and Thorpe, 1982). Production from the Main Orebody began in 1977.

1.2   Geology of the Nanisivik Area

The regional geology of the area has been most recently discussed by Jackson and Iannelli (1981) and forms the basis for the description to follow. A thick middle-to-late Proterozoic sequence unconformably overlies early Precambrian basement in the Borden Basin of northwest Baffin

FIGURE 1.1
LOCATION MAP

NANISIVIK

BAFFIN ISLAND

CHURCHILL PROVINCE

NORTH AMERICA

0   800
KILOMETERS
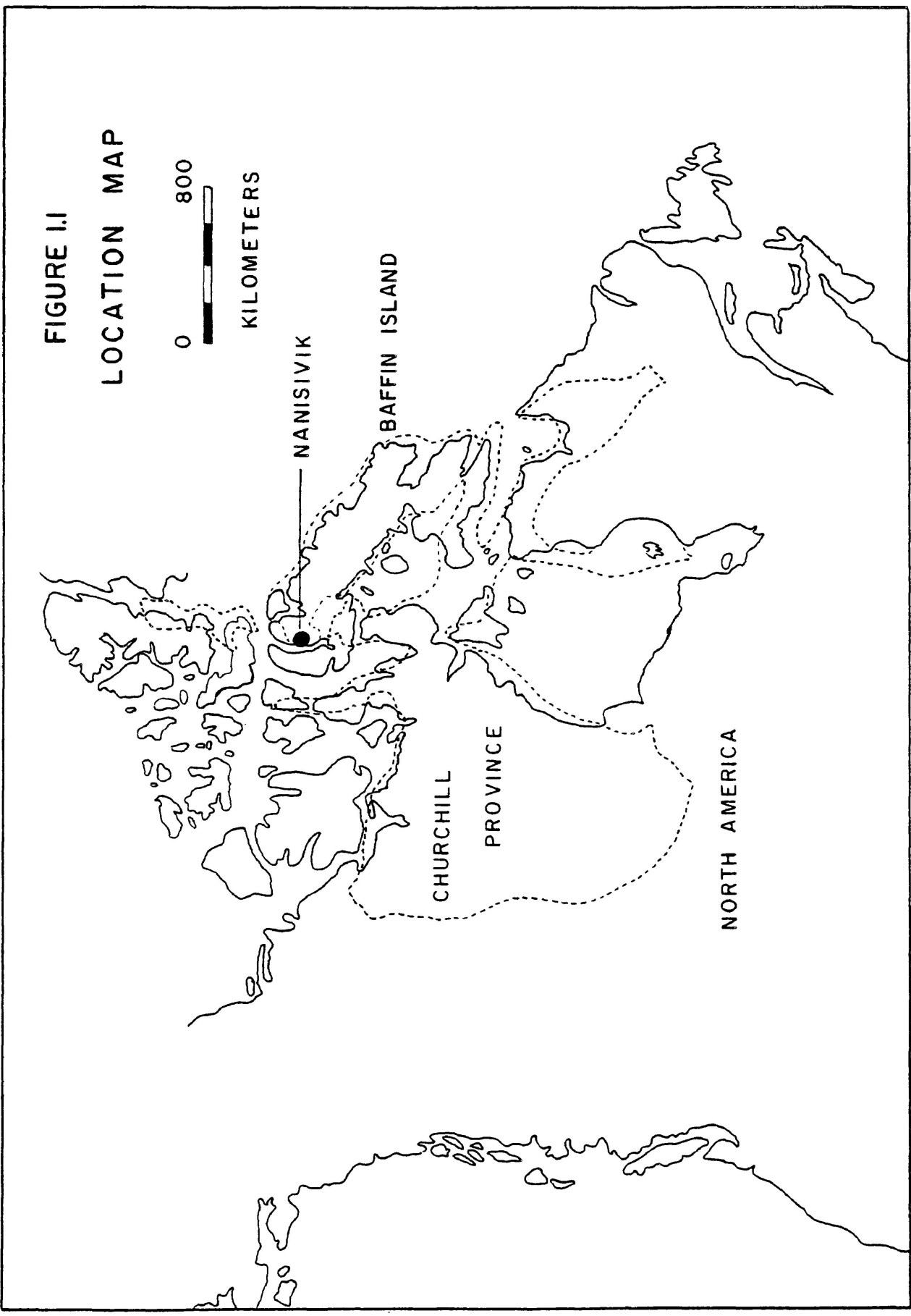
Island. Deposition within the basin took place in three west to northwest tending fault-bounded troughs, which together comprise the North Baffin Rift Zone (Figures 1.2 and 1.3). Sulfide mineralization in the Nanisivik region occurs within the Milne Inlet Trough, which is the middle of the three. The Milne Inlet Trough is centered on Strathcona Sound and may extend as far northwest as Somerset and Cornwallis Islands. The North Baffin Rift Zone was considered to represent an aulocogen by Olson (1977) and has been correlated with a number of other rift basins within the Canadian Arctic by Jackson and Iannelli (1981). These rift basins are orientated at a high angle to the northwest edge of the former Canadian-Greenlandic Shield and are believed to have formed during a period of rifting about 1,200 million years ago.

Jackson and Iannelli (1981) recognized three distinct groups within the basin which collectively comprise the Bylot Supergroup (Table 1.1). The lowermost Eqalulik Group consists predominantly of terrigenous clastics with minor continental tholeiitic basalts of the Nauyat Formation. These volcanics yield an average K-Ar age of 946 m.y. and a Rb-Sr age of 1,129 m.y. (Jackson and Iannelli, 1981). The latter age agrees well with a paleomagnetic age of 1,220 m.y. for the Nauyat Formation (Fahrig et al., 1981). Shallow water carbonates and minor clastics of the Uluksan Group over-lie the Eqalulik Group. An upper clastic unit, the Nanatsiaq Group in turn overlies the Uluksan Group. Syndepositional

4.
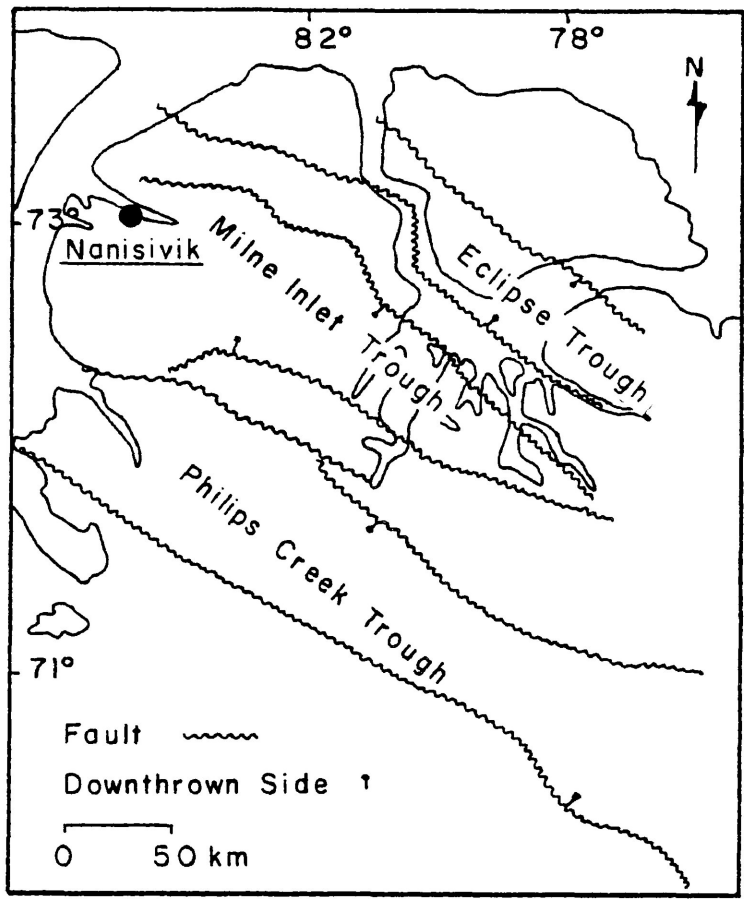
NORTH BAFFIN
RIFT ZONE

FIGURE I.2 - DEPOSITIONAL
BASINS (MODIFIED AFTER
JACKSON AND IANNELLI,
1981).

FIGURE I.3 - GENERALIZED
GEOLOGY (AFTER CLAYTON
AND THORPE, 1982).
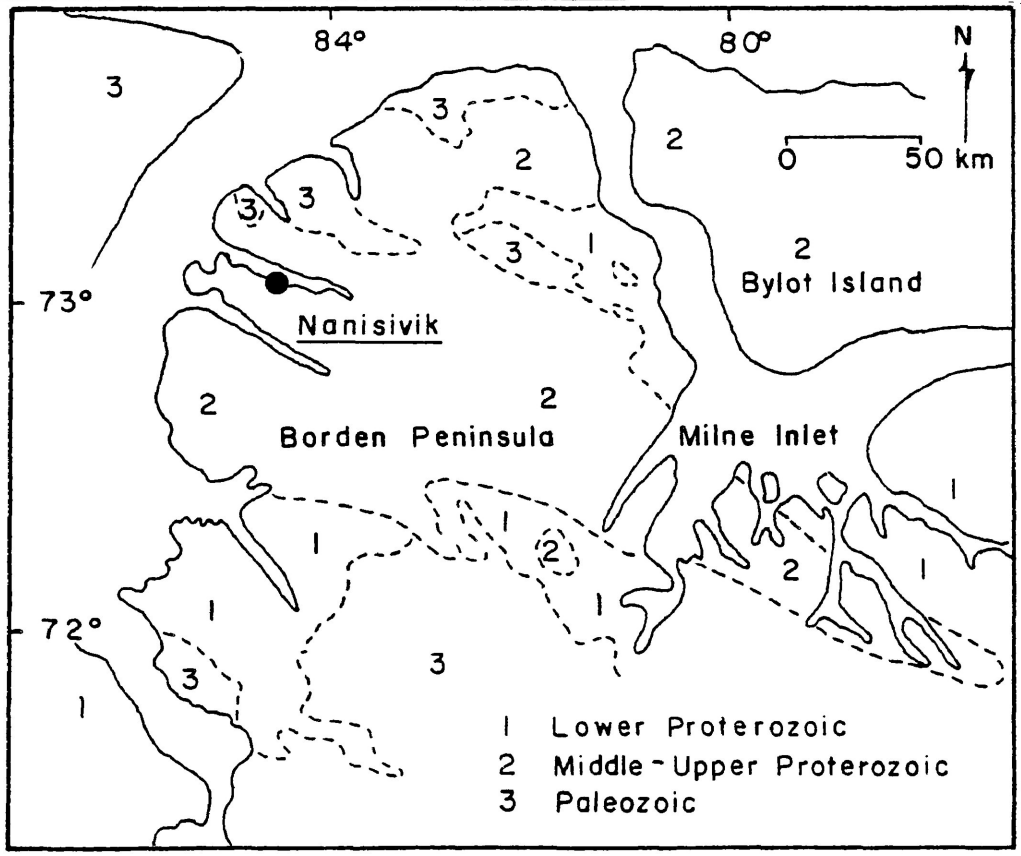
TABLE 1.1 : FORMATIONS OF THE BYLOT SUPERGROUP (MODIFIED AFTER JACKSON AND IANELLI, 1981).

Era	Supergroup	Group	Formations / Contacts
Hadrynian			FRANKLIN INTRUSIVES: DIABASE
			Intrusive Contact
		Nunatsiaq Group	ELWIN FORMATION
Neohelikian	Bylot Supergroup		Gradational Contact
			STRATHCONA SOUND FORMATION
			Gradational Contact
			ATHOLE POINT FORMATION
			Gradational / Gradational to Conformable
		Uluksan Group	VICTOR BAY FORMATION
			Conformable, Abrupt to Gradational
			SOCIETY CLIFFS FORMATION
		Eqalulik Group	Unconformable (?) / Gradational to Unconformable
			FABRICIUS FIORD FORMATION / ARCTIC BAY FORMATION
			Conformable, Abrupt to Gradational
			ADAMS SOUND FORMATION
			Conformable Contact
			NAUYAT FORMATION
Archean/Aphebian			Nonconformaty
			GRANITIC GNEISS BASEMENT COMPLEX

faulting in Borden Basin has resulted in abrupt lateral facies and thickness variations.

Jackson and Iannelli (1981) presented numerous K-Ar ages from various northwest and north striking diabase dikes that range from 472±11 m.y. to 1,128±38 m.y. Christie and Fahrig (1983) argued that many of these ages are too low, possibly because coarse-grained material more susceptible to argon loss was analyzed. Christie and Fahrig (1983) recognized two distinct igneous events; a predominantly northwest-striking dike swarm, the Borden Dikes, having an average age of 950 m.y. and a north-striking dike swarm, the Franklin Dikes, that have an average age of 750 m.y. and crosscut the older set. Although diabase dikes in the Strathcona Sound region usually strike northwest, they consistently yield whole rock K-Ar ages less than 800 m.y. suggesting that there has been some argon loss, perhaps due to subsequent regional reheating. Using the Rb-Sr and paleomagnetic ages of the Nauyat Formation as a maximum, and the average K-Ar age for the Borden Dikes as a minimum, it can be estimated that the Bylot Supergroup was deposited between 1,200 and 950 m.y. ago.

The Society Cliffs Formation of the Uluksan Group hosts Zn-Pb-Ag mineralization in the Nanisivik region. Jackson and Iannelli (1981) identified two members of the formation, a lower clastic-rich member and an upper clastic-poor member. Four major dolostone lithological types are recognized by Jackson and Iannelli (1981) on a regional scale

in both members:

1)   Thick bedded to massive dolostone.

2)   Regularly laminated algal dolostone to thin bedded dolostone.

3)   Nodular to elliptical, irregularly laminated dolostone.

4)   Dolostone conglomerate and breccia.

Dolomitic shale and dolostone of the Victor Bay Formation overlie the Society Cliffs Formation. Generally the two formations are in gradational contact, but locally, minor karsting of the Society Cliffs Formation has preceded Victor Bay deposition.

In the immediate Nanisivik area, dolostone of the Society Cliffs Formation is conformably overlain by dolomitic shales of the Victor Bay Formation. Although a complete section is not exposed at Nanisivik, the thickness of the Victor Bay Formation is estimated to have been as much as 300 m, while the Society Cliffs Formation is considered to have a thickness of between 500 and 600 m (Clayton and Thorpe, 1982). Gröepper (1978) subdivided the Society Cliffs Formation in the immediate Nanisivik area into seven lithofacies units deposited in intertidal to subtidal environments. Solution features such as collapse breccias and vugs are most common in the upper Society Cliffs Formation (Olson, 1977) but have been reported throughout the formation in the Nanisivik area. Sulfide mineralization is generally restricted to the upper Society Cliffs Formation or the overlying contact with the Victor Bay Formation.

Structure within the Nanisivik area is dominated by block faulting (Figure 1.4). Proterozoic strata dip slightly northward near the Main Orebody (Clayton and Thorpe, 1982). Two sets of normal faults predominate. One set strikes east and parallels the main graben centered on Strathcona Sound, delineating a series of horst and graben that are progessively down dropped towards the Sound. Ore mineralization of the Main Orebody transects one of the east striking faults on the north side of the Keystone Graben with little apparent offset. Whether faulting accompanied or followed deposition of the Victor Bay shale is unclear, but faulting brought the shale into abrupt lateral contact with the Society Cliffs Formation. Less common north striking faults offset the east striking series as well as the sulfide mineralization (Olson, 1977).

Northwest striking gabbro dikes 20 - 30 m wide occur in the immediate Nanisivik area. Olson (1977) observed that these dikes are offset by the east striking fault series. Olson (1977) also reported K-Ar ages of 531 ± 20 m.y. and 463 ± 17 m.y. for dikes in the area, including a gabbro dike which crosscuts the Main Orebody.

1.3   **Geology of the Nanisivik Ore Deposits**

Figure 1.5 illustrates the various sulfide bodies outlined to date in the Nanisivik area. The majority of these sulfide bodies, and by far most of the sulfide mineralization
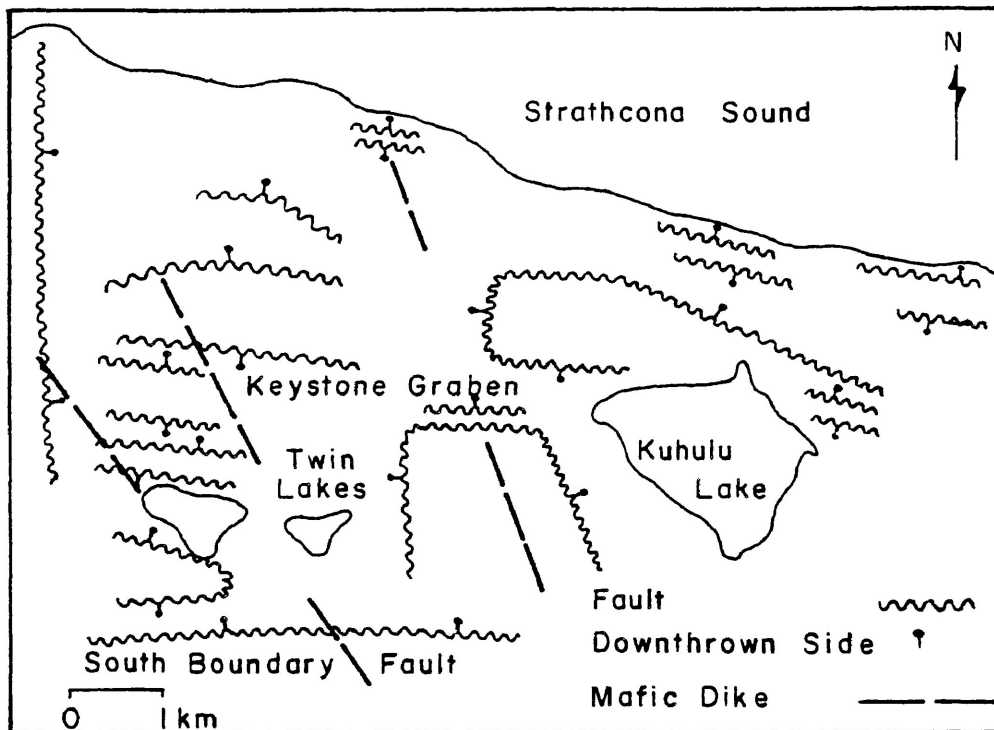
FIGURE I.4 - BLOCK FAULTING OF THE NANISIVIK AREA.
(AFTER CLAYTON AND THORPE, 1982).
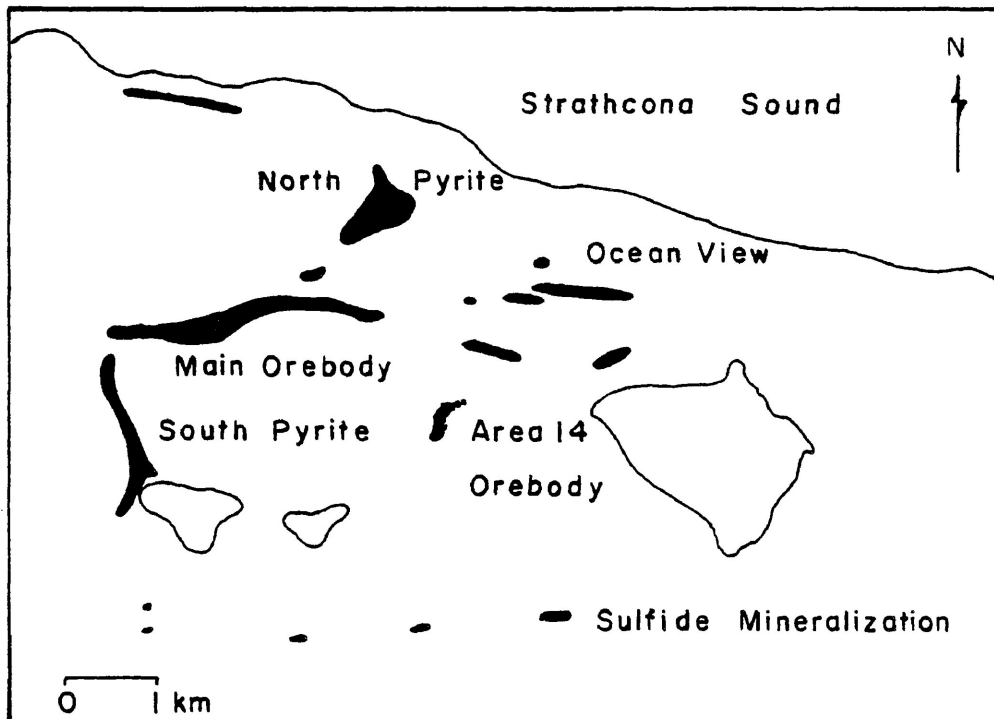
FIGURE I.5 - SULFIDE MINERALIZATION AT NANISIVIK
(AFTER CLAYTON AND THORPE, 1982).

at Nanisivik, consists of barren iron sulfide. However, the Main Orebody contains economic quantities of zinc, lead and silver, as do a number of satellite bodies, the most important of which is in Area 14 (Figure 1.5). Most of the ore bodies have lenticular cross sections and are elongate in plan view. Clayton and Thorpe (1982) emphasized the nearly horizontal nature of individual sulfide bodies, as well as an overall drop in sulfide body elevation above sea level towards Strathcona Sound. They attributed this consistent drop in sulfide body elevation to a paleokarstic control of sulfide mineralization in the area, an idea first proposed by Geldsetzer (1973) and later expanded by Olson (1977, 1984). The South Boundary Fault appears to have localized sulfide mineralization in the southern portion of the area, and the Shale Hill Zone to the north of the Main Orebody also appears to be fault-controlled (Ron Sutherland, pers.comm., 1985).

1.3A   **Geology of the Main Orebody**

The Main Orebody is hosted in an upthrown block of Society Cliffs dolostone that is situated immediately north of the Keystone Graben, a prominent structural and topographical feature in the area (Figure 1.5). The Upper Lens of the Main Orebody is an elongate, nearly horizontal ore zone approximately 3.0 kilometers long, 100 meters wide, and 10 meters thick (Figure 1.6). In cross-section the Upper
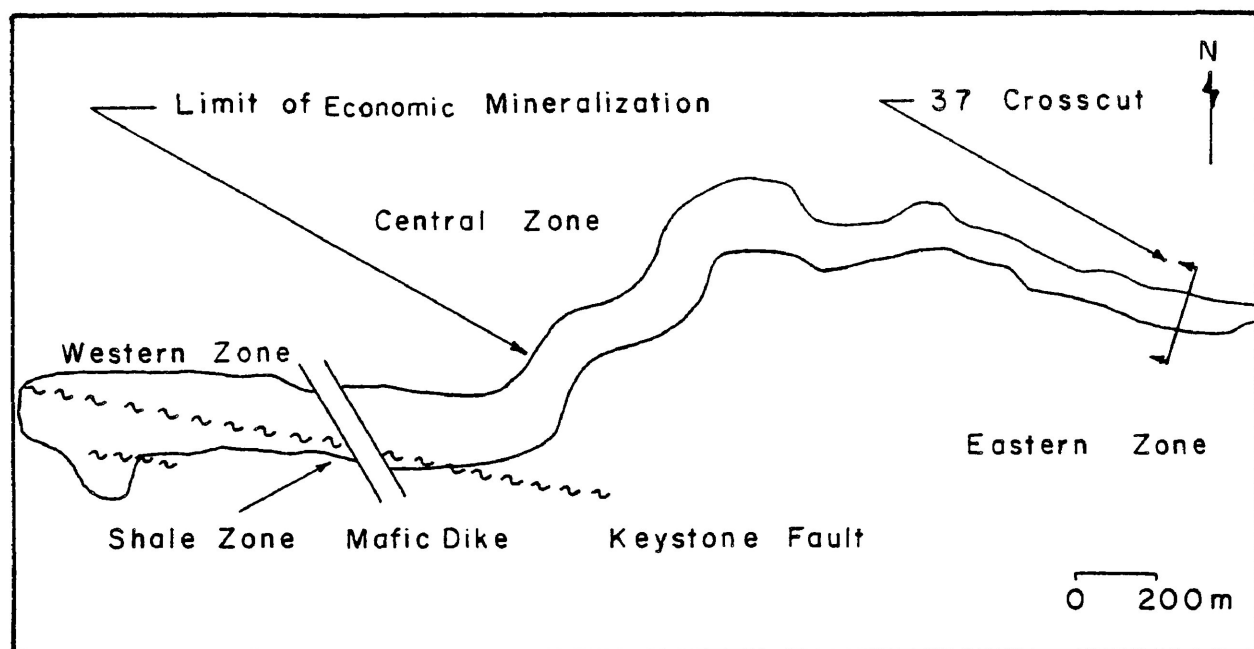
FIGURE I.6 - NANISIVIK MAIN OREBODY, PLAN SECTION
(MODIFIED AFTER OLSON, 1984).
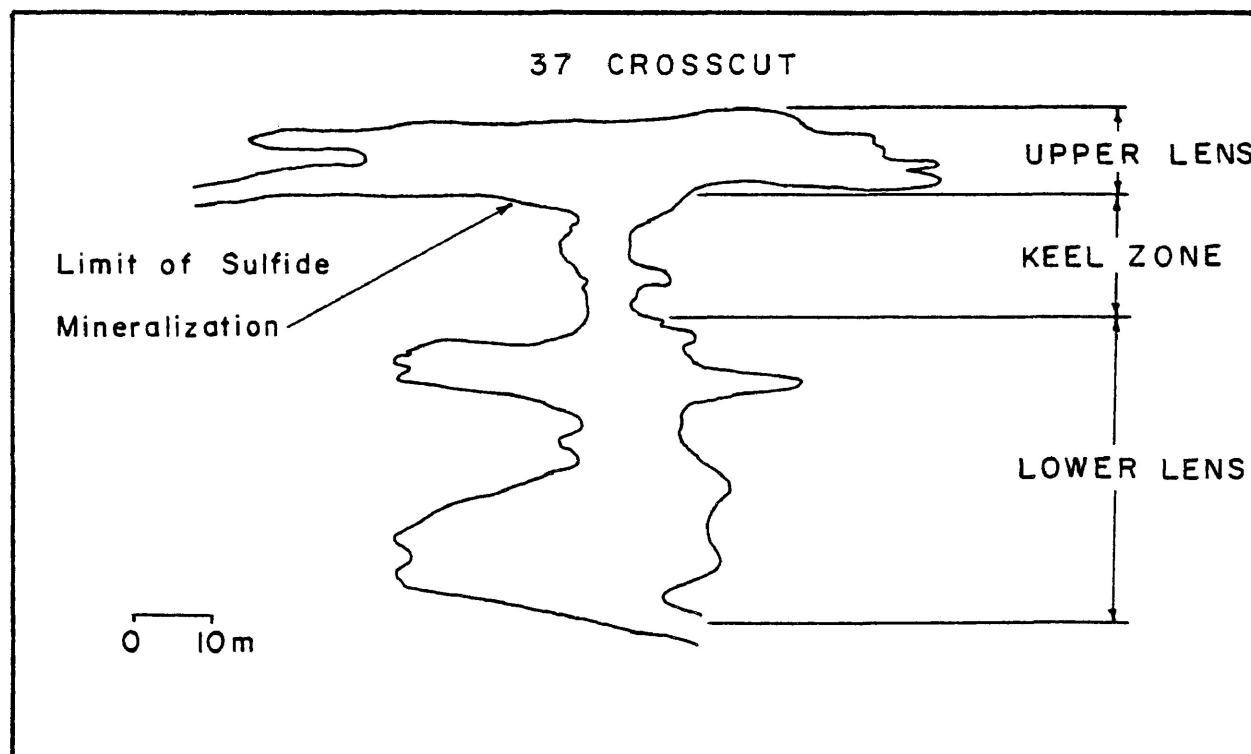
FIGURE I.7 - NANISIVIK MAIN OREBODY, CROSS SECTION
(COURTESY OF NANISIVIK MINE STAFF).

Lens is roughly lenticular in shape with "fins" of wall rock that extend laterally for a considerable distance into the ore, particularly in the central and eastern portions (Figure 1.7). Mineralization in the Lower Lens occurs 20 to 60 m below the Upper and is considerably more irregular. In places Lower Lens mineralization is connected to the Upper by a vertical zone of uneconomic sulfide mineralization known as the Keel Zone (Figure 1.7). To date, no strict control on Lower Lens mineralization has been identified (Doug Dumka, pers.comm., 1984) although Clayton and Thorpe (1982) report that Lower Lens mineralization conforms to bedding in the Society Cliffs Formation north of the central portion of the Main Orebody.

To avoid confusion in the discussion to follow, the term dolomite will be restricted to carbonate gangue associated with mineralization and the term dolostone will be used to refer to the dolomitic host rock. The footwall contact of the Upper Lens varies from gradational, where the wall rock is in contact with coarsely banded pyrite and white, sparry dolomite, to sharp, where the wall rock is in contact with massive sulfide. Gradational contacts between sulfide ore and dolostone are characterized by a progressive increase in the amount of fine grained pyrite present and by an increase in recrystallization of dolostone to coarse dolomite rhombs towards the ore zone. The footwall contact is often irregular and appears to dip towards the center of the orebody. Sulfide banding in the west open pit is conformable

to the hanging wall, as is generally the case throughout most of the Upper Lens. Vertical wall rock contacts along the sides of the orebody are generally abrupt and here banded sulfides may be seen to dip away from the contact. As in the case of the footwall, the upper contact of the dolostone fins may vary from abrupt to gradational. Along the underside of the fins, dolostone is often separated from sulfides by a band of sparry dolomite about 5 cm thick. Contacts between sulfides and dolostone in the Lower Lens are usually sharp. Beneath the Lower Lens the dolostone is often fractured, consisting of rubble to crackle breccias. Crackle breccias consist of fractured dolostone in which there has been little relative movement between fragments, while fragments in the rubble breccia have been rotated and displaced. Breccia fragments generally have a bleached appearance, relative to Society Cliffs dolostone, due to recrystallization and partial replacement. Sparry dolomite is the most common breccia cement.

Ford (1981) suggested that the dolostones fins are too large to have been unsupported in a cavern system and estimated that as much as 95% of the Upper Lens volume was created during ore formation. Enlargement of an initial cavern system is supported by the observation of unsupported fins "floating" in ore (Kissin, 1983; Curtis, 1984) and by the occurrence of replacement textures along the margins of the Upper Lens (Curtis, 1984).

Irregular stringers and patches of a white, highly altered material, known informally at the mine as "white rock", occur within approximately 600 m of the gabbro dike along the exploration ramp into the Lower Lens. The origin of this material is uncertain but in its less altered form feldspar crystals have been observed, suggesting that the "white rock" represents a highly altered igneous intrusive (Neumann, 1984). In its most altered form the "white rock" consists predominantly of clay minerals (Curtis, 1984). A sample of white rock is reported to give a Rb-Sr age of 485±7 m.y. (Curtis, 1984), suggesting that it is coeval with, or slightly younger than, the gabbro dike that cuts the Main Orebody.

One of the most striking features of the Upper Lens of the Main Orebody is the well banded nature of much of the mineralization. Banding may be defined by sulfides alone or by sulfides and white, sparry dolomite. Detailed underground mapping by Curtis (1984) in the eastern portion of the Upper Lens delineated a mine stratigraphy consisting of seven mine units that are characterized on the basis of texture and mineralogy (Figure 1.8). Contacts between units are typically abrupt. Neumann (1984) offered an alternative classification that emphasized the similarities between certain units. However, the units, as described by Curtis (1984), will form the basis of the description to follow, with Neumann's (1984) nomenclature included in brackets. Descriptions apply mainly to the eastern and central portions of the Upper Lens.
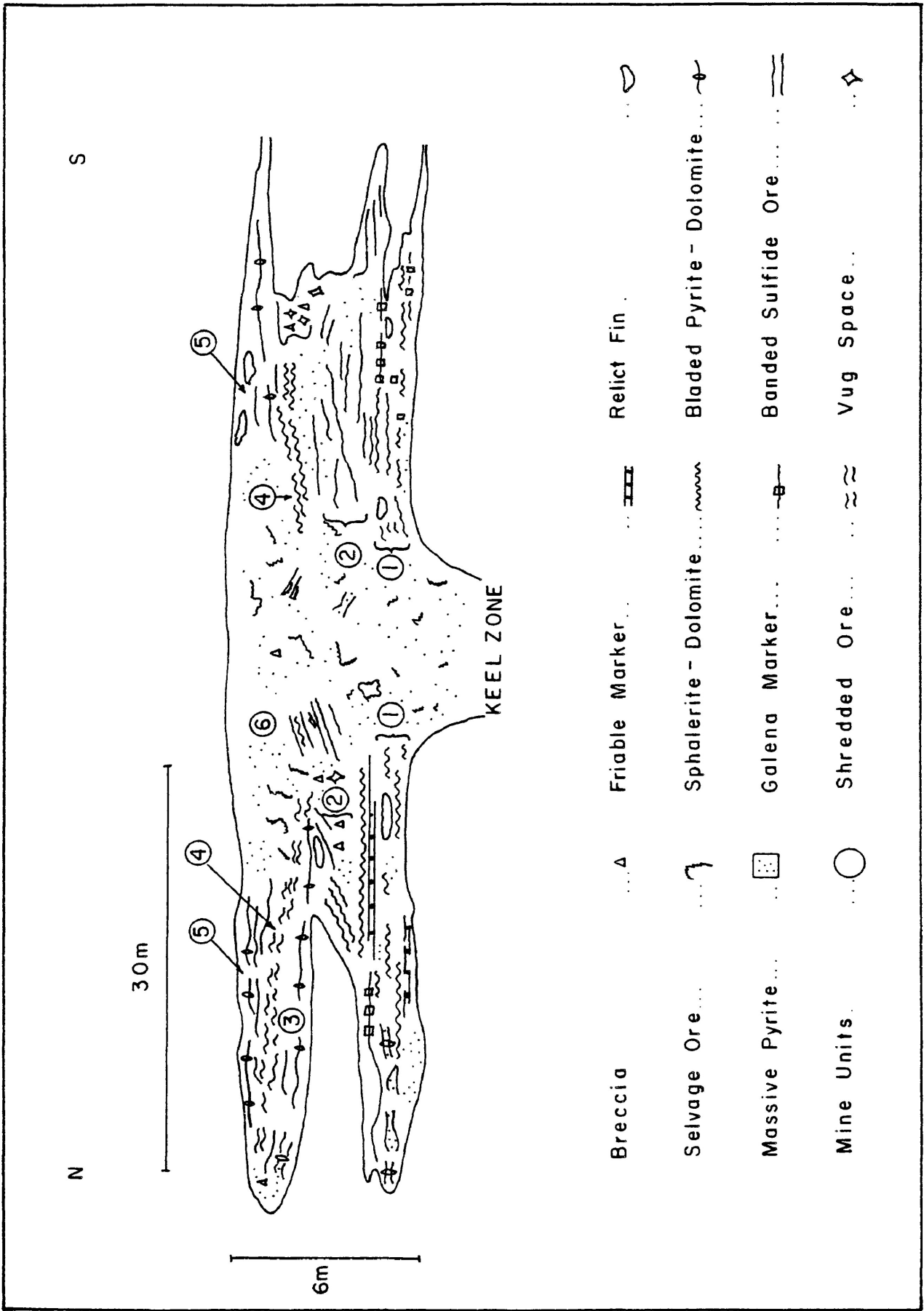
FIGURE I.8 – SCHEMATIC CROSS SECTION OF THE EASTERN UPPER LENS (AFTER CURTIS, 1983).

Unit 1 (A₁)

Unit 1, the lowermost mine unit, is most often in contact with footwall dolostone and typically consists of bands 2 - 3 cm wide of coarse, bladed pyrite and white, sparry dolomite (Figure 1.9). In places the contact with the footwall is gradational and characterized by replacement of dolostone (Figure 1.10). White sparry dolomite rhombs up to 1 cm across have grown at the expense of dolostone in areas of replacement and a small amount of black, bituminous material may sometimes be found interstitial to the dolomite crystals. Fine grained pyrite partially replacing dolostone forms bands several centimeters across. Remnants of dolostone are occasionally isolated within the banded ore and may be in various stages of replacement. Unit 1 also contains rhythmically banded ore consisting of a central band of sphalerite surrounded on either side by pyrite and then by sparry dolomite (Figure 1.11). Friable dolomite marker horizons up to 10 cm thick enclose ice-filled cavities. The top of the unit is considered to be the lower contact of the projecting dolostone fins (Figure 1.12).

Unit 2 (B₁)

Unit 2 consists predominantly of massive or finely banded sulfide laterally equivalent to the dolostone fins. In some areas it appears that sulfides have totally replaced dolostone fins (Figure 1.13) but, generally, replacement textures are lacking in this Unit. Pyrite and sphalerite are the predominant sulfides. Curtis (1984) emphasized the occur-
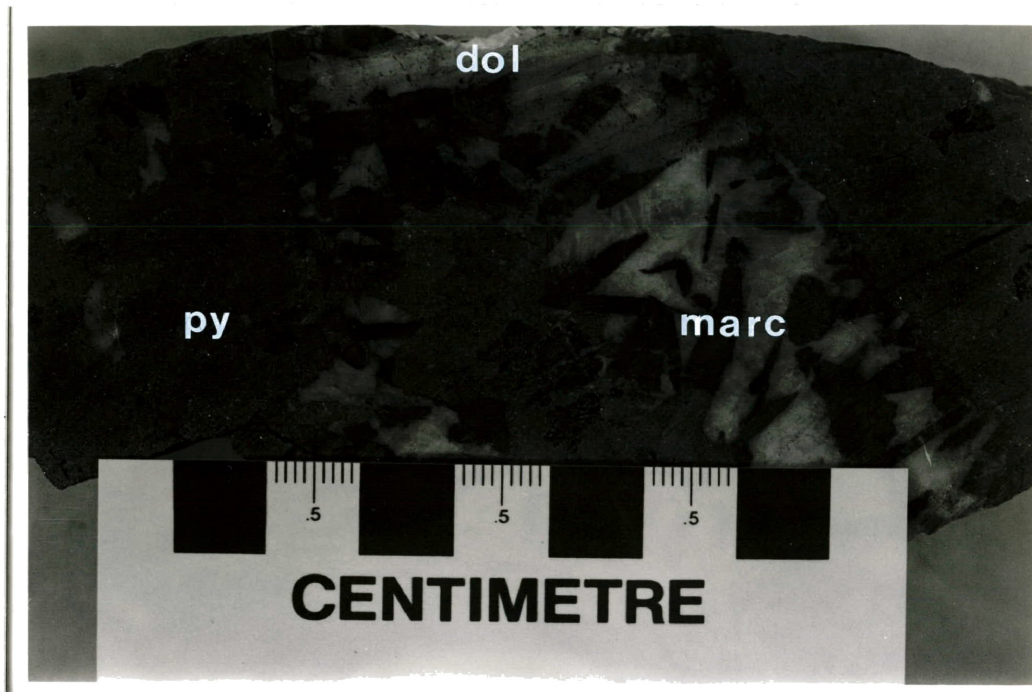
FIGURE 1.9 – BLADED PYRITE PSEUDOMORPHS AFTER MARCASITE IN COARSELY BANDED MINERALIZATION FROM UNIT 1.
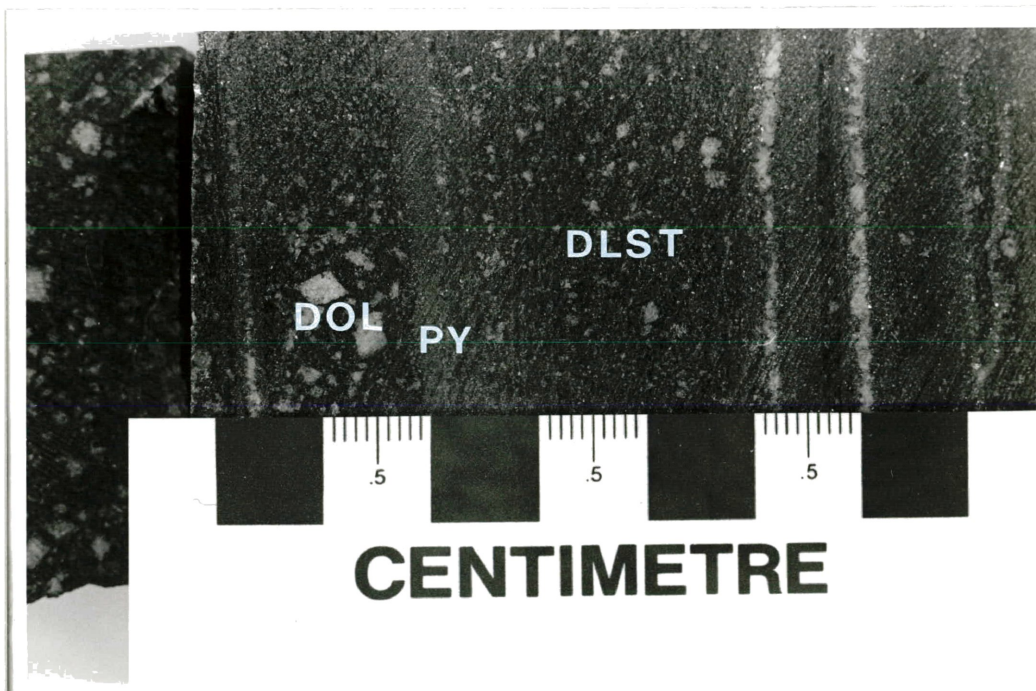
FIGURE 1.10 – REPLACEMENT TEXTURE IN SOCIETY CLIFFS DOLOSTONE CHARACTERIZED BY THE RECRYSTALLIZATION OF DOLOMITE AND PRECIPITATION OF FINE-GRAINED PYRITE.
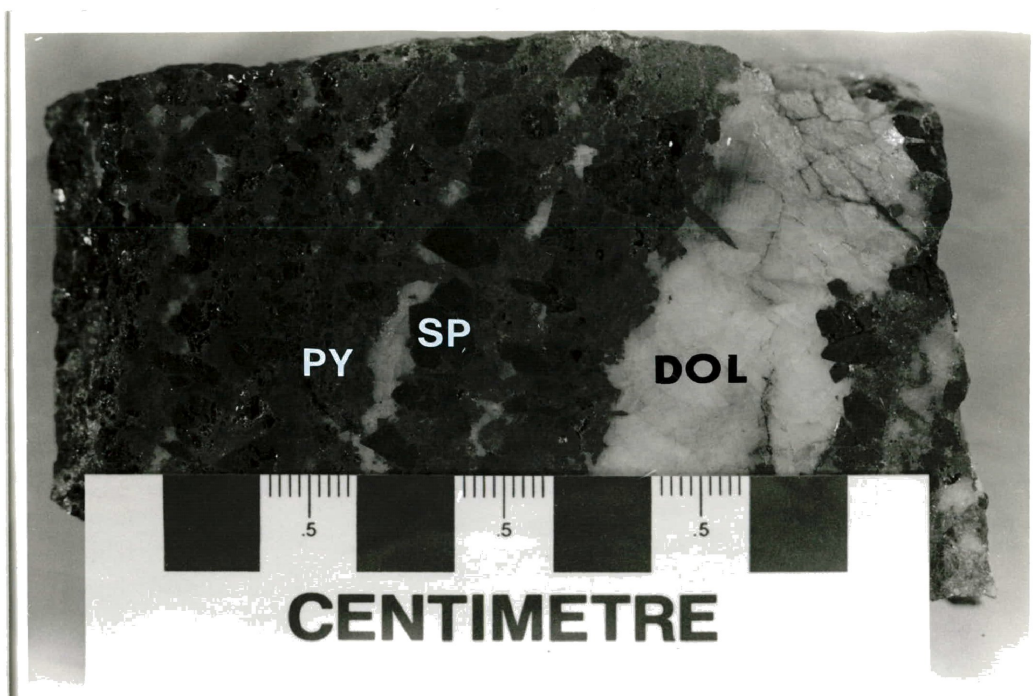
FIGURE 1.11 - COARSE, BANDED ORE FROM UNIT 1.

FIGURE 1.12 - COARSELY BANDED ORE FROM UNIT 1 IN CONTACT
WITH AN OVERLYING DOLOSTONE FIN. UNITS 2 AND 3 ALSO INDICATED.

rence of "cross bedding" or inclined banding in the sulfides that parallels the dolostone contact (Figure 1.14).

Unit 3 (A₂)

Unit 3 is similar to Unit 1, consisting of coarsely banded, bladed pyrite-sparry dolomite couplets. However, Unit 3 is not as well developed or as widespread as Unit 1. The contact with the underlying dolostone fin is generally gradational. Where Unit 2 contains inclined bands, these may be truncated by Unit 3.

Unit 4 (B₂)

Unit 4 consists of well banded sulfide and sulfide-sparry dolomite couplets approximately 1 - 2 cm in width (Figure 1.15). Often the bands are irregular or disrupted, giving the ore a "shredded" appearance (Figure 1.16). Where both Units 3 and 4 are present, the contact may be marked by a friable dolomite band at the top of Unit 3, or by a band of massive, dark sphalerite ore 10 - 20 cm thick at the base of Unit 4. The lower contact of Unit 4 is abrupt whether it overlies Unit 3 or rests directly on a dolostone fin. In the vicinity of crosscut 22, Unit 4 is locally disrupted and appears to fill collapse structures characterized by sparry dolomite filling open spaces.

Unit 5 (A₃)

Unit 5 is best developed on the extreme edges of the orebody in contact with the hanging wall. In many respects it is similar to Units 1 and 3, consisting primarily of bladed pyrite-sparry dolomite couplets and massive pyrite
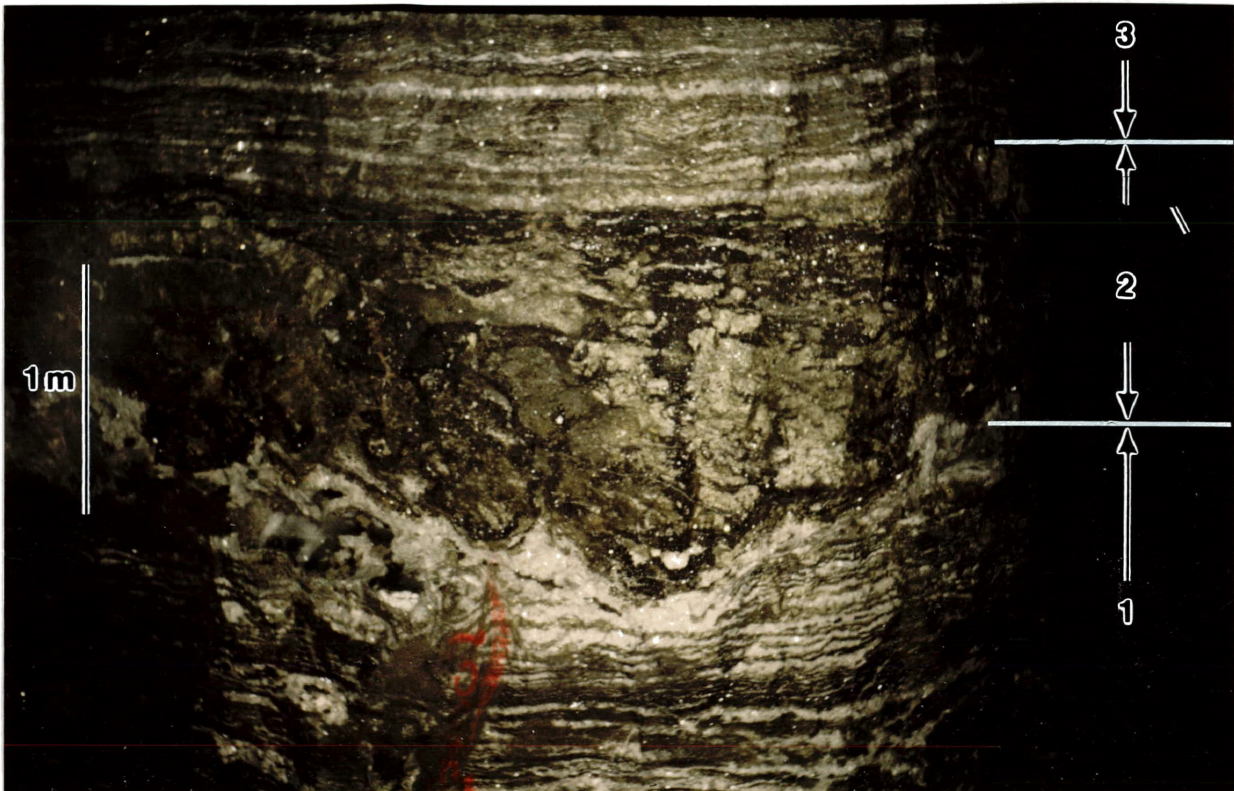
FIGURE 1.13 - REPLACEMENT OF A DOLOSTONE FIN BY MASSIVE
PYRITE AND SPHALERITE IN UNIT 2.
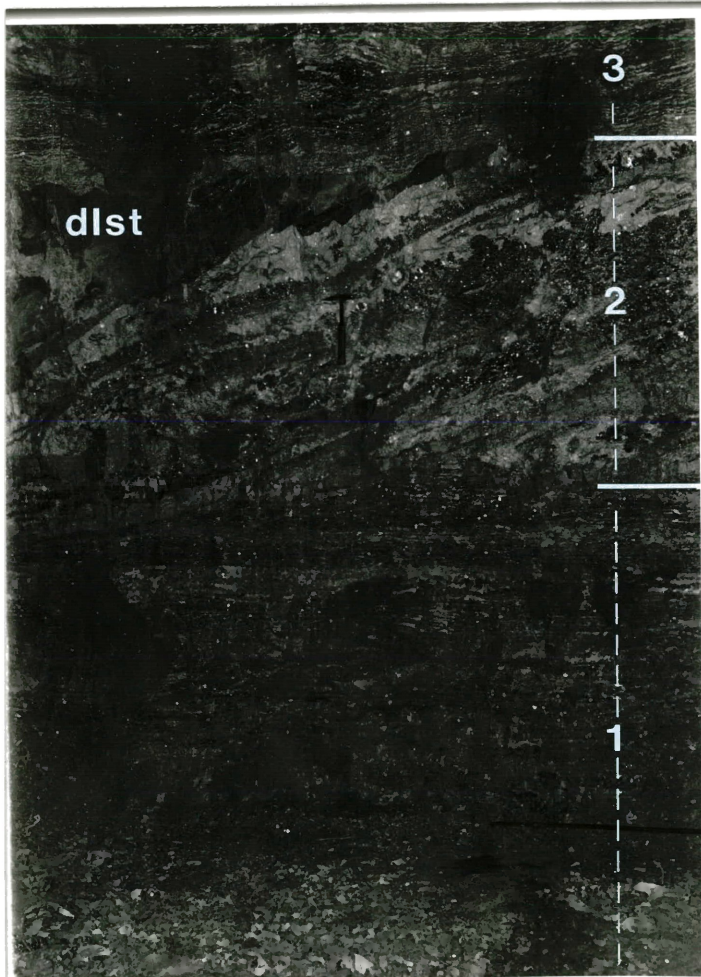
FIGURE 1.14 - INCLINED BANDING
IN ORE FROM UNIT 2.
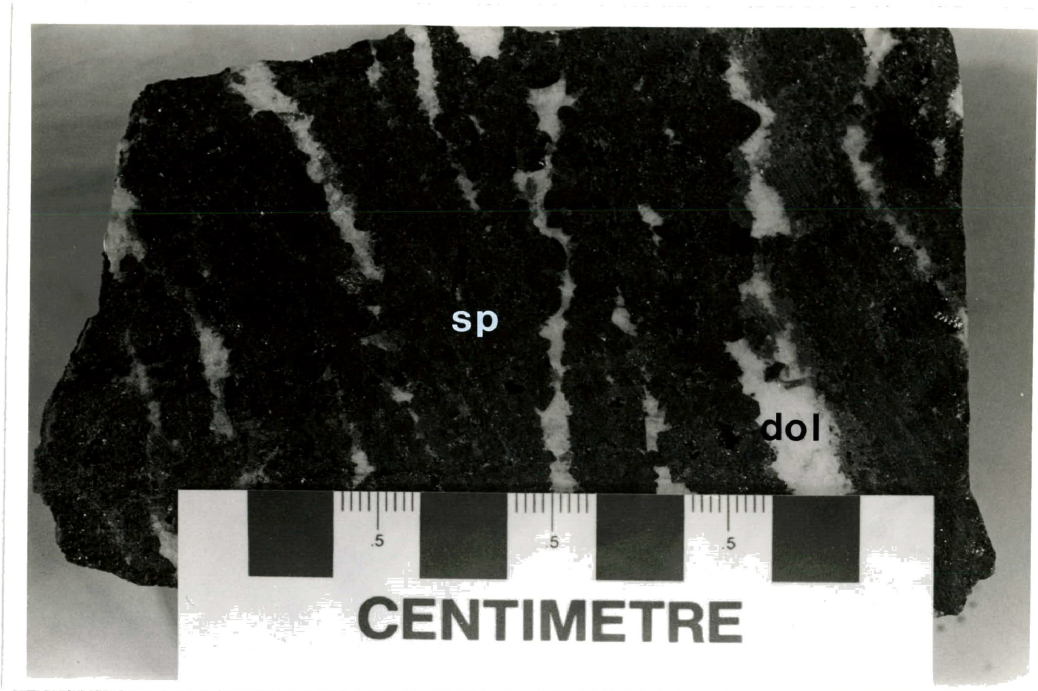
FIGURE 1.15 – REPETITIVE BANDING IN SPHALERITE – RICH
ORE FROM UNIT 4.

FIGURE 1.16 – "SHREDDED" ORE
FROM UNIT 4.

bands. Curtis (1984) reported evidence of replacement in this unit and interpreted it as having a similar origin as Units 1 and 3, although Unit 5 is slightly enriched in galena.

Unit 6 (C)

Unit 6 is an irregular, chaotic unit containing sel-vage-textured ore and "ribs" of massive pyrite (Figure 1.17). Pyrite and sphalerite are found intergrown around the outside of the selvages, followed by a layer of darker sphalerite towards the center. The centers of selvages contain coarse-grained, occasionally vuggy, sparry dolomite (Figure 1.18). Ribs of pyrite dip away from the center of the orebody in contrast to the slightly inward orientation of banding in Units 1 and 5. Fragments of dolostone floating in ore may also occur in this unit. The lower contact of Unit 6 is typically abrupt and locally truncates the lower banded units, creating a contact that dips toward the center of the orebody (Figure 1.17).

Keel Zone (E₂)

Curtis (1984) included both the Keel and Shale Zones in his Unit 7 without implying a common genesis. Given the significant differences between the Keel and Shale Zones, they are treated separately here. Towards the center of the orebody the ore becomes more massive and pyrite becomes the predominant sulfide, although some Unit 6 textures are locally preserved. Along with Unit 6, the Keel Zone truncates the underlying banded ore units towards the center

FIGURE 1.17 - "SELVAGE" TEXTURED ORE OF UNIT 6.

FIGURE 1.18 - "SELVAGE" TEXTURE IN HAND SAMPLE.

of the orebody. The contact between Units 1 to 6 and the Keel Zone is poorly exposed by the mine workings so that its exact nature remains unclear. The Keel Zone is in sharp contact with footwall dolostone in the center of the Main Orebody and this contact dips moderately inward.

Shale Zone

Shale Zone mineralization occurs on the south side of the Main Orebody where it intersects an easterly trending fault with no apparent offset. Mineralization of the Shale Zone is partially hosted in a graben overlain by Victor Bay shale and consists mainly of massive pyrite with zones of very coarse-grained sphalerite and minor sparry dolomite. The Shale Zone is best exposed along a decline on the south side of the upper lens that begins near crosscuts 7 and 8.

Lower Lens

Lower Lens mineralization is best exposed along the exploration ramp that begins near the northwest margin of the Upper Lens. Irregular patches of "white rock" are common, as previously mentioned, and these are often surrounded by massive, dark red sphalerite, which appear to have been remobilized during white rock emplacement. Sulfide minerali- zation generally consists predominantly of pyrite. Locally, massive fine-grained pyrite contains poorly developed bands of medium-grained sphalerite. Massive sulfides are often disrupted by irregular patches of sparry dolomite and fractures containing fine-grained sphalerite.

Western Portion of the Upper Lens (West Zone)

The mine stratigraphy outlined above for the central and eastern portions of the upper lens is not as well developed west of the gabbro dike (Figure 1.6), although banding is still pervasive. Dolostone fins are not as extensive as elsewhere in the Upper Lens, and the orebody is wider at this point. Pyrite and sphalerite occur either alone as massive layers or interbanded together. White sparry dolomite gangue is not as common as it is in the central and eastern portions of the Upper Lens. Galena commonly occurs as irregular patches, although it is well banded in the west open pit. The Zn/Pb ratio is reported to increase from east to west in the Upper Lens (Olson, 1984).

1.3B   Geology of the Area 14 Orebody

The recently discovered Area 14 Orebody is situated just over two kilometers southeast of the Main Orebody (Figure 1.5). Ore grade mineralization is restricted to the western portion of an elongate, east-west trending, discontinuous sulfide body. Compared to the Main Orebody, zonation at Area 14 is relatively simple. A lower pyritic unit with minor white, sparry dolomite may be in either sharp or gradational contact with the footwall. Neumann (1984) suggested that the lower pyritic unit replaces dolostone. The lower pyritic unit is abruptly overlain by a coarse-grained, massive sphalerite unit approximately one meter thick. Locally,

the lower pyritic unit may be absent, in which case the central sphalerite unit is in sharp contact with the foot- wall. An upper pyritic zone, typically less than one meter thick, separates the hanging wall from the central sphalerite unit. In the southwest portion of the orebody zones of high-grade lead mineralization (6 - 10% Pb) correspond to downward extensions of the sphalerite unit below the mining level. These zones of high-grade lead content appear to have a north- west trend (Michael Neumann, pers.comm., 1984).

1.4   Previous Work

Mineralogical Investigations

The mineralogy of sulfide deposits at Nanisivik is relatively simple, consisting predominantly of pyrite with local, economic concentrations of sphalerite and galena (Olson, 1977; Clayton and Thorpe, 1982). White sparry dolomite is the main non-sulfide gangue mineral although late quartz crystals occur in open vugs with sulfides and pink dolomite.

Olson (1977, 1984) considered some of the coarse, bladed pyrite to be pseudomorphous after marcasite, an obser- vation supported by Gait (1985), although no relict marcasite has been reported in the Main Orebody. The presence of marcasite in the Area 14 Orebody was reported by Lakefield Research (1984). Olson (1977) reported the presence of minor wurtzite in the Main Orebody on the basis of X-ray powder

diffractometer studies and confirmation was obtained by Neumann (1985) using the same technique. In neither case was the exact structure of the ZnS polymorph described. Neumann (1985) suggested that most wurtzite has inverted to sphalerite. Several generations of differently colored sphalerite have been reported from the Main Orebody (McNaughton, 1983; Neumann, 1984). Pyrrhotite has also been reported as a minor constituent of the Main Orebody (Olson, 1977) and of the Area 14 Orebody (Neumann, 1985). Growth banding is apparent in the dolomite gangue when viewed under cathodoluminescence, and this effect has been used for regional correlations by Curtis (1984) and Bending (1984).

Although recoverable amounts of silver occur within the Main Orebody, no discrete silver minerals have been identified. In a study of the silver contents of sphalerite and galena mineral separates using atomic absorption spectrophotometry, Neumann (1984) found that silver was associated with sphalerite rather than galena. Correlation of silver with sphalerite was confirmed in a recent study by Cabri *et al.*, (1985) using proton-microprobe analysis in which Ag concentrations from three sphalerite grains ranged from 600 to 700 ppm. In the same study, all three sphalerite grains analyzed contained between 3,000 and 6,000 ppm Cd, while single grains were reported to contain 149 ± 51 ppm Se and 86 ppm Ge. Jonassen and Sangster (1978), using atomic absorption spectrophotometry, reported Cd values between 0.1760 and 0.2290 wt.% in Nanisivik sphalerite. Silver appears to

correlate with galena in the Area 14 Orebody (Lakefield Research, 1984).

Fluid Inclusion Studies

The earliest study of fluid inclusions from northwest Baffin Island was that of Olson (1977) involving a total of 89 inclusions, mostly from sparry dolomite. A range of homogenization temperatures, from 50 to 300°C, was reported although inclusions from the Main Orebody grouped around 190 and 130°C. Individual samples in Olson's (1977) study were characterized by a range in homogenization temperature of as much as 150°C, possibly due to the accidental use of secondary inclusions in the study. Limited inclusion work by Jalonen (1982) reported in Olson (1984) indicated a narrower range of homogenization temperature for the Main Orebody of 170 - 240°C.

The most intensive study of fluid inclusions at Nanisivik to date is that of McNaughton (1983), who reported homogenization temperatures from approximately 200 inclusions and information on freezing behavior from about 160 of those. Inclusions were from sphalerite and sparry dolomite and were considered by McNaughton (1983) to be mainly primary, although it is likely that some of the sphalerite inclusions were actually pseudo-secondary. Due to the low estimated pressure of ore formation, the homogenization data presented was not corrected for pressure.

McNaughton's (1983) data for the Main Orebody may be differentiated on the basis of host mineralogy and position

within the orebody. Data from sparry dolomite was mainly
from the Lower Lens and represented a single population
approximately centered at 180°C (Figure 1.19). Homogeniza-
tion temperatures from sphalerite were primarily from the
Upper Lens and indicated two main temperature groupings, one
centered at 115° and the other at 170°C (Figure 1.19).
McNaughton (1983) estimated salinities to range from 20 to 40
wt.% $CaCl_2$ eq. on the basis of the final melting temperature
of ice and eutectic melting points. Inclusions in dolomite
contained about 33 wt.% $CaCl_2$ eq. while inclusions in
sphalerite typically contained approximately 24 wt.% $CaCl_2$ eq.
(Figure 1.20). Eutectic melting temperatures ranged from -30
to -60°C reflecting the dominance of cations other than $Na+$
in the fluids.

Although McNaughton's (1983) sampling was done prior
to the delineation of mine units by Curtis (1984), it is
believed that samples along the length of the Upper Lens are
from a fairly constant horizon (Ron Sutherland, pers.comm.,
1984). McNaughton (1983) reported that the homogenization
temperature and salinity of inclusions decreased towards the
west-central portion of the Upper Lens. Re-evaluation of
these trends on the basis of mineralogy indicates that this
trend of decreasing homogenization temperature and salinity
is relfected in both sphalerite and dolomite. However, the
salinity trend is poorly developed in sphalerite and the
overall decrease towards the west-central portion of the
Upper Lens is largely due to the measurement of very saline
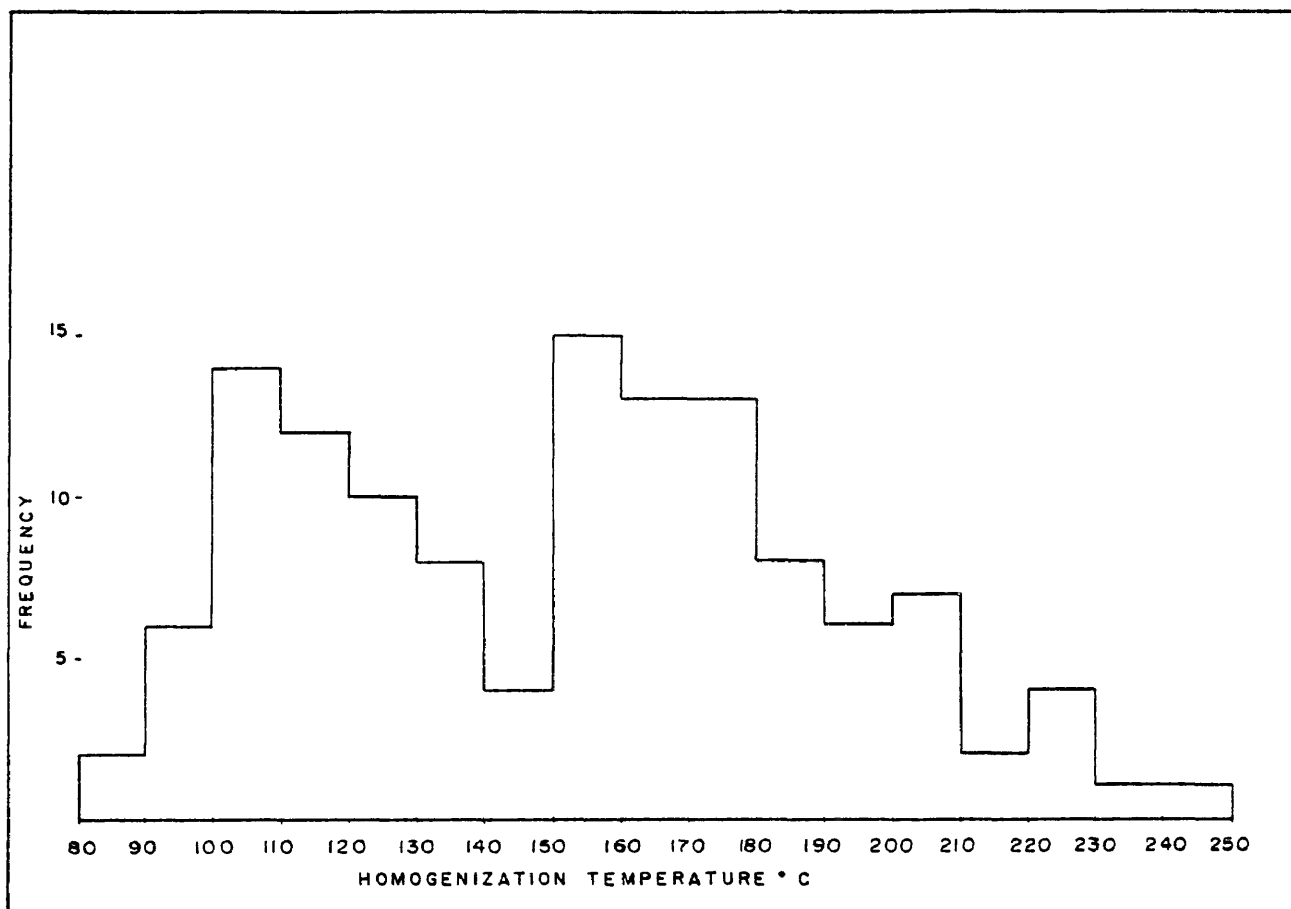
FIGURE I.19a-SUMMARY OF SPHALERITE INCLUSION TEMPERATURE
DATA FROM McNAUGHTON (1983).
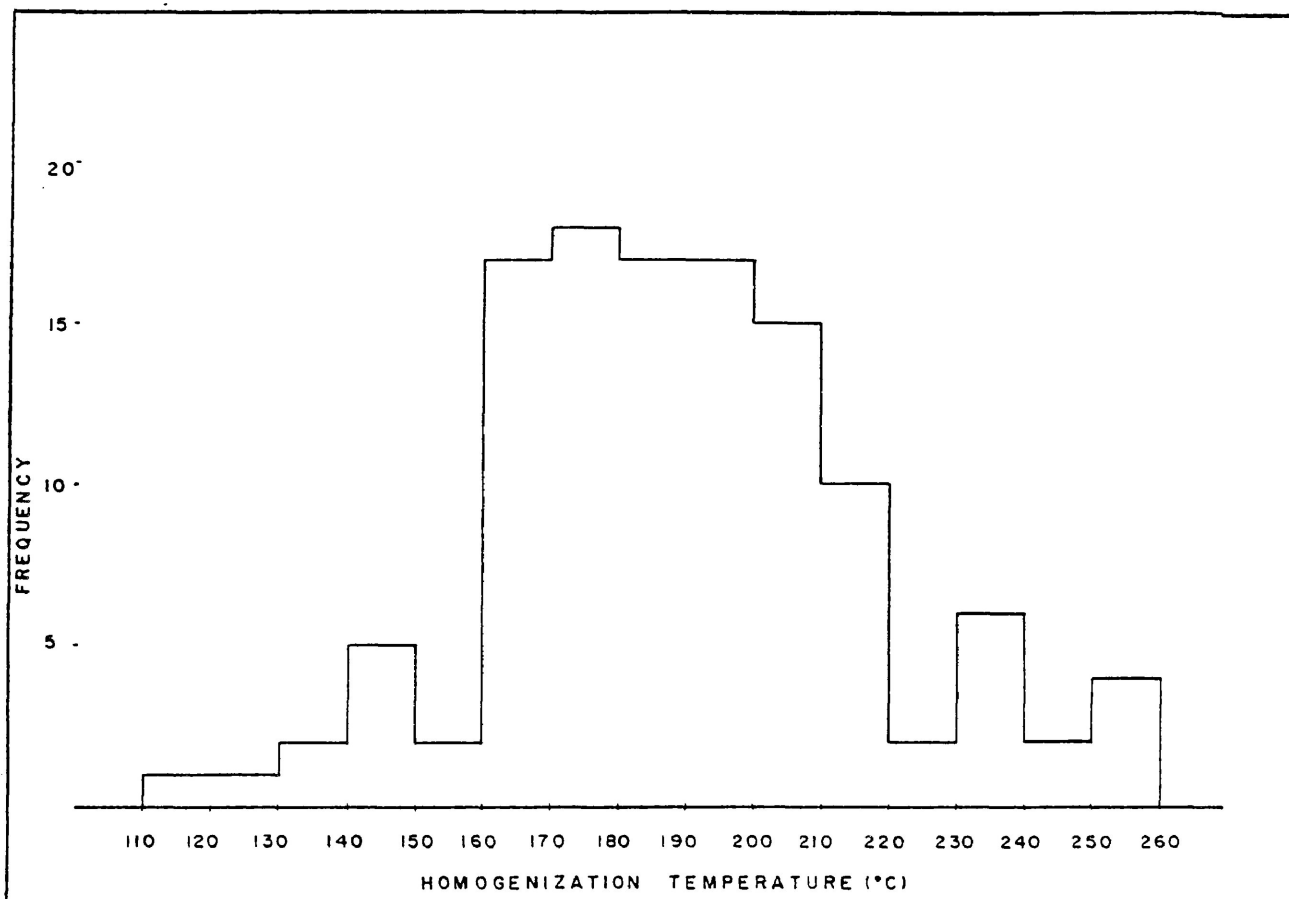
FIGURE I.19b- SUMMARY OF DOLOMITE INCLUSION TEMPERATURE
DATA FROM McNAUGHTON (1983).

31.
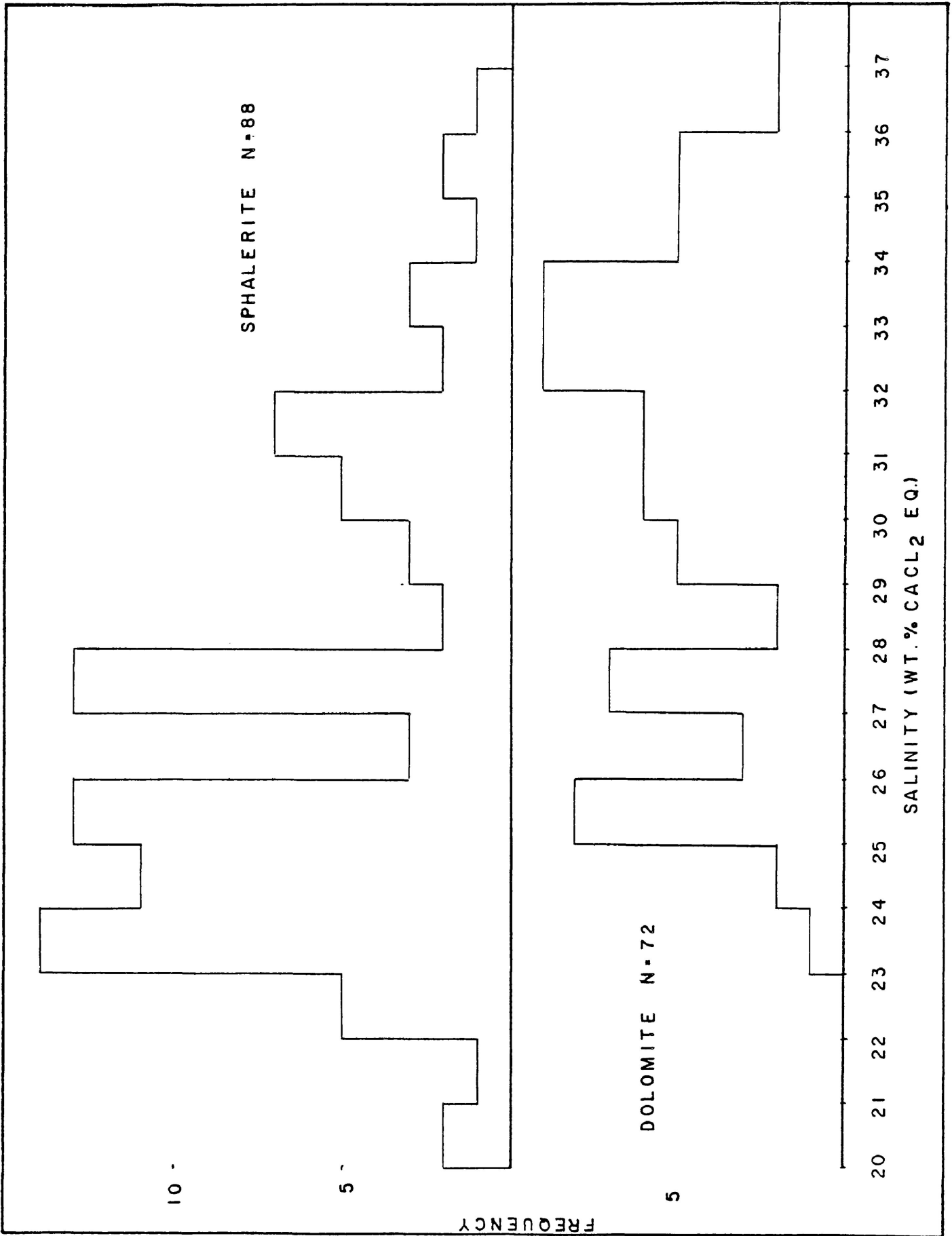
FIGURE 1.20-SALINITY DATA OBTAINED BY McNAUGHTON (1983) FOR THE MAIN OREBODY.

inclusions from dolomite in the extreme eastern portion of
the Upper Lens. McNaughton (1983) also reported an increase
in homogenization temperature and salinity with depth through
the Keel Zone and Lower Lens. Examination of the data
indicates that inclusions from sphalerite alone reflect this
trend.

A limited amount of fluid inclusion work was reported
by D. Bending in Curtis (1984). Bending reported that
inclusions from sparry dolomite associated with generally
barren satellite sulfide bodies homogenized near 100°C, with
the exclusion of inclusions from Area 14 - west, which homo-
genized at a mean temperature of 142°C. An examination of
inclusions immediately adjacent to the gabbro dike cutting
the orebody indicated that large inclusions within several
meters of the dike had decrepitated, while smaller inclusions
had developed a negative crystal habit and homogenized in the
temperature range 200 - 300°C. In a hand sample of repeti-
tively banded sphalerite and sparry dolomite ore, Bending
(1984) reported a regular variation in temperature and salin-
ity between the two minerals. In going from a sphalerite
band containing primary and pseudo-secondary inclusions to
sparry dolomite containing primary inclusions, a drop in homo-
genization temperature and salinity was observed. Inclusions
within a particular host mineral from a single hand sample
sometimes homogenized over a range of as much as 60°C.
Unusual freezing behavior during the course of inclusion
experiments was attributed to the possible presence of

CH_4 and H_2S within inclusions (Bending, 1984).

Sulfur Isotopes

Olson (1977, 1984) analyzed sulfides from Nanisivik, the nearby Hawker Creek showing and from minor fissure-fill occurrences. Values of $\delta^{34}S$ from pyrite ranged from 25.2 to 28.2% with the lowest value occurring in a marcasite-pyrite stalactite. Fractionation between co-existing sphalerite and galena indicated temperatures of 180 to 195°C which were in good agreement with inclusion homogenization temperatures obtained in the same study. Pyrite-galena pairs gave temperatures ranging from 210 to 245°C. Bedded gypsum from the Society Cliffs Formation east of Milne Inlet gave an average $\delta^{34}S$ composition of 23.7% while minor gypsum associated with sulfides in the Nanisivik area yielded values slightly greater than 26%.

Primary sulfur isotope results of pyrite from various satellite sulfide bodies in the Nanisivik area were reported by D. Sangster in Curtis (1984). The data were similar to Olson's (1984), although pyrite from the Main Orebody appeared to be slightly heavier than pyrite from the barren sulfide bodies. Pyrite from the South Boundary zone, the Raven Claims and from a single sample of Lower Lens mineralization from the Main Orebody gave anomalously low $\delta^{34}S$ values. Diagenetic pyrite from the Victor Bay Formation had a heavy sulfur isotopic composition similar to that obtained from sulfides in the Nanisivik area.

The heavy nature of sulfur from the Main Orebody has

also been confirmed by the work of Ghazban (1984) at McMaster University who reported a range of $\delta^{34}S$ composition from +23 to +32‰. Pyrite samples from the Main Orebody varied from +26.68 to +31.2‰. Three samples of pyrite from the Arctic Bay Formation gave very negative $\delta^{34}S$ values while six fracture-fill occurrences of evaporite gave values from +30.2 to +36.2‰.

Organic Material

Very little work has been done on organics at Nanisivik to date, although Olson (1977) reported the presence of the asphaltic bitumen Albertite in Nanisivik ore. In a study of bitumen from Society cliffs dolostone, Gize and Rimmer (1984) discussed the thermal effects of dike emplacement. Curtis (1984) described a "salt and pepper" texture resulting from the recrystallization of dolomite in Society Cliffs Formation, which was reported to exude a petroliferous odor when freshly broken (Olson, 1977). In a recent study of organic and related volatiles in Society Cliffs dolostone, Thiede (1984) concluded that hydrocarbons, sulfur gases and organo-halide compounds formed anomalies up to several hundred meters away from mineralization.

Ore Genesis

There is general agreement among most recent investigators of ore formation at Nanisivik concerning the nature of the ore fluid. The ore fluid is considered to have been a warm, very saline brine derived from basinal dewatering (Olson, 1977, 1984; McNaughton, 1983). Flow of the ore fluid

is believed to have been channelled by karstic features (Olson, 1977, 1984; Clayton and Thorpe, 1982) and by faults (Curtis, 1984). Most recent workers also agree that the ore fluid was reduced at the site of ore deposition upon contact with hydrocarbons (Olson, 1984; Curtis, 1984).

In the most comprehensive analysis of ore genesis at Nanisivik to date, Olson (1984) evaluated ore formation on the basis of fluid inclusions, stable isotopes and mineral equilibria. The pH of the ore fluid was restricted to values near neutrality by the stability of dolomite. Oxygen activities were constrained by carbon and oxygen isotopes and were considered to have decreased during ore deposition. On the basis of sulfur isotopes, the ore fluid was interpreted to have had a $\delta^{34}S$ composition of +28.0% with H_2S as the dominant sulfur species. Olson (1984) evaluated the possible causes of sulfide deposition and concluded that neither temperature, dilution nor pH changes played a significant role, while changes in reduced sulfur and metal chloride activities were considered to be of prime importance.

Olson (1977, 1984) and Clayton and Thorpe (1982) stressed the role of karstic features in the localization of mineralization and considered the sulfide bodies to have filled pre-existing caverns. However, Ford (1981) and Curtis (1984) contended that most of the ore body volume had been created by the ore fluid itself, although it is quite likely that the ore fluid was initially channelled by karstic features. Ford (1981) proposed a meteoric ore fluid to

explain the configuration of the Main Orebody and McNaughton (1983) suggested the mixing of two distinct fluids to explain observed temperature and salinity trends. However, on the basis of stable isotope work, Olson (1984) concluded that meteoric water had little effect on ore deposition.

1.5 Statement of Problem

The purpose of this investigation is to study the physical and chemical parameters responsible for the various mine units described by Curtis (1984). Fluid inclusion homogenization temperatures should reflect variations in the temperature of the ore fluid. The sulfur isotopic composition of pyrite from the various mine units should reflect changes in temperature, dominant sulfur species and source of the ore fluid. The distribution of marcasite and wurtzite should place constraints on the nature of the ore fluid given information concerning the stabilities of these minerals. Limits may also be placed on sulfur and oxygen activities by the iron content of sphalerite co-existing with iron sulfides. Given the amount of wall rock replacement which is believed to have occurred, and the high organic content of Society Cliffs dolostone, hydrocarbons associated with both mineralization and wall rock will be compared to investigate the possible role of wall rock organics in sulfate reduction. Additional fluid inclusion work will be done to confirm temperature trends indicated by McNaughton (1983) for the

Main Orebody and by Bending (1984) for the satellite sulfide bodies. A better understanding of the physical and chemical factors responsible for mineral zonation should place constraints on possible theories of ore genesis.

CHAPTER 2 : DETAILED DESCRIPTION OF MINERALOGY

2.1   Introduction

During the course of this study, nearly 100 doubly polished thick sections were examined in reflected and transmitted light to provide a paragenetic control for fluid inclusion, mineralogic and isotopic investigations. On the microscopic and hand sample scale, the paragenetic sequence is usually quite simple, consisting of early sphalerite followed by pyrite and galena, and finally by sparry dolomite. However, variations of this simple paragenesis do occur.

Sample locations are shown in Figure 2.1 for the Main Orebody and Figure 2.2 for the Area 14 Orebody. The numbering system commonly used at the mine has been retained for the present study. The first number refers to a particular crosscut and the second to a drift. Bold letters refer to the orientation of the working face. The letters "cc" refer to a sample location along a crosscut. A final number or lower case letter refers to individual samples taken at each sampling location. For example, sample 37-11 E #2 refers to the second sample taken along an east face exposed near the intersection of crosscut 37 and drift 11. Sampling was concentrated in the eastern and central portions of the mine where the mine units described by Curtis (1984) are best developed. Accordingly, most samples are from locations

39.

FIGURE 2.1

NANISIVIK MAIN OREBODY - PLAN VIEW OF MINE DEVELOPMENT AS OF MAY, 1984

SAMPLE LOCATIONS INDICATED.
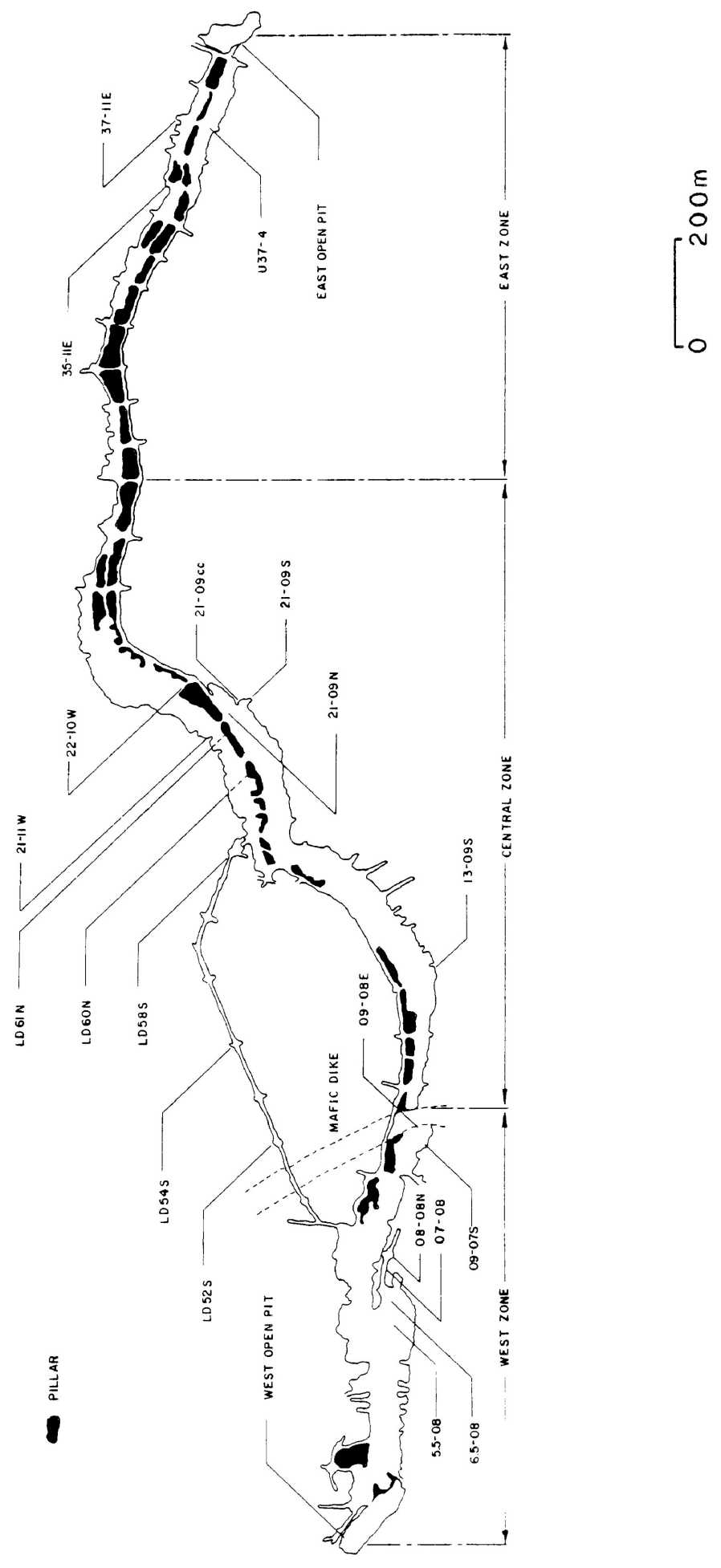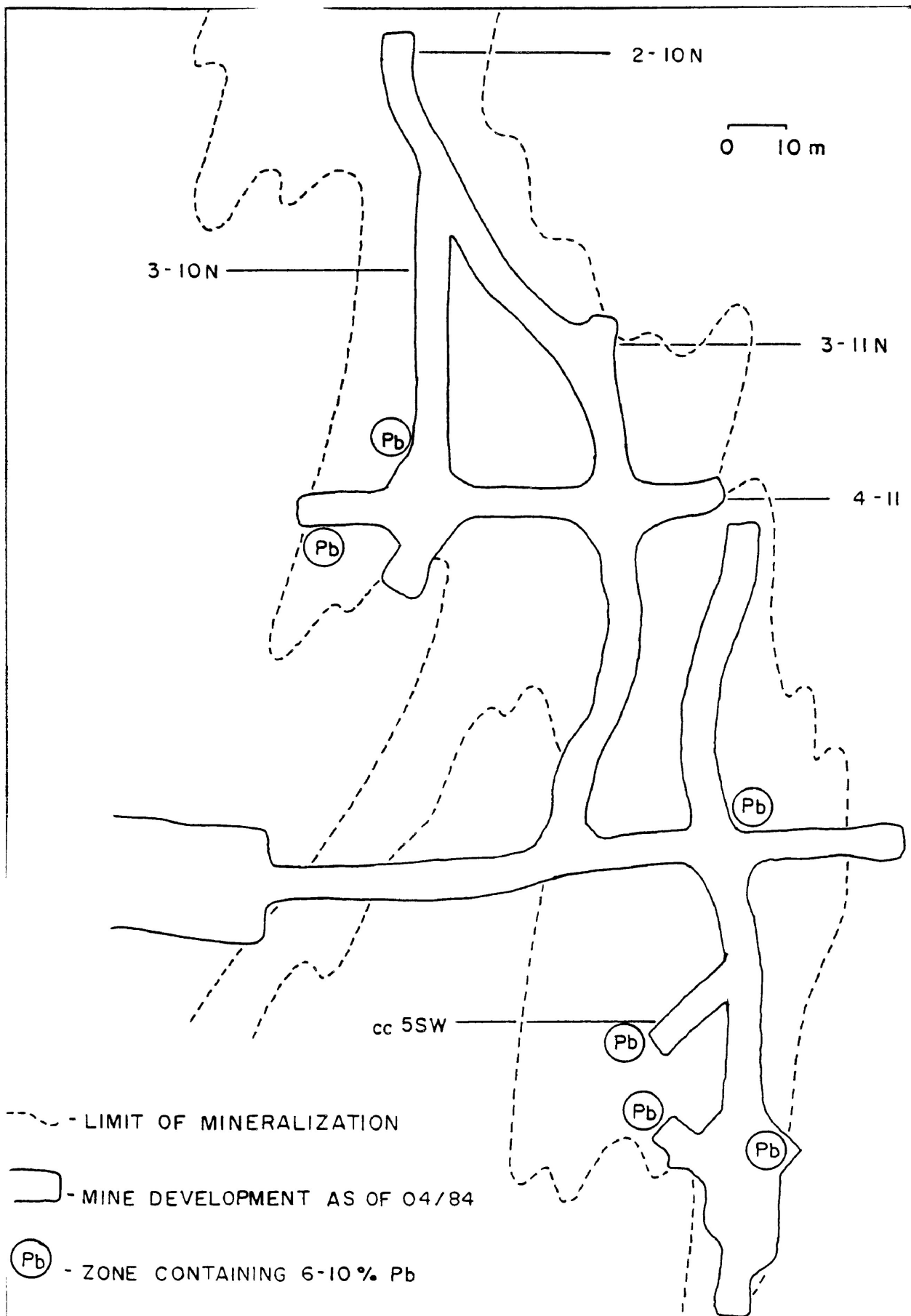
FIGURE 2.2 - AREA 14 OREBODY, PLAN VIEW WITH SAMPLE LOCATIONS (COURTESY OF NANISIVIK MINE STAFF).

13-09 S, 21-09 S, 21-09 cc, 35-11 E and 37-11 E. Detailed
sample location maps are given for each of these main
sampling locations in Figures 2.4 to 2.7 with the exception
of 21-09 cc. A legend describing the units is given in
Figure 2.3.

2.2   Description of Ore Zones

Upper Lens - Eastern and Central Portions

As previously discussed, the ore units described by
Curtis (1984) are best developed in these portions of the
Main Orebody and, therefore, much of the description to
follow will concentrate on these zones. Where all three main
sulfide minerals are found together, sphalerite is typically
early, followed by pyrite having a variety of crystal habits
(Figures 2.8, 2.9). Galena often occurs intergrown with
pyrite or as irregular masses cutting earlier sulfides
(Figure 2.10). White, sparry dolomite occurs as interstitial
filling between sulfides, as interbanding with sulfides, or
as late veins and open space fillings.

Sphalerite generally occurs as coarse, euhedral to
subhedral crystals up to one centimeter across, either as
massive crystal aggregates or as distinct bands. Under trans-
mitted light, thick sections of sphalerite display colour
zoning, which typically varies from dark red in crystal
centers, through orange and yellow to colourless along
crystal rims (Figure 2.11). Colour zoning may also involve

Pyrite breccia

Massive pyrite band

Massive pyrite

Banded sphalerite

Banded dolomite and coarsely bladed iron sulfide

Ice filled vugs

White, sparry dolomite (D_3)

Selvage ore

Banded pyrite and dolomite

Banded sphalerite and pyrite $\pm$ dolomite

Disseminated sphalerite

Pyrite and dolomite replacing dolostone

Society Cliffs dolostone

Textural Types	Mineralogy	Other
1 - Banded	S- Sphalerite	B- Brecciated
2 - Massive	P- Pyrite	◯- Sample
3 - Chaotic	D- Dolomite	Location
4 - Disseminated	G- Galena	
5 - Selvage		

FIGURE 2.3- LEGEND FOR SAMPLE LOCATION SKETCHES (AFTER CURTIS, 1984).
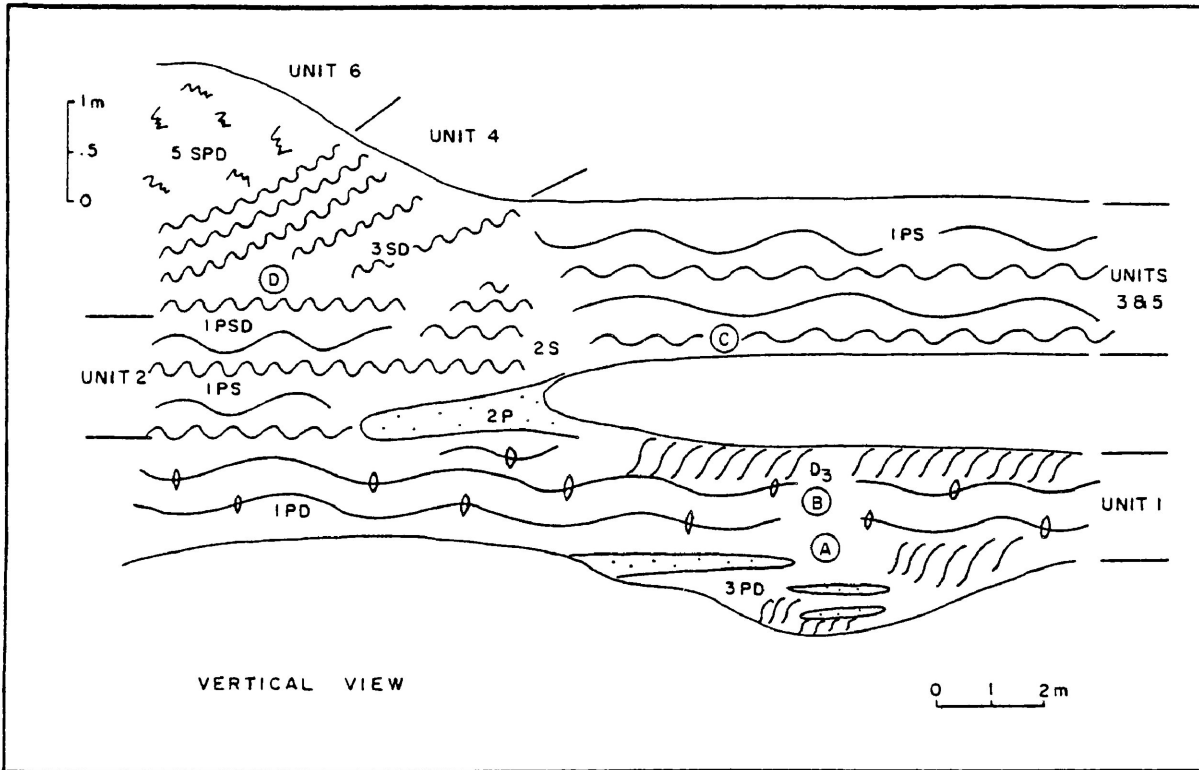
FIGURE 2.4 - SAMPLING LOCATION 13.- 09 S.
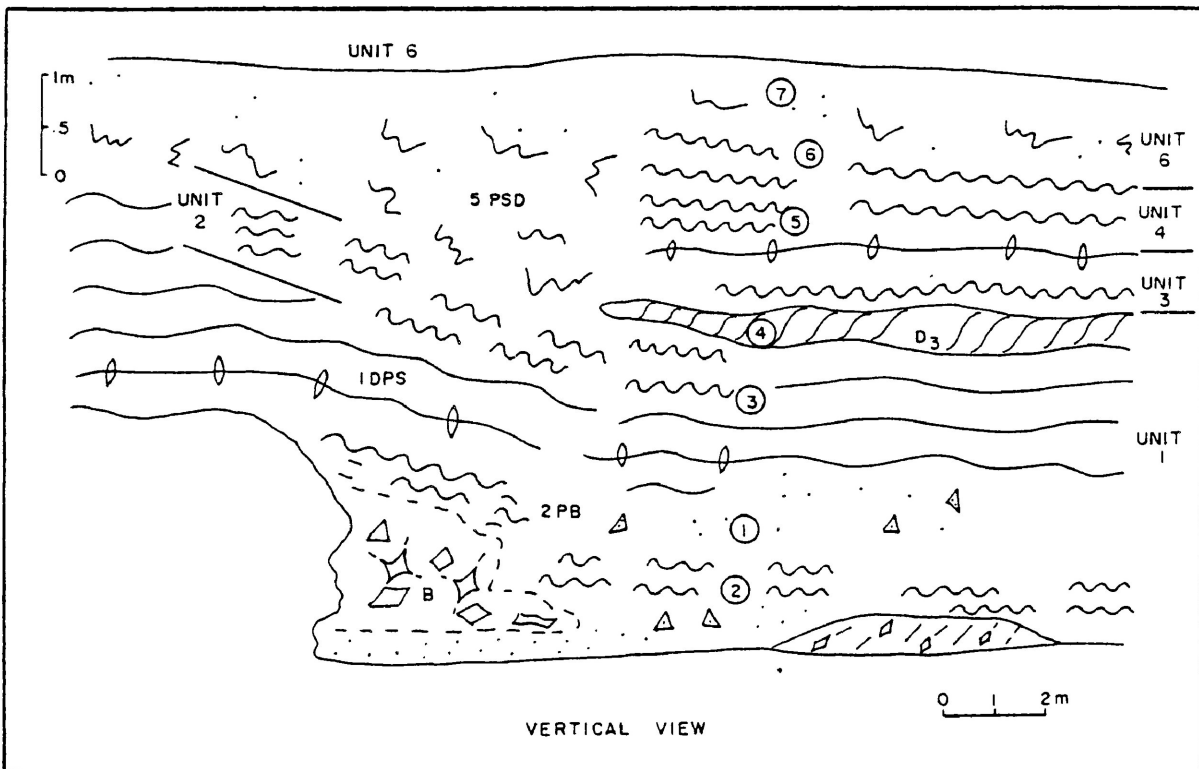
FIGURE 2.5 - SAMPLING LOCATION 21-09S
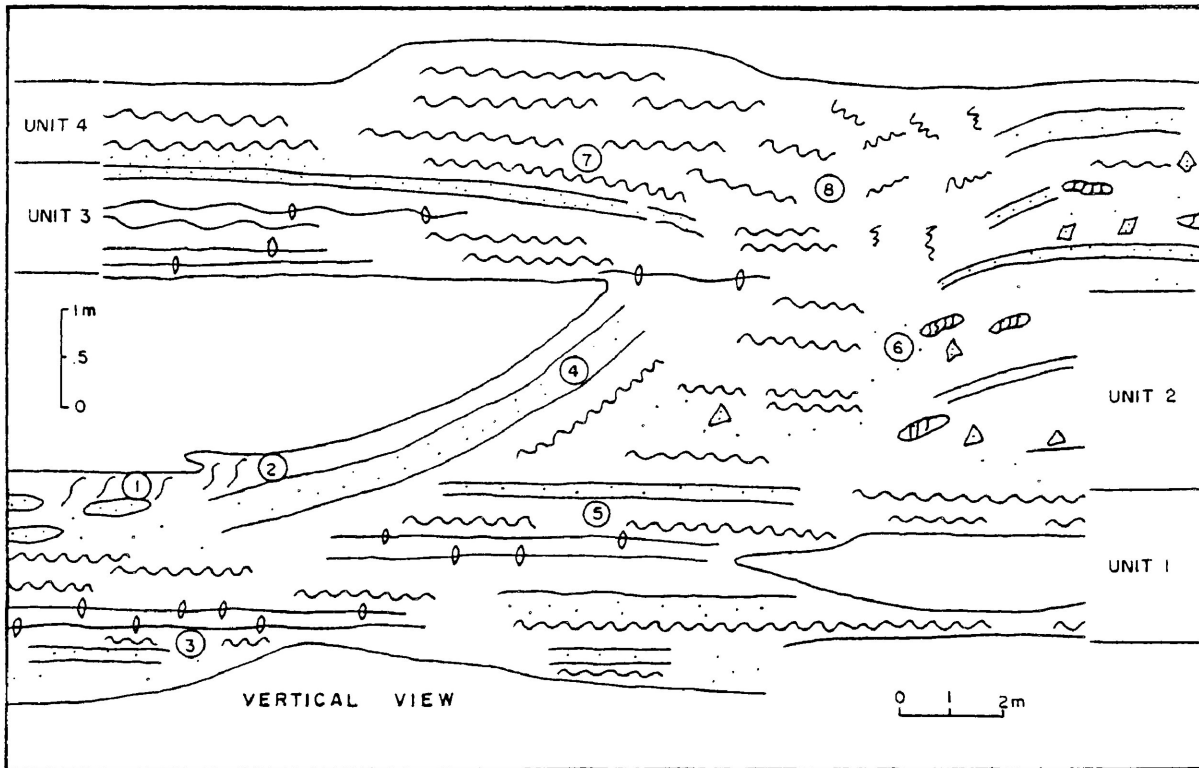
FIGURE 2.6 - SAMPLE LOCATION 37-IIE
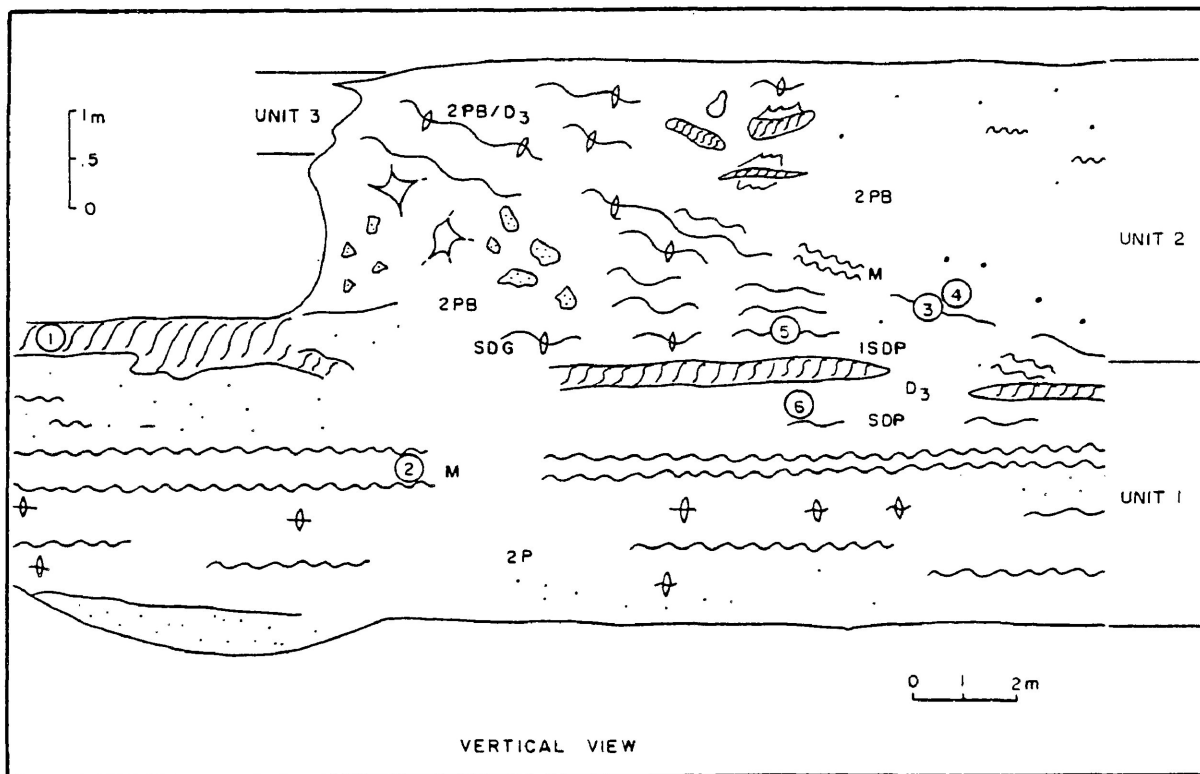
FIGURE 2.7 - SAMPLING LOCATION 35-IIE
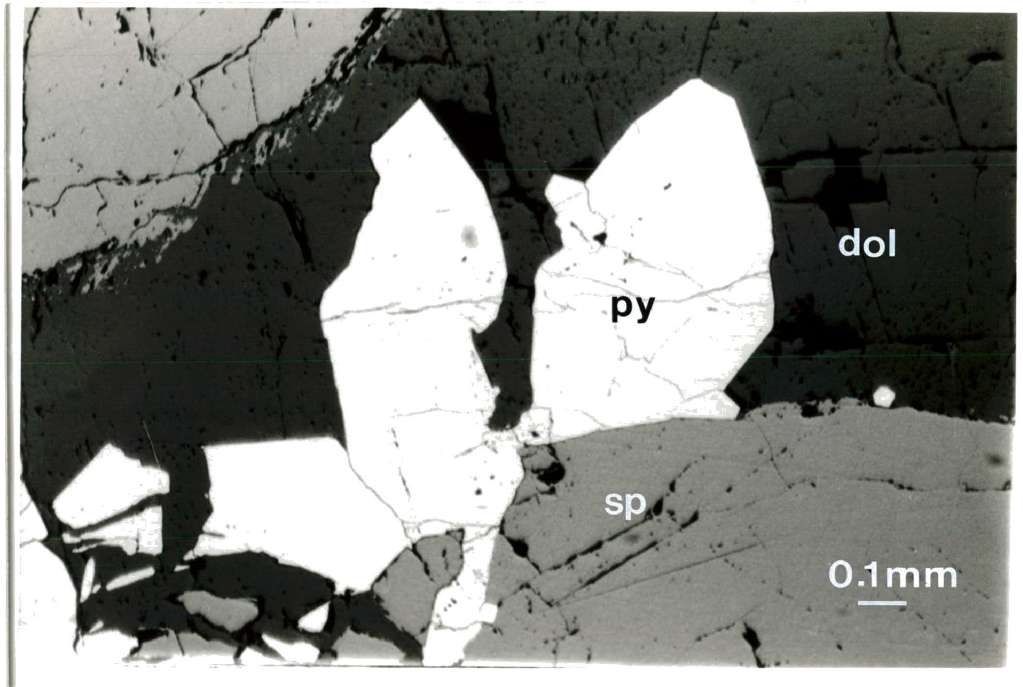
FIGURE 2.8 – REFLECTED LIGHT PHOTOMICROGRAPH OF BLADED
PYRITE CRYSTALS PROJECTING FROM A SPHALERITE CRYSTAL.
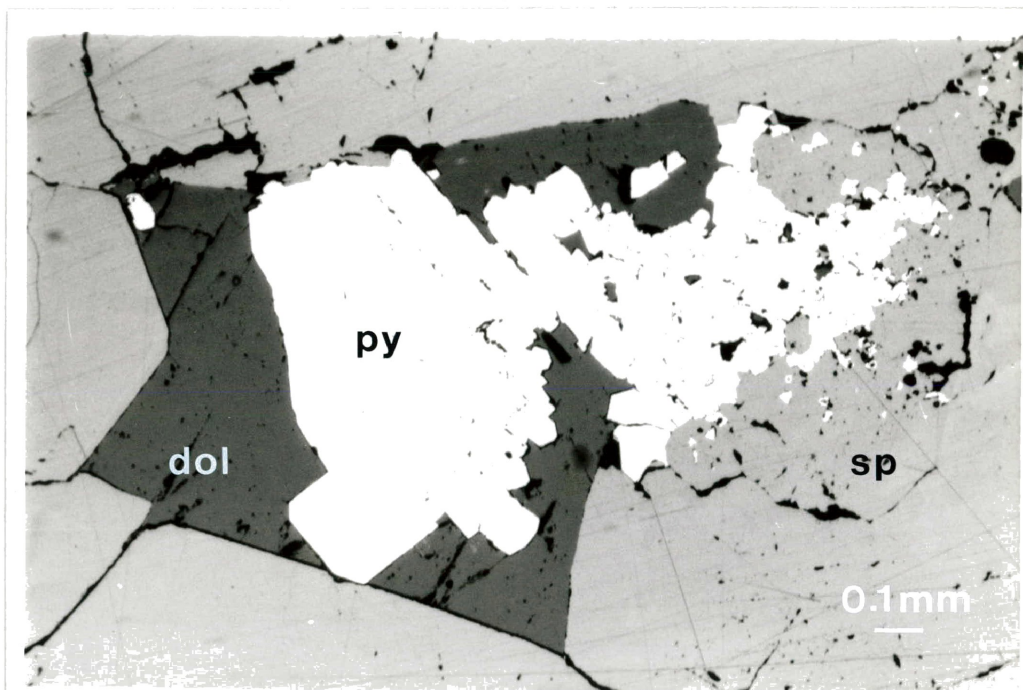
FIGURE 2.9 – REFLECTED LIGHT PHOTOMICROGRAPH OF CUBIC
PYRITE INTERSTITIAL TO SPHALERITE.
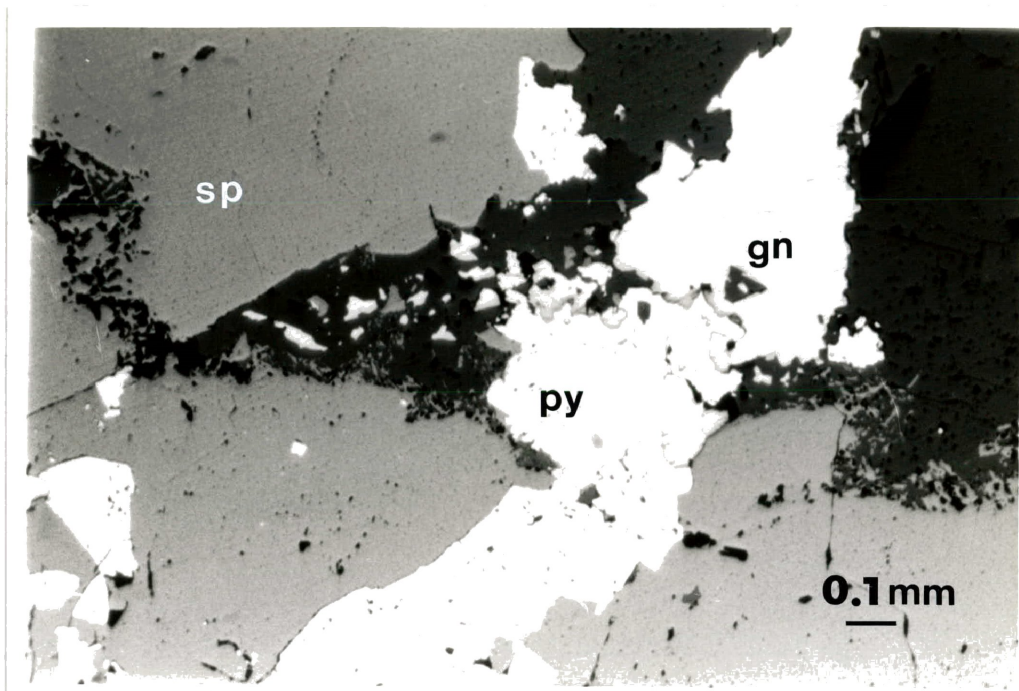
FIGURE 2.10 - REFLECTED LIGHT PHOTOMICROGRAPH SHOWING PYRITE AND GALENA INTERSTITIAL TO SPHALERITE.
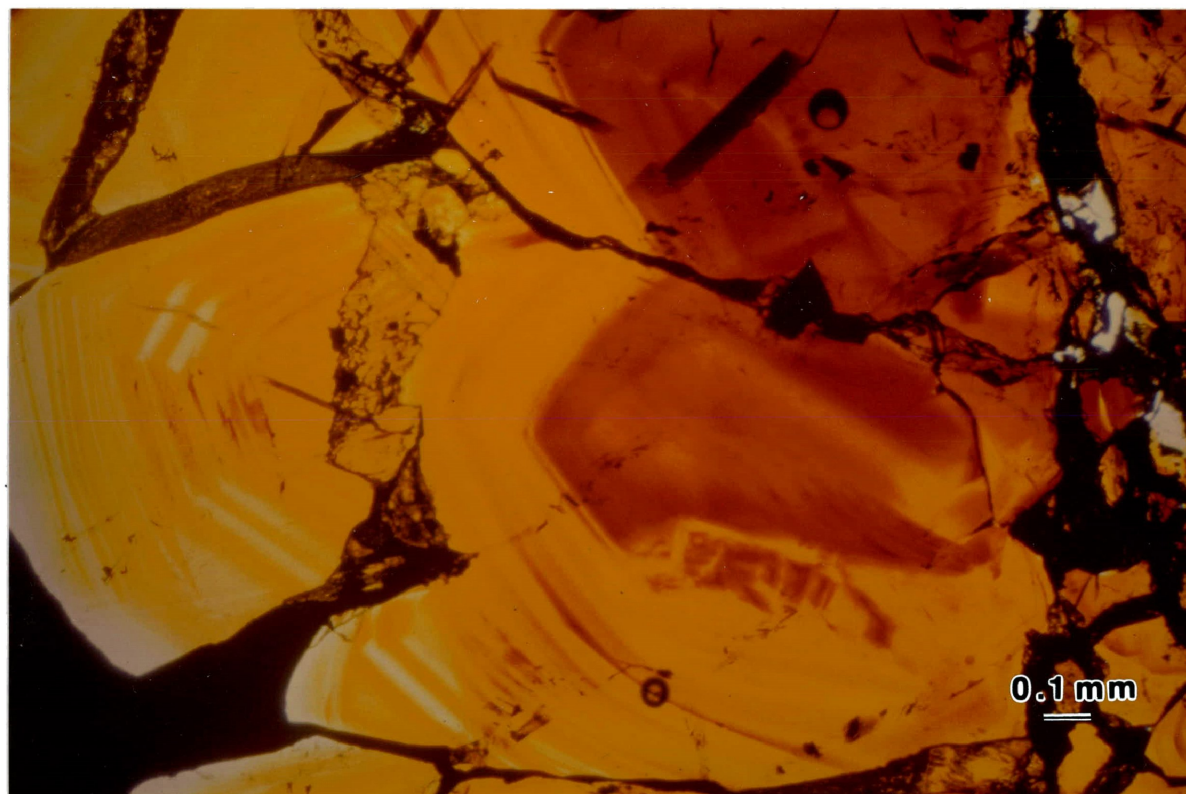
FIGURE 2.11 - TRANSMITTED LIGHT PHOTOMICROGRAPH OF COLOR ZONING IN SPHALERITE.

the repetition of two or more colours or may not be developed
at all. In Units 1, 3, 5 and 6, fibrous, pale coloured
sphalerite occasionally rims sphalerite crystals, particular-
ly where they appear to have grown into open space. Late
fibrous sphalerite also occurs in fine veinlets. Under ultra-
violet illumination this late sphalerite fluoresces orange-
red (Figure 2.12). Locally, a spectacular polysynthetic twin-
ning is developed in some sphalerite crystals (Figure 2.13).

Sphalerite is often anisotropic, although this effect
is usually masked by colouration. Anisotropy is best dis-
played in colourless sphalerite rims (Figure 2.14) and local-
ly anisotropic domains may be seen to crosscut colour zoning.
Anisotropic domains are commonly birefringent and may give a
positive uniaxial figure under conoscopic light. The bire-
fringence usually varies across anisotropic domains with
bands of different interference colour typically parallel to
the crystal boundary. Observations on a universal stage
suggest that maximum retardation occurs perpendicular to the
plane of the optic axis, which is in turn parallel to the
crystal boundary.

A bladed iron sulfide is characteristic of Units 1, 3
and 5. It occurs intergrown with sparry dolomite as crystals
up to several centimeters in length, which appear to have
grown outward from either side of a massive sulfide band.
Although the bladed crystal habit is suggestive of marcasite,
examination of polished sections indicates that the blades
consist of a porous, fine-grained crystalline mass of
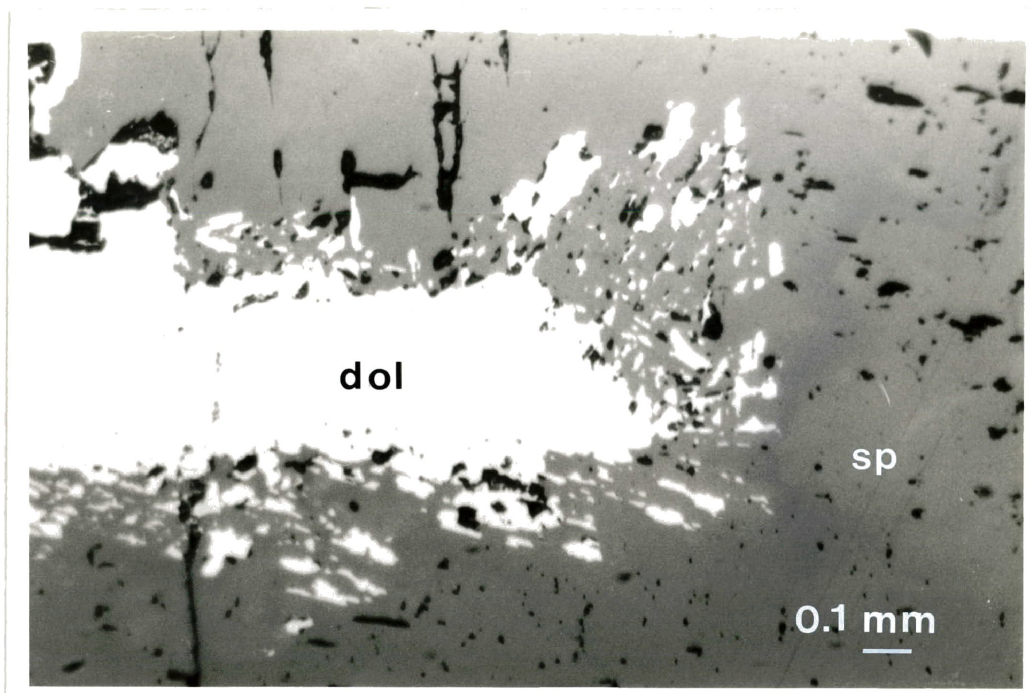
FIGURE 2.12 – REFLECTED LIGHT PHOTOMICROGRAPH OF A FLUORESCENT SPHALERITE – DOLOMITE INTERGROWTH.
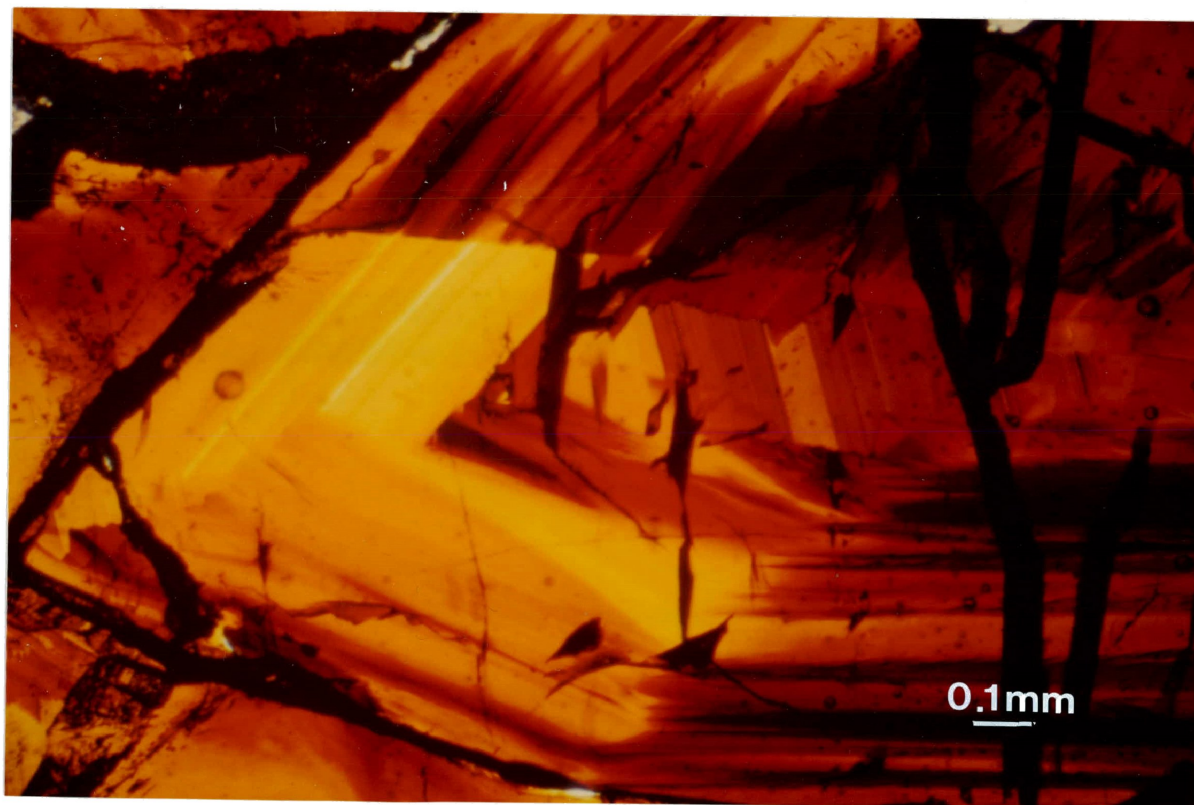
FIGURE 2.13 – TRANSMITTED LIGHT PHOTOMICROGRAPH OF A TWINNED SPHALERITE CRYSTAL.

anomalously anisotropic pyrite. Massive pyrite bands occa-
sionally contain large zoned crystals in which the zoning is
defined by a regular alignment of solid inclusions. Zoning
in pyrite is often suggestive of an earlier, bladed marcasite
habit (Figure 2.15).

The cloudy appearance of white, sparry dolomite is
due to the presence of abundant fluid and solid inclusions.
Sparry dolomite often exhibits undulose extinction, probably
due to distortion of the crystal lattice during growth, and
is triboluminescent. Ore stage sparry dolomite exhibits
growth banding when viewed under cathodoluminescence (Dave
Bending, pers.comm., 1984). Staining with alizarine red and
Feigl's solution (Friedman, 1959) indicates that dolomite is
the only ore stage carbonate gangue mineral.

Upper Lens - Western Portion

From the small number of samples studied in the vici-
nity of crosscuts 5 and 6 (Figure 2.1), it appears that the
paragenetic sequence of the western Upper Lens is similar to
that of the eastern portion of the Upper Lens. Pyrite local-
ly exhibits both stubby and tabular crystal habits. The
latter is pale and strongly anisotropic. There is local
evidence of microbrecciation in pyrite prior to the
deposition of galena and dolomite. Colour zoning could not
be evaluated from the few sections studied. However, as no
fluorescence is observed, it is unlikely that late, clear
sphalerite was deposited.
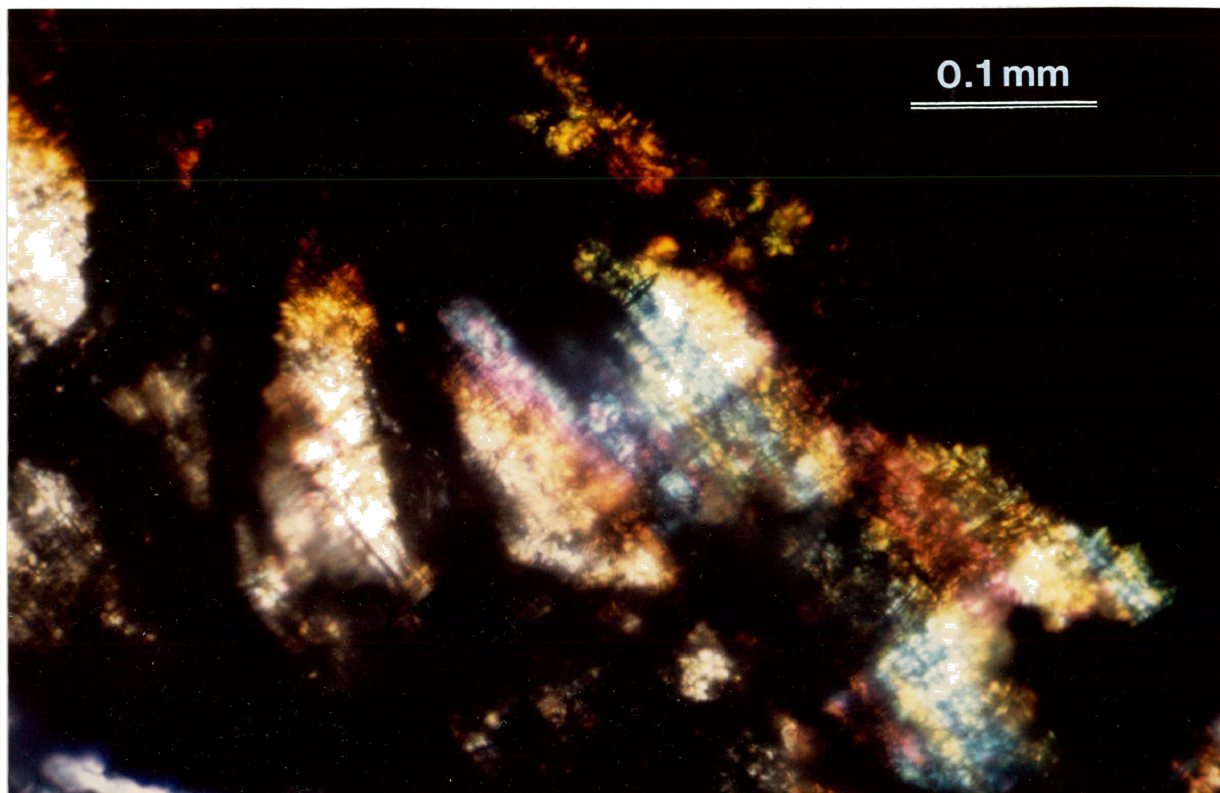
FIGURE 2.14 – TRANSMITTED LIGHT PHOTOMICROGRAPH OF AN ANISOTROPIC DOMAIN IN SPHALERITE UNDER CROSSED POLARIZED LIGHT.
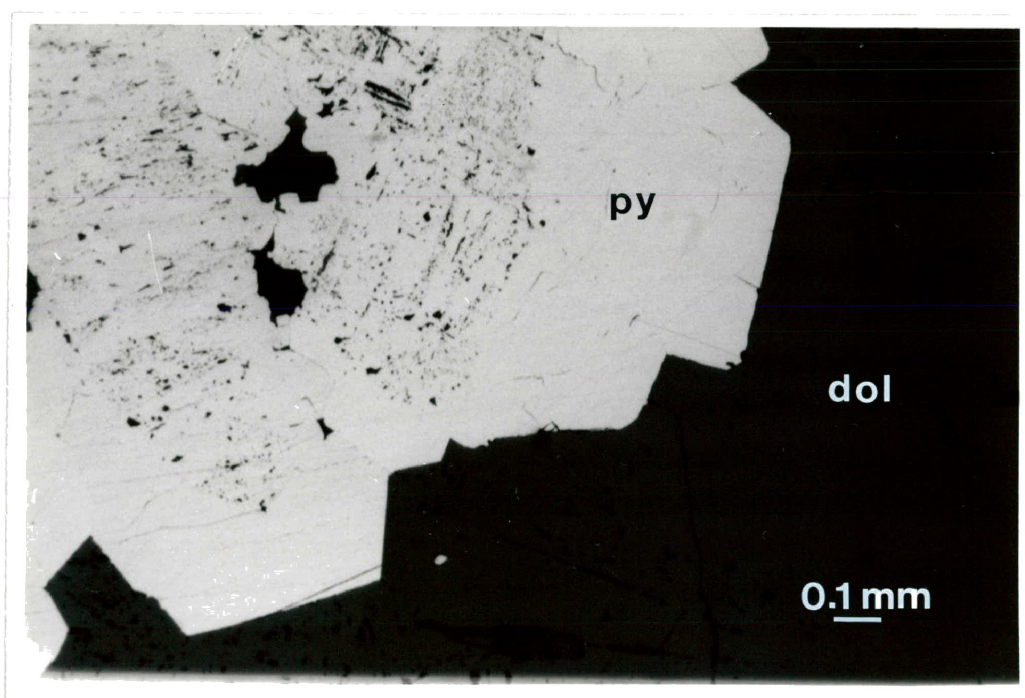
FIGURE 2.15 – REFLECTED LIGHT PHOTOMICROGRAPH OF RELICT MARCASITE HABIT DEFINED IN PYRITE.

Keel Zone

Study of two hand samples from the vicinity of pillar 19-11/01 indicates that Keel Zone mineralization consists of massive, vuggy, fine to medium grained pyrite enclosing less than 1% pyrrhotite. The pyrite is weakly anisotropic. Approximately 5% of the sample volume is open pore space. Pyrrhotite forms irregular microscopic inclusions approximately 0.025 mm across. Sphalerite is a minor component (<5%), either intergrown with pyrite or as late crystal euhedra in open vugs. The sphalerite is very dark making it unsuitable for fluid inclusion work.

Lower Lens

Examination of a number of samples from drill core and from the lower decline on the north side of the Upper Lens indicates that the paragenesis of the Lower Lens is slightly different from that of the Upper. An early generation of pyrite is strongly anisotropic and finely laminated, consisting of fine crystals less than 1 mm across, which are often surrounded by rectangular "laths" of pyrite (Figure 2.16). The early iron sulfide is disrupted by later sulfide mineralization, which is similar in paragenesis to that of the Upper Lens. Rhythmically banded ore occurs in a core sample of Lower Lens material from the eastern portion of the Main Orebody (U37/4). This rhythmically banded ore is well developed and consists of a central layer of sphalerite less than 0.25 mm across surrounded on either side by pyrite and then dolomite (Figure 2.17). Colour zoning in sphalerite
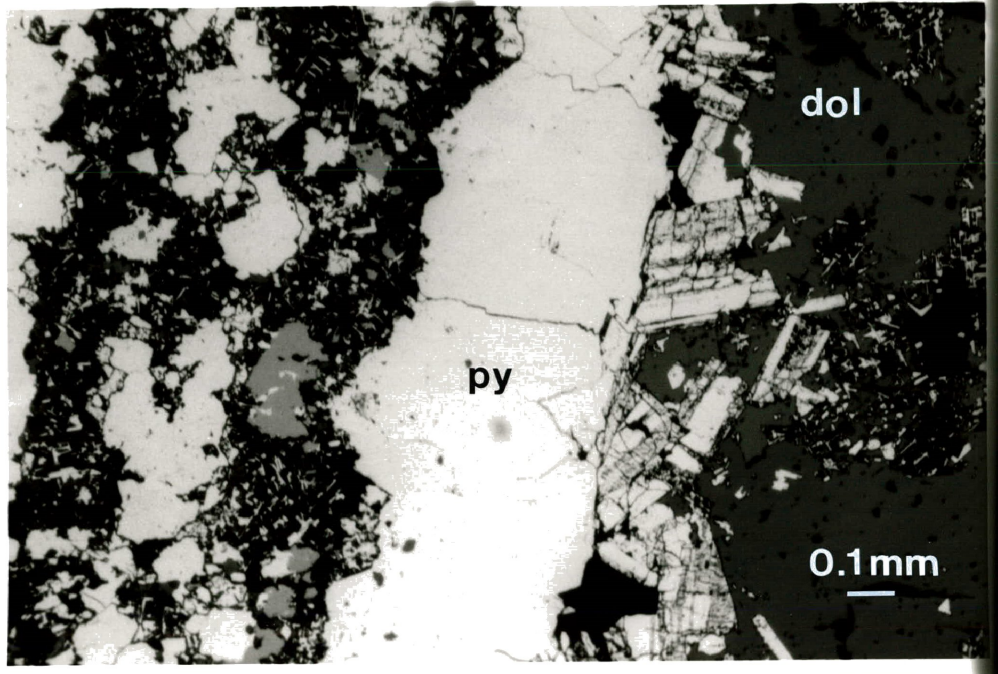
FIGURE 2.16 - REFLECTED LIGHT PHOTOMICROGRAPH OF EARLY
IRON SULFIDE FROM THE LOWER LENS OF THE MAIN OREBODY.
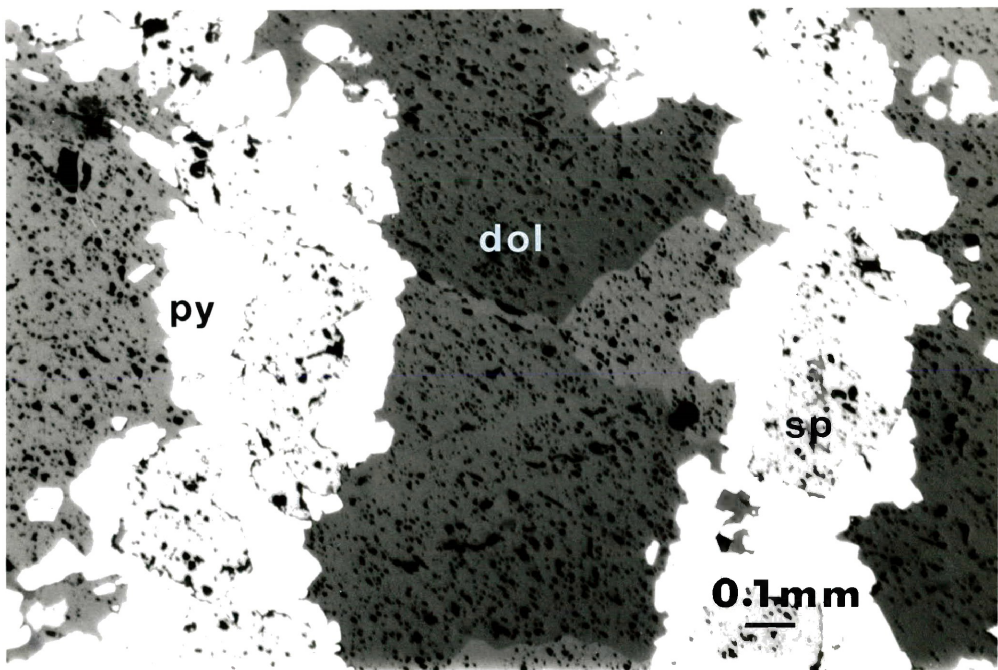
FIGURE 2.17 - REFLECTED LIGHT PHOTOMICROGRAPH OF RHYTHMIC
BANDING IN ORE FROM THE LOWER LENS OF THE MAIN OREBODY.

is not as well developed as it is in the Upper Lens, although different combinations of red, orange and yellow zones are present. Colourless, late sphalerite is not present, and fluorescence is rare. Occasionally, colour zoning varies from yellow in the centers of some crystals to dark red at the rim (Figure 2.18).

Shale Zone

Mineral paragenesis in the Shale Zone is more complex than elsewhere in the Main Orebody, although a basic sequence of mineralization similar to that observed in the eastern portion of the Upper Lens is present. This simple paragenesis has been disrupted by apparent remobilization. Pyrite crystals display yellow to white anisotropy and often share triple joint junctions suggestive of annealing. Sphalerite forms medium-grained red-brown masses, which are sometimes in sharp contact with a darker, coarser-grained variety. Colour zoning in sphalerite crystals is similar to that normally found in the Upper Lens, but has been disrupted by a late, colourless sphalerite that crosscuts earlier zoning (Figure 2.19). No fluorescence of sphalerite rims is present.

Area 14 Orebody

From the small number of samples studied, it appears that the paragenesis of Area 14 is somewhat different than that of the Main Orebody. In the central sphalerite band, an early, finely laminated generation of iron sulfide has been disrupted by late sphalerite, pyrite and dolomite, usually
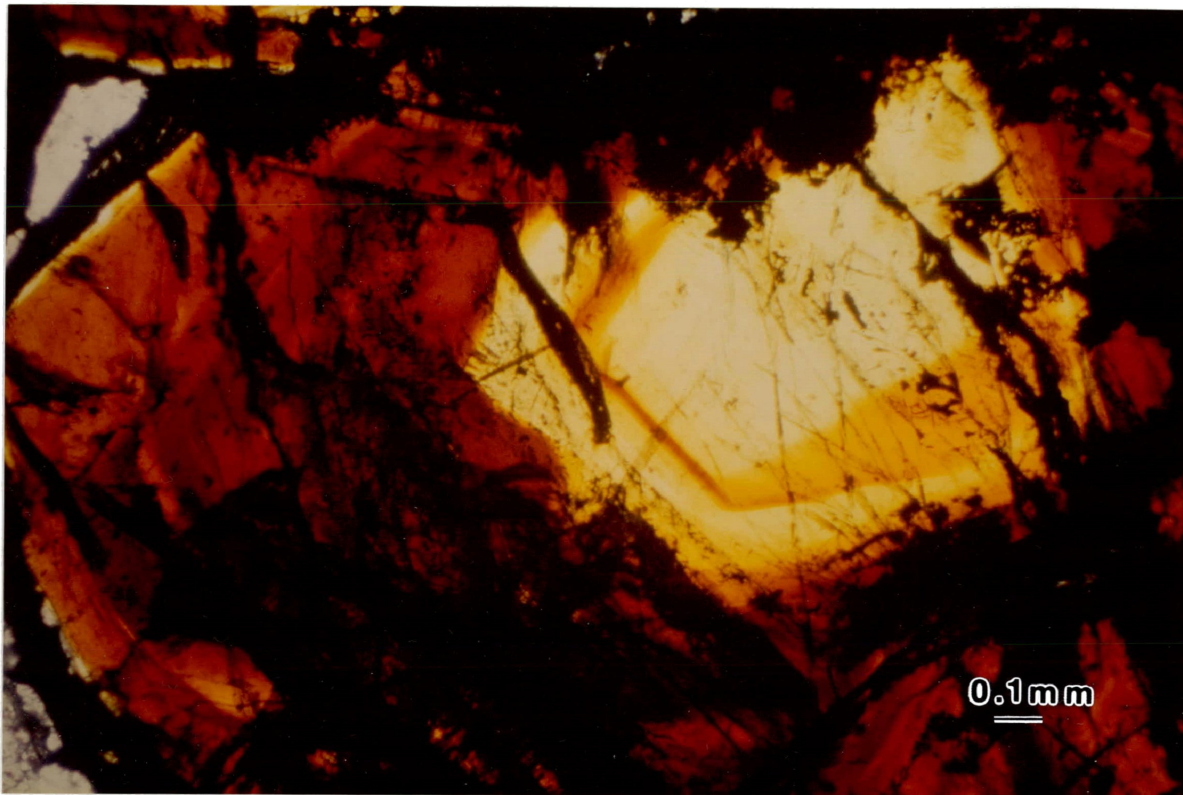
FIGURE 2.18 – TRANSMITTED LIGHT PHOTOMICROGRAPH OF "REVERSE" COLOR ZONING IN SPHALERITE FROM THE LOWER LENS.
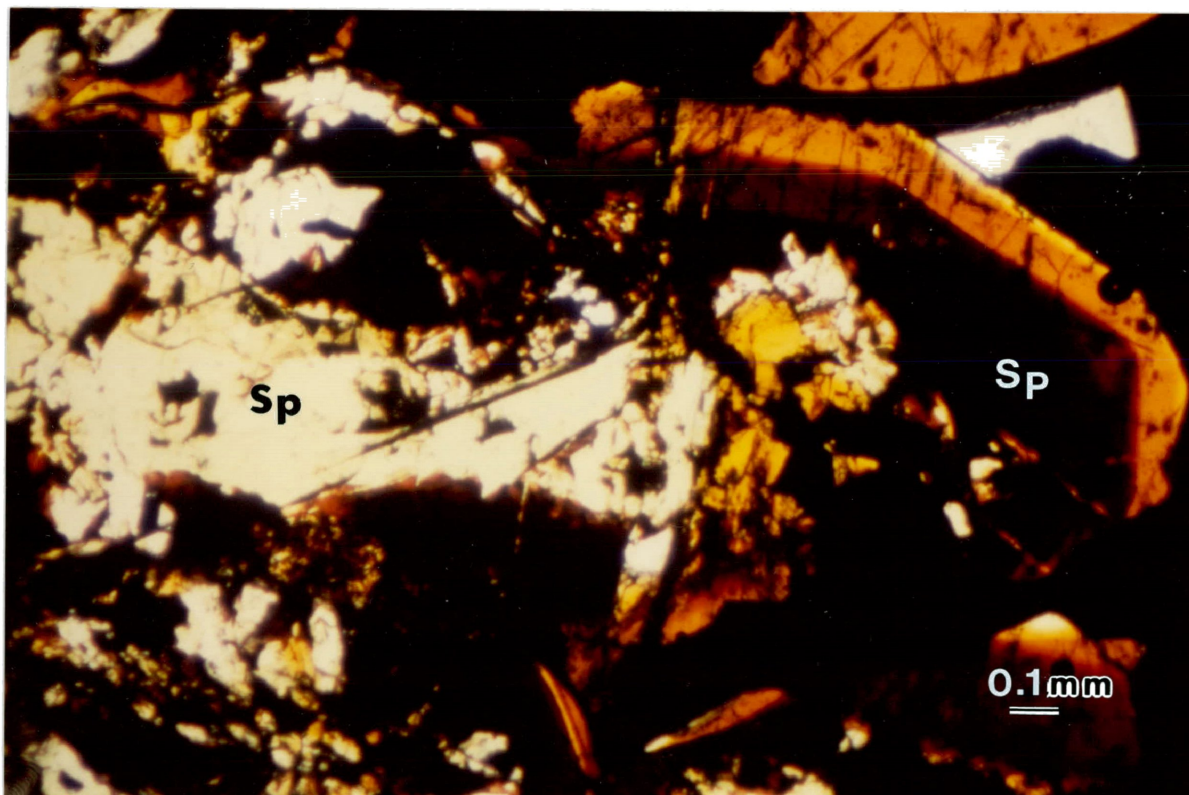
FIGURE 2.19 – TRANSMITTED LIGHT PHOTOMICROGRAPH OF LATE, CLEAR SPHALERITE FROM THE SHALE ZONE OF THE MAIN OREBODY.

deposited in that order (Figure 2.20). In the lower pyritic zone, tabular pyrite was the earliest sulfide deposited, followed by coeval sphalerite and pyrite. As in the case of the Main Orebody, white, sparry dolomite was typically the last mineral to form. Spectacular colour zoning in sphalerite similar to that observed in the eastern portion of the Upper Lens occurs, although locally this has been disrupted by a late, colourless sphalerite. Fluorescence is rare in this material.

2.3 Distribution of Sulfide Minerals

Relative sulfide mineral abundances and sulfide to sparry dolomite ratios have been calculated from the estimated proportions of minerals in hand samples. Calculations are based on a small sampling of ore that was biased towards material suitable for fluid inclusion studies. Despite these sampling problems, the calculated ratios are considered to reflect general trends. All calculated ratios are recorded in Table 2.1, along with average ore compositions.

The eastern and central portions of the Upper Lens, along with the Lower Lens, may be distinguished from the Shale Zone, western portion of the Upper Lens and the Area 14 Orebody in having a generally greater proportion of sparry dolomite gangue. Within the eastern and central portions of the Upper Lens the individual ore units described by Curtis
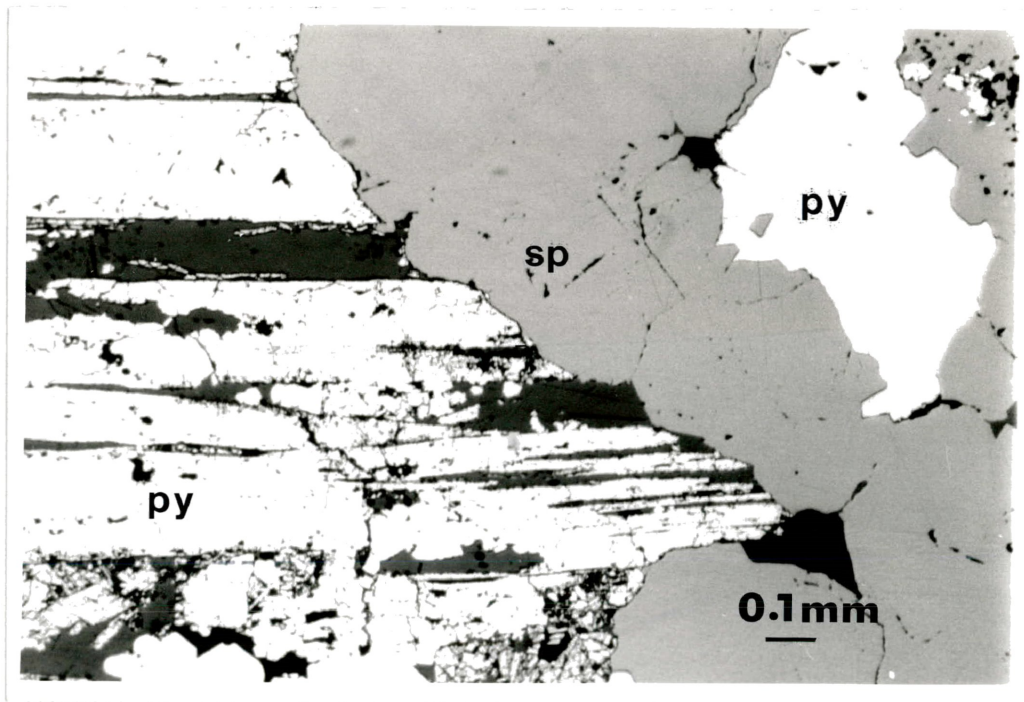
FIGURE 2.20 — REFLECTED LIGHT PHOTOMICROGRAPH OF EARLY, FINELY LAMINATED PYRITE TRUNCATED BY SPHALERITE AND PYRITE IN A SAMPLE FROM THE AREA 14 OREBODY.

TABLE 2.1 - RELATIVE SULFIDE MINERAL ABUNDANCES AND SULFIDE TO SPARRY DOLOMITE RATIOS

ORE ZONE OR MINE UNIT (No. of samples)	AVERAGE ORE COMPOSITION (VOL.%)				RATIOS		
	Sp	Py	Gn	Dol	Sp/Sp+Gn	Sp/Sp+Py	Dol/Sp+Gn+Py
Main Orebody (Eastern)							
Unit 1 (9)	29	48	1	22	0.96	0.37	0.27
Unit 2 (4)	50	28	1	21	0.97	0.64	0.26
Unit 3 (5)	41	37	0	22	1.00	0.52	0.28
Unit 4 (6)	56	33	4	7	0.93	0.63	0.08
Unit 5 (2)	29	52	1	18	0.96	0.36	0.21
Unit 6 (6)	66	21	1	12	0.98	0.75	0.13
Main Orebody							
West Zone (5)	56	32	7	5	0.88	0.63	0.05
Lower Lens (5)	41	40	1	18	0.97	0.50	0.21
Shale Zone (6)	64	31	2	3	0.96	0.67	0.03
Area 14 Orebody	74	16	3	7	0.96	0.81	0.08

Sp - Sphalerite, Py - Pyrite, Gn - Galena, Dol - Sparry dolomite gangue

(1984) may be further distinguished. Units 1, 2, 3 and 5 are relatively rich in dolomite compared to Units 4 and 6. The higher Units 4, 5 and 6, contain slightly more galena than underlying Units 1, 2 and 3. Mine Units 1, 3 and 5 also appear to contain more iron sulfide than Units 2, 4 and 6. Although the Sp/(Sp+Gn) ratio for the western portion of the Upper Lens suggests galena enrichment in that area of the mine, the Zn/Pb ratio is considered to increase from east to west in the Main Orebody. The Sp/(Sp+Py) ratio for the Area 14 Orebody is unrepresentative because sampling was biased towards the central sphalerite zone.

CHAPTER 3: MINERALOGICAL INVESTIGATIONS

3.1   Introduction

Although the presence of wurtzite and marcasite has previously been reported at Nanisivik (Olson, 1977; Neumann, 1985; Gait, 1985; Lakefield Research Report, 1984), neither of these minerals has been adequately studied by detailed X-ray techniques to define their structures. The presence of wurtzite and/or marcasite, along with their distribution and position within the paragenetic sequence should have impor-tant implications for the physical and chemical conditions of ore formation. The presence of anisotropic sphalerite may have some importance in relation to the wurtzite-sphalerite transition. Although different sphalerite generations have been noted at Nanisivik (McNaughton, 1983), and a general correlation of colour with iron content has been suggested (Neumann, 1984), a detailed study of sphalerite composition and its relationship to colour zoning has yet to be carried out. Fluorescent sphalerite has not previously been reported at Nanisivik, and its association with particular ore units suggests that it deserves further investigation. Pyrrhotite, if present in sufficient quantities with pyrite, may contribute to the understanding of the physical and chemical conditions of sulfide mineralization in the Keel Zone.

Pure hexagonal wurtzite (2H) is relatively rare and most naturally occurring wurtzite consists of a mixture of

polytypes having structures intermediate between those of cubic and hexagonal ZnS (Smith, 1955). Scott and Barnes (1972) suggested that wurtzite is slightly deficient in sulfur relative to sphalerite. Deviations from stoichiometry may also be responsible for various intermediate polytypes (Scott, 1974), as point defects appear to affect the sulfur-dependent phase boundaries. Curie (1963) noted that minor element impurities appear to stabilize the hexagonal struc-ture during the firing of high temperature synthetic ZnS, and Geilkman (1982) suggested that Cd, Fe or Mn impurities may be important in the stabilization of wurtzite polytypes.

Anisotropic domains in sphalerite exhibiting cross hatched twinning were reported from Tennessee by Seal et al (1985), where they were attributed to regions of disordered hexagonal packing corresponding to an increase in the unit cell parameter of sphalerite from 0.006 to 0.010Å. Although thermal and mechanical stress may also stabilize the hexagonal structure in ZnS, Seal et al (1985) concluded that the disordered hexagonal packing resulted from the replace-ment of Zn by Fe and Cd in the ZnS structure. Schalenblende, a mixture of wurtzite and sphalerite, has been reported from Pribram, Czechoslovakia, where disordered hexagonal wurtzite corresponds to anisotropic domains (Fleet, 1977; Akizuki, 1981), the biretringence of which indicates the percentage of disordered hexagonal packing. Fleet (1977) concluded that disordered hexagonal ZnS in schalenblende from Pribram represents the first step in the wurtzite-sphalerite inver-

sion process.

The iron content of sphalerite in carbonate-hosted deposits of the Mississippi Valley Type is generally low (Anderson and MacQueen, 1982). At the lower end of the reported range, sphalerite from East Tennessee is reported to contain less than 0.5 wt. % Fe (Churnet, 1979), while Appalachian deposits in general usually contain less than 2 wt. % Fe (Craig *et al*, 1983). McLimans (1977) reported maximum FeS contents from sphalerite of the Upper Mississippi Valley District of 19.9 mole %, or 22.2 wt. % Fe assuming negligible trace element contamination and perfect stoichiometry.

Colour zoning of sphalerite is not uncommon in deposits of this type and has been used as a stratigraphic tool in some districts (McLimans, 1977). Roedder and Dwornik (1968) reported that Fe content did not correlate with colour at Pine Point, as did Hardy (1979) for Gayna River and Churnet (1979) for East Tennessee. However, McLimans (1977) was able to demonstrate a regional correlation between iron content and sphalerite stratigraphy for the Upper Mississippi Valley District. Craig *et al* (1983) found dark coloured sphalerite to correlate with iron contents greater than 2.0 wt % in ore from the Appalachians.

Fluorescence in sphalerite often results from trace element impurities, the most common of which are Au, Ag and Cu, although Cd, Hg, Al, Ga, In, or Mg may also be involved (Curie, 1963). Au, Ag and Cu substitute for Zn and produce a

blue or green visible fluorescence. Copper may produce a red fluorescence, if present in large enough quantities, and if sulfur vacancies are present (Shionoya, 1966). The presence of Ag substituting in CdS, which forms an almost perfect solid solution with ZnS, will result in a red fluorescence. Ga and In may produce a red fluorescence in ZnS, as might Pb if the ZnS is prepared under sulfurizing conditions (Shionoya, 1966). Iron, which is usually considered to inhibit fluorescence, may actually produce a red emission but this is usually accompanied by blue fluorescence as well. Manganese is a common activator in silicates and is reported to fluoresce yellow-orange under ultraviolet light in ZnS (Curie, 1963).

In a study of pure, or self-activated ZnS, Uchida (1964) attributed emissions less than 400 nm to inferred deviations from stoichiometry. For example, an emission of 357 nm may indicate an excess of Zn. In the visible part of the spectrum, a green fluorescence in pure ZnS may be due to an excess of Zn (Kröger and Vink, 1954), while Shionoya (1966) argued that self-activated fluorescence in ZnS may actually require the presence of a halogen co-activator substituting for S . The creation of sulfur vacancies by electron bombardment may produce a red fluorescence with a maximum wavelength of 720 nm in pure CdS crystals (Kulp and Kelley, 1960). The presence of hexagonal rather than cubic structure in ZnS results in only a very minor shift of emission wavelengths (Curie, 1963; Shionoya, 1966).

The significance of anomalously anisotropic, porous pyrite was noted by Rising (1973) and Murowchick and Barnes (1984). Such textures at Nanisivik support the contention of Olson (1977) that much of the bladed iron sulfide had at one time been marcasite. The crystallography of the inversion of marcasite to pyrite at Nanisivik has been described by Gait (1985), but the structure of inverted crystals has not yet been examined in detail. Anisotropic pyrite is not restricted to the bladed pyrite of the eastern and central Upper Lens, so that the possibility of marcasite occurring elsewhere in the Main Orebody cannot be overlooked. Although marcasite has been reported in the Area 14 Orebody, its position in the paragenetic sequence has not been defined.

3.2   Experimental Technique

In an attempt to identify wurtzite and marcasite, ten single-crystal samples were analyzed on both large and small diameter Gandolfi cameras. Zinc sulfide crystals were X-rayed with filtered Cu K α radiation (1.54178Å), while iron sulfide crystals were X-rayed with filtered Fe Kα radiation (1.93728Å). Data obtained from ZnS crystals were compared to reported X-ray diffraction patterns for 2H wurtzite available in the JCPDF files and to calculated diffraction patterns for the 3R, 9R, 12R, 15R and 21R polytypes generated on a VAX/780 computer with the CRYSTINDX FORTRAN program (J.T. Szymanski, pers.comm.). Unit cell parameters were also calculated on

the VAX/780 system using a least-squares refinement FORTRAN program (E.J. Gabe, pers.comm.). Fluorescent sphalerite-sparry dolomite intergrowths and fibrous yellow ZnS suspected of having wurtzite morphology were also analyzed by X-ray powder diffraction using a Phillips diffractometer with monochromated Cu $K\alpha$ radiation. Powder diffraction data were indexed with the aid of a CYBERNEX APL-100 computer. Unusual sphalerite crystals were further nalyzed using a Supper precession camera with filtered Mo $K\alpha$ radiation.

Major and trace elements were analyzed by ARL Electron Microprobe at the University of Toronto operating at 20 kv and 120 nA beam current. Detection was by energy-dispersive analysis using a 100 second counting time. Data reduction was done by a peak stripping procedure using PESTRIP, a University of Toronto modification of Stratham's (1976) procedure. Major elements in sphalerite were cali-brated with a synthetic (Zn, Fe)S standard containing 25 mole % FeS. Synthetic FeS was used as a standard for pyrrhotite analyses. Detection limits were calculated using the following formula:

$$CDL = C \quad X \quad \frac{3\sqrt{Ib}}{Ip}$$

where CDL   = calculated detection limit in wt. %

     C   = composition of the standard in wt. %

     Ib   = background intensity during calibration

     Ip   = peak intensity during calibration.

The calculated detection limits for minor elements in

sphalerite are as follows: Mn = 0.01 wt.%, Cd = 0.02 wt.%, Cu = 0.02 wt.%, Ag = 0.03 wt.% and Fe = 0.01 wt.%. For pyrrhotite the calculated detection limits are: Ni = 0.10 wt.%, Co = 0.04 wt.%, Cu = 0.06 wt.% and Mn = 0.05 wt.%. The latter two minor element detection limits for pyrrhotite were calculated from pure Cu metal and MnS respectively.

The gallium contents of two sphalerite crystals were analyzed by radiochemical neutron activation analysis (RNAA) by D. McKay at Lakehead University. Samples were irradiated at McMaster University and returned to Lakehead where the gallium was extracted using a solvent extraction technique involving isopropol ether. Gallium peak areas were determined on a germanium crystal gamma-ray spectrometer. A detection limit of 1.4 ppm was calculated on the basis of the peak to background ratios. The standard error of the gallium analyses is based on a standard error of ±4% calculated from ten multiple analyses of the U.S.G.S. standard G-2, which contains 23.0 ppm Ga (Doug McKay, in prep.).

3.3   Experimental Results

X-Ray Diffraction Studies

Ten ZnS crystals were analyzed with the Gandolfi camera, including anisotropic, fibrous and fluorescent varieties. In none of the crystals analyzed was the (100) reflection at 29.943°2θ characteristic of the 2H wurtzite structure observed. However, in some of the X-ray

diffraction patterns produced there is an unusual splitting of diffraction lines not attributable to $K\alpha_1-K\alpha_2$ resolution. The (111) and (220) reflections are most commonly split, although the (311), (200) and (400) lines are also affected in some crystals. The observed X-ray diffraction patterns do not conform exactly to any of the patterns calculated for wurtzite polytypes, although the 15R polytype does allow for splitting of some diffraction lines. Powder diffractometry analysis of late, fibrous ZnS and a fluorescent ZnS-sparry dolomite intergrowth also failed to indicate the presence of hexagonal structure.

The birefringence of anisotropic domains in sphalerite may be used to estimate the amount of disordered hexagonal packing within the crystal structure (Fleet, 1977). An estimate of 0.004 for the birefringence of some well developed anisotropic domains in Nanisivik sphalerite is based on the maximum retardation observed on a universal stage and a direct measure of the section thickness with a micrometer. A value of 0.004 would correspond to 20% hexagonal close-packed layering in the cubic structure according to Figure 3.1. Zero-level precession camera photographs failed to indicate anything unusual about the structure of anisotropic sphalerite.

Calculated unit cell parameters range from 5.400 to 5.425Å, although the majority fall between 5.400Å and 5.412Å (Table 3.1). Splitting of diffraction lines does not affect the unit cell parameter a great deal but does introduce a
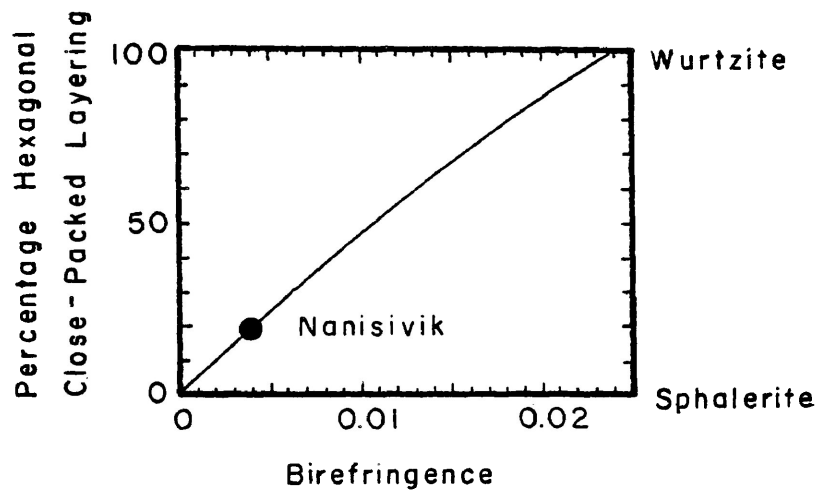
FIGURE 3.1 - RELATIONSHIP BETWEEN
BIREFRINGENCE OF ANISOTROPIC ZnS
AND HEXAGONAL CLOSE - PACKED
LAYERING (AFTER FLEET, 1977).

considerable error into the calculation. Therefore, when calculating the unit cell parameter for crystals exhibiting split diffraction lines, an average 2θ value for the split line was used. Crystals having a large unit cell parameter include late, fibrous sphalerite, an anisotropic domain within sphalerite, and sphalerite having estimated iron contents greater than 5 wt.%. A single unusual value of 5.425Å corresponds to a crystal having an X-ray pattern that shows evidence of splitting along the (111), (200), (220) and (400) directions.

Table 3.1: CALCULATED UNIT CELL PARAMETERS OF SPHALERITE

Sample Description	Lattice Constant (Å)	Standard Error
Late, fibrous sphalerite	5.4009	0.0012
Sphalerite-dolomite intergrowth	5.4056	0.0021
Fluorescent sphalerite	5.4077	0.0015
Anisotropic sphalerite	5.4077	0.0019
Sphalerite; 3-4 wt.% FeS	5.4071	0.0017
Fibrous, yellow sphalerite	5.4104	0.0014
Sphalerite; 5 wt.% FeS	5.4120	0.0019
Anisotropic sphalerite	5.4122	0.0026
Sphalerite; 7-8 wt.% FeS	5.4125	0.0033
Sphalerite; 2-3 wt.% FeS	5.4256	0.0051

Single crystal X-ray diffraction patterns of both late and main stage bladed iron sulfide crystals indicate that marcasite has inverted to pyrite, confirming the findings of Gait (1985) and the suspicions of Olson (1977). A

crystal of strongly anisotropic iron sulfide from the western Upper Lens consisted only of pyrite. A sample of finely laminated, anisotropic iron sulfide from Area 14 consisted only of pyrite while a sample of similar, early iron sulfide from the Lower Lens contained minor amounts of marcasite.

Microprobe Analyses

The major and minor element microprobe results for sphalerite are presented in Table 3.2. Colour zoning within sphalerite crystals correlates well with iron content. In mine Units 1, 3, 5 and 6 where colour zoning is best developed, colourless rims generally contain less than 1 wt.% Fe, whereas dark crystal centers contain up to 7 wt.% Fe. In Units 2 and 4 colourless rims are usually absent, and the iron content varies from 1 wt.% Fe at the edges of the crystals to approximately 8 wt.% Fe in crystal centers. Although very dark red, sphalerite from the Keel Zone contains almost negligible Fe. Metal to sulfur ratios generally lie outside of the expected range of 0.995 to 1.005 for stoichiometry. The observed ratios vary from 0.9834 to 1.0370 with the majority of ratios being greater than 1.0100. Graphs of metal to sulfur ratios versus iron content, analysis total, and colour fail to explain these high metal to sulfur ratios, suggesting that sphalerite at Nanisivik is generally non-stoichiometric and sulfur deficient.

Although Cd and Ag are common minor element constituents in Nanisivik sphalerite, neither Cd nor Ag contents were high enough for detection by microprobe analysis.

TABLE 3.2 - SUMMARY OF MICROPROBE DATA FOR SPHALERITE

SAMPLE	UNIT	COLOUR ZONE	ANALYSES IN WT. %					TOTAL	METAL/SULFUR
			Zn	Fe	S	Mn	Cu		
37 - 11 #3	1	Orange rim	65.11	2.12	33.41	ND	o.53	101.17	0.9999
		Orange and yellow	67.77	0.78	33.20	ND	0.22	101.97	1.0152
		Orange and yellow	66.88	1.46	33.39	ND	0.27	102.00	1.0113
		Red core	62.03	5.85	33.19	ND	ND	101.07	1.0174
		Orange rim	64.76	1.85	33.17	ND	0.50	100.27	0.9969
		Red	63.15	4.94	33.40	ND	ND	101.49	1.0119
		Red core	61.65	5.55	33.43	ND	ND	100.64	0.9996
37 - 11 #2	1	Sp-dol intergrowth	66.61	ND	32.90	1.15	0.29	100.95	1.0166
		Orange rim	67.51	0.15	32.89	ND	ND	100.55	1.0110
		Orange	65.90	1.93	33.06	ND	ND	100.89	1.0109
		Red and orange	65.75	2.96	32.93	ND	0.18	101.83	1.0333
		Red and orange core	63.78	3.86	33.04	ND	0.19	100.87	1.0178
21 - 09S #1	2	Colourless rim	67.37	1.28	33.02	ND	0.19	101.86	1.0255
		Yellow	67.21	1.17	32.85	ND	ND	101.23	1.0235
		Orange	62.61	5.33	33.00	ND	0.24	101.18	1.0262
		Red	59.83	8.02	33.15	ND	ND	101.00	1.0239
		Red	59.99	7.66	33.29	ND	0.19	101.13	1.0184
		Red core	61.42	6.60	33.20	ND	ND	101.23	1.0211
37 - 11 #5	2	Complex rim	65.60	2.38	32.95	ND	0.24	101.17	1.0213
		red	65.37	2.98	33.04	ND	0.22	101.62	1.0238
		and	62.47	5.80	33.20	ND	0.19	101.66	1.0256
		orange	63.97	4.82	32.86	ND	ND	101.65	1.0370
		core	63.23	4.60	33.04	ND	0.22	101.09	1.0106

SAMPLE	UNIT	COLOUR ZONE		Zn	Fe	S	Mn	Cu	TOTAL	METAL/SULFUR
35 - 11 #4	3	Orange rim		62.39	4.68	33.17	ND	0.19	100.43	1.0060
		Red core		60.91	6.70	33.31	ND	ND	100.92	1.0120
		Orange rim		62.99	4.26	33.15	ND	0.28	100.68	1.0097
		Red core		62.02	6.13	33.51	ND	0.23	101.89	1.0159
21 - 09S #4	4	Complex	rim	61.99	5.82	33.25	ND	0.23	101.30	1.0181
		red and		60.95	7.13	33.54	ND	ND	101.62	1.0072
		orange	core	60.43	7.44	33.45	ND	ND	101.32	1.0134
21 - 09S #5	4	Red band		60.54	7.22	33.20	ND	ND	100.95	1.0188
		Orange band		63.29	5.15	33.29	ND	0.27	102.00	1.0251
		Red band		60.13	7.70	33.02	ND	ND	100.84	1.0267
		Red band		60.25	7.42	33.17	ND	0.22	101.06	1.0223
21 - 09S #6	4	Orange rim		62.00	5.77	33.21	ND	0.31	101.29	1.0198
		Orange core		61.18	6.35	33.51	ND	0.22	101.26	1.0072
		Red rim		59.53	8.32	34.02	ND	0.21	101.90	0.9988
		Red core		59.81	7.94	33.16	ND	0.19	101.10	1.0246
21 - 09S #7	5	Colourless rim		65.72	0.16	32.95	ND	0.19	99.02	0.9836
		Red and orange		60.87	6.49	33.74	ND	0.20	101.30	0.9980
		Red and orange core		61.42	6.37	33.55	ND	0.25	101.59	1.0104
13 - 09S F	6	Sp-dol intergrowth		66.65	0.19	32.83	ND	ND	99.67	1.0027
		Colourless rim		68.19	0.25	33.03	ND	0.18	101.66	1.0193
		Orange		62.52	5.54	33.18	ND	ND	101.24	1.0196

SAMPLE	UNIT	COLOUR ZONE	Zn	Fe	S	Mn	Cu	TOTAL	METAL/SULFUR
13 - 09S E	6	Orange rim	65.54	2.33	33.05	ND	0.27	101.18	1.0169
		Orange (?)	65.52	2.89	32.80	ND	0.20	101.41	1.0331
		Orange (?)	65.59	3.09	32.86	ND	ND	101.54	1.0326
		Red core	63.70	4.39	33.12	ND	0.28	101.48	1.0235
Keel Zone		Red core	68.73	ND	33.04	ND	ND	101.78	1.0200
		Red rim	68.18	0.13	32.95	ND	ND	101.26	1.0168
		Red core	68.51	0.12	32.80	ND	0.19	101.62	1.0291
		Red rim	68.38	0.12	33.18	ND	0.19	101.86	1.0153

ND - Not detected at calculated detection limits of Fe = 0.01 wt.%, Mn = 0.01 wt.% and Cu = 0.02 wt.%.
Ag and Cd were not detected in any analyses at detection limits of Ag = 0.03 wt.% and Cd = 0.02 wt.%.
Error in precision based on duplicate analyses for major elememts are as follows; Zn = ± 0.00
Fe = ± 0.01 and S = ± 0.13.

Copper trace element contents vary from 0.18 wt.% to 0.53 wt.%. Manganese is occasionally associated with sphalerite crystal rims and, in one case, 37-11#2, this corresponds with a fluorescent dolomite-sphalerite intergrowth. However, sample 37-11#3, which fluoresces along sphalerite rims, contains no detectable Mn. Two samples of sphalerite analyzed for Ga by radiochemical neutron activation analysis contained 1512.81±60.51 ppm and 192.59±7.70 ppm corresponding to late, fibrous, yellow sphalerite and a dark red sphalerite crystal, respectively. The Ga contents are in general agreement with those reported for low temperature Mississippi Valley Type deposits (Shaw, 1957).

Results from microprobe analyses of pyrrhotite from the Keel Zone are presented in Table 3.3. The atomic percent Fe iron varies from 47.11% to 47.81%. Nickel and manganese contents are below detection limits, while small amounts of copper and cobalt are present.

Table 3.3: MICROPROBE ANALYSES OF PYRRHOTITE

	Fe	Elemental Composition (wt.%) S	Ni*	Co	Cu*	Mn*	Total	At % Fe
1.	62.12	38.93	N.D.	0.27	0.23	N.D.	101.55	47.81
2.	61.23	39.17	N.D.	0.25	N.D.	N.D.	100.65	47.29
3.	61.13	39.39	N.D.	0.33	0.22	N.D.	101.25	47.11
4.	61.72	39.18	N.D.	0.30	N.D.	N.D.	101.20	47.49

* not detected at calculated detection limits of Ni $\leq$ 0.10 wt.%; Cu $\leq$ 0.06 wt.% and Mn $\leq$ 0.05 wt.%.

CHAPTER 4:   FLUID INCLUSION STUDIES

4.1   Introduction

The validity of utilizing fluid inclusions to esti-
mate the temperature and salinity of ore fluids at the time
of mineral deposition is dependent upon four major assump-
tions, listed below in their approximate order of importance.

1)   Fluid inclusions contain representative samples of ore
     fluid at the time of mineralization;

2)   The age of inclusion entrapment relative to the host
     mineral may be determined;

3)   No appreciable change in inclusion volume has occurred
     since entrapment;

4)   No leakage or contamination of the inclusion has
     occurred.

Roedder (1979) has discussed the first assumption,
that inclusions contain samples of ore fluid, and it will not
be dealt with any further here other than to say that the
assumption is considered valid.

Determining the age of inclusions relative to the
host mineral is essential for the proper interpretation of
inclusion data. Inclusions are classified as primary,
secondary or pseudo-secondary, and exhaustive criteria are
available for this distinction (Roedder, 1979). Primary
inclusions are considered to form during growth of the

immediate host mineral, usually due to imperfections along the growth face. Secondary inclusions form after growth of the host mineral has ceased, typically developing along annealed fractures. During growth of the host mineral, fracturing may occur, trapping pseudo-secondary inclusions. Pseudo-secondary inclusions appear very similar to true secondary inclusions, making the distinction very difficult. Many inclusions that have been classified as secondary may in fact be pseudo-secondary and are therefore representative of the ore fluid during mineralization (Roedder, 1984).

Volume changes occurring in inclusions after trapping have recently been discussed by Roedder (1981, 1984). Two of the more common causes of volume changes are necking down and stretching. Necking down occurs when elongate inclusions or secondary fractures anneal in order to reduce internal surface areas. If necking down occurs after nucleation of a vapor phase, the vapor bubble may become isolated, resulting in erroneous homogenization values. Stretching has recently been studied quantitatively by Bodnar and Bethke (1984) who analyzed the effects of overheating inclusions past their homogenization point. As little as 8°C overheating can cause stretching in fluorite, depending upon the inclusion size, while generally at least 40°C is required to cause stretching in sphalerite. When cooled and reheated, stretched inclusions homogenize at new, higher temperatures (Larson *et al*, 1973). Stretching may also be caused by mechanical abrasion or by freezing (Lawler and Crawford, 1983).

Leakage of fluid from inclusions may be relatively difficult to detect if the fracture has healed. Inclusions in brittle minerals, such as sphalerite, often tend to fracture rather than stretch (Bodnar and Bethke, 1984), and the presence of such decrepitated inclusions may often be the only evidence of leakage.

The behavior of an idealized fluid inclusion with regard to temperature and pressure during trapping is illustrated in Figure 4.1. During warming of a simple two-phase inclusion, homogenization occurs at the point where the fluid leaves the liquid-vapor curve to follow a trend of constant density (isochore). The actual trapping temperature may lie anywhere along the isochore depending upon the density of the inclusion fluid, which is in turn related to salinity, pressure and specific volume. It is therefore often necessary to add a pressure correction to the homogenization temperature using an estimate of salinity obtained from freezing determinations and an independent estimate of the pressure of formation. Given this information, the graphs in Potter (1977) may be used to quickly calculate the necessary temperature corrections for brines approximated by the $NaCl-H_2O$ system. Roedder (1984) has pointed out that these graphs apply only to inclusions that homogenize in the liquid phase.

4.2   Experimental Technique

The sample preparation technique followed for the
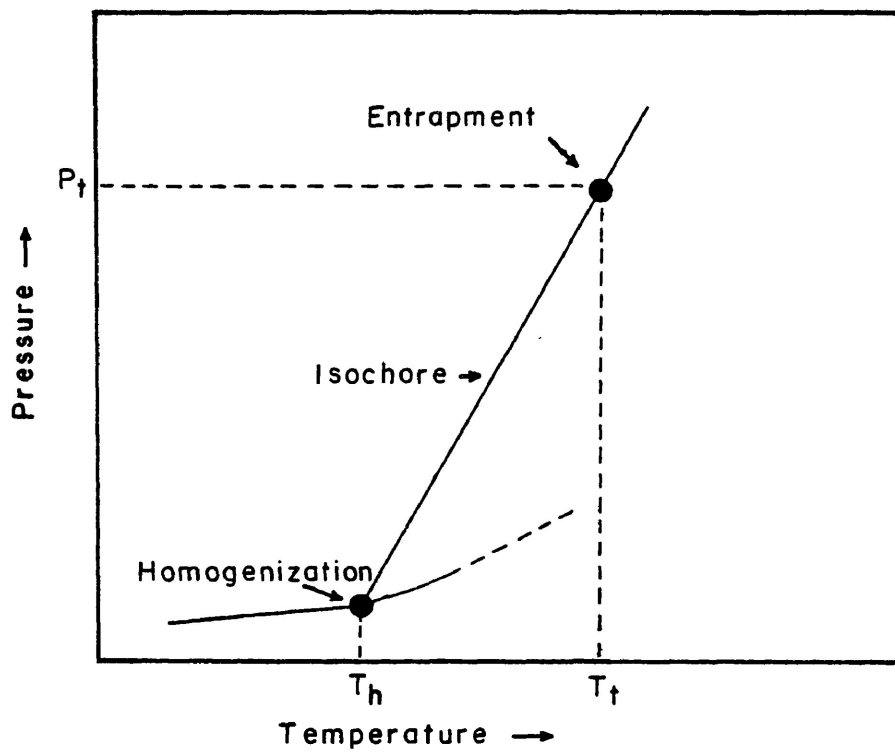
FIGURE 4.1- IDEALIZED BEHAVIOR OF A SIMPLE
TWO-PHASE INCLUSION (AFTER BURRUSS, 1981).

production of doubly polished thick sections was modified after Hollister *et al* (1981). Section thickness varied with the mineral being examined and its clarity, but averaged 100 μm. A detailed description of the sample preparation technique is given in Appendix II. Most sections were heated to approximately 100°C during preparation. Given the findings of Bodnar and Bethke (1984), the possibility exists that very low temperature inclusions in dolomite were thermally stretched during sample preparation. A cold mounting technique, perfected towards the end of the study, is also described in Appendix II.

Approximately 100 doubly polished sections were prepared at Lakehead University during the course of this study, of which half were found to contain suitable inclusions. White, sparry dolomite was found to contain mainly primary inclusions, some of which were localized at the intersection of cleavages (Figure 4.2). Inclusions in sphalerite were mainly pseudo-secondary, although some primary inclusions were also observed (Figure 4.3). Planes of pseudo-secondary inclusions could occasionally be traced to a termination within the crystal (Figure 4.4). Definite secondary inclusions were observed to cut numerous crystals of sphalerite. Secondary inclusions often showed evidence of necking down (Figure 4.5) and either lacked a discrete vapor phase or homogenized at very low temperatures.

Microthermometric observations were made on a Chaixmeca heating/freezing stage mounted on a Leitz micro-
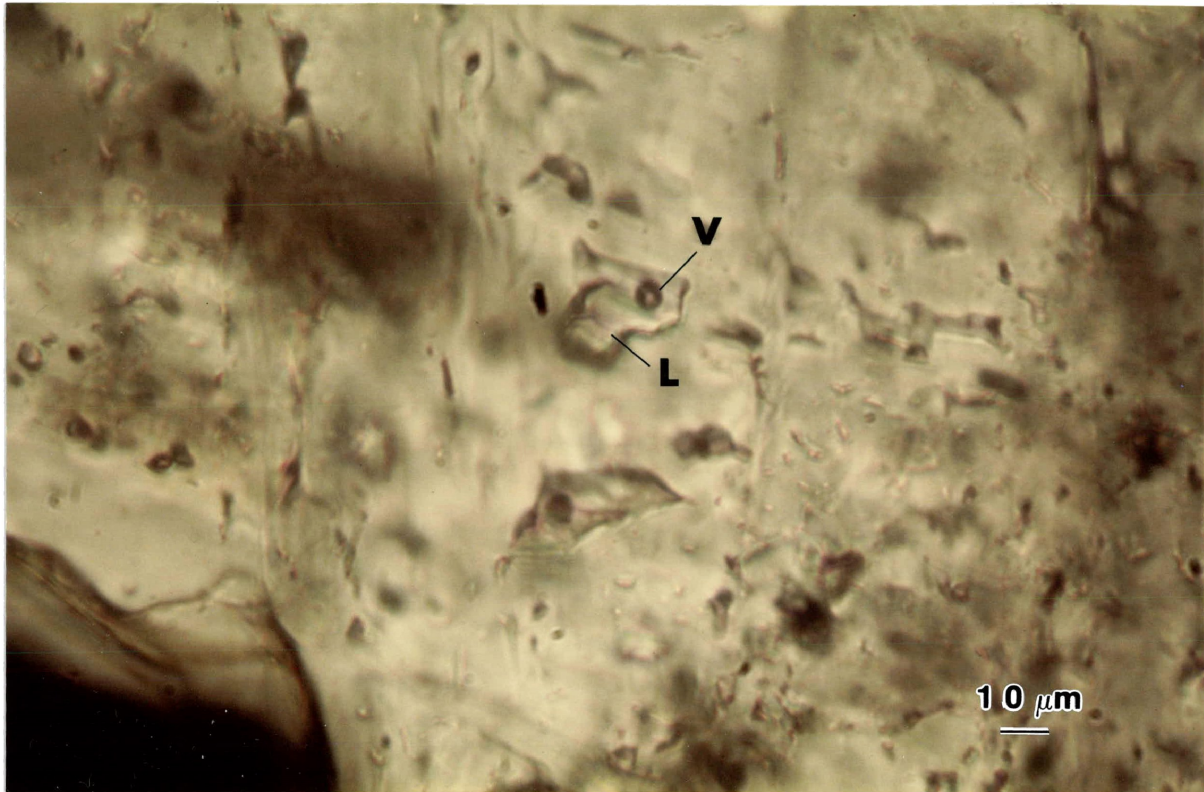
FIGURE 4.2 - PRIMARY FLUID INCLUSION IN SPARRY DOLOMITE GANGUE. LIQUID (L) AND VAPOR (V) PHASES INDICATED.
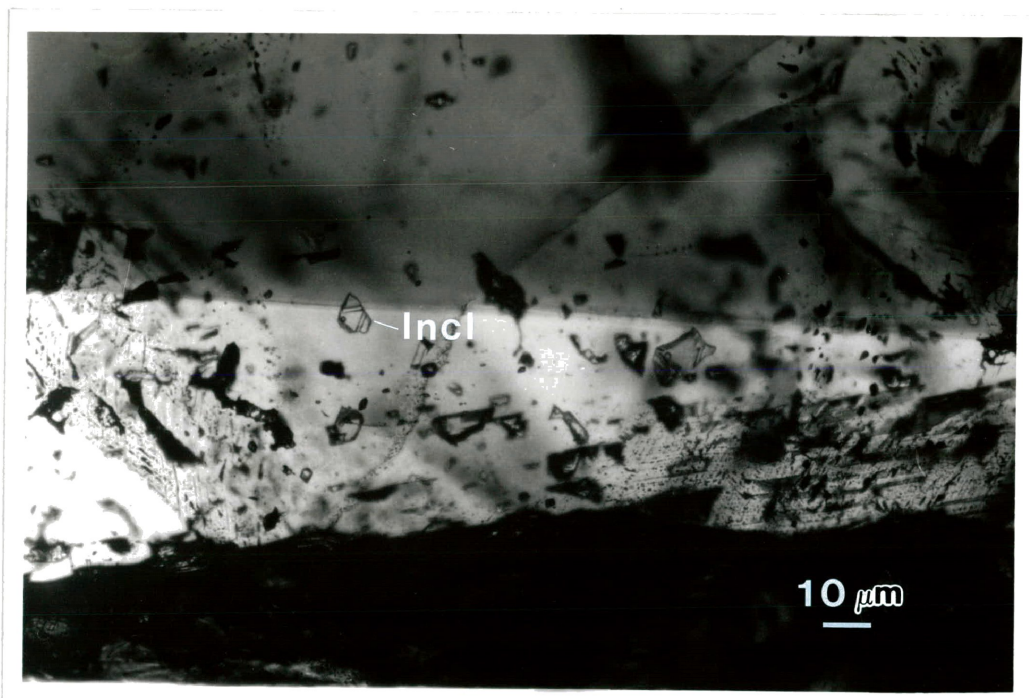
FIGURE 4.3 - PRIMARY FLUID INCLUSIONS IN COLOUR BANDED SPHALERITE.
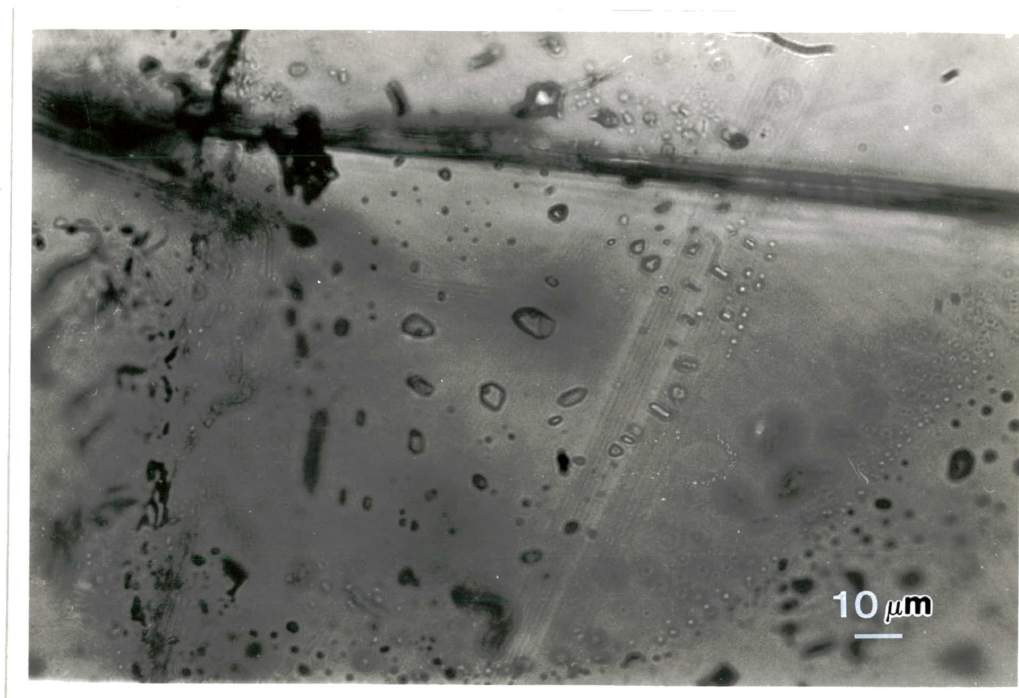
FIGURE 4.4 – PLANE OF PSEUDO – SECONDARY FLUID INCLUSIONS
IN SPHALERITE. NOTE THE CONSTANT VAPOR VOLUME IN EACH.
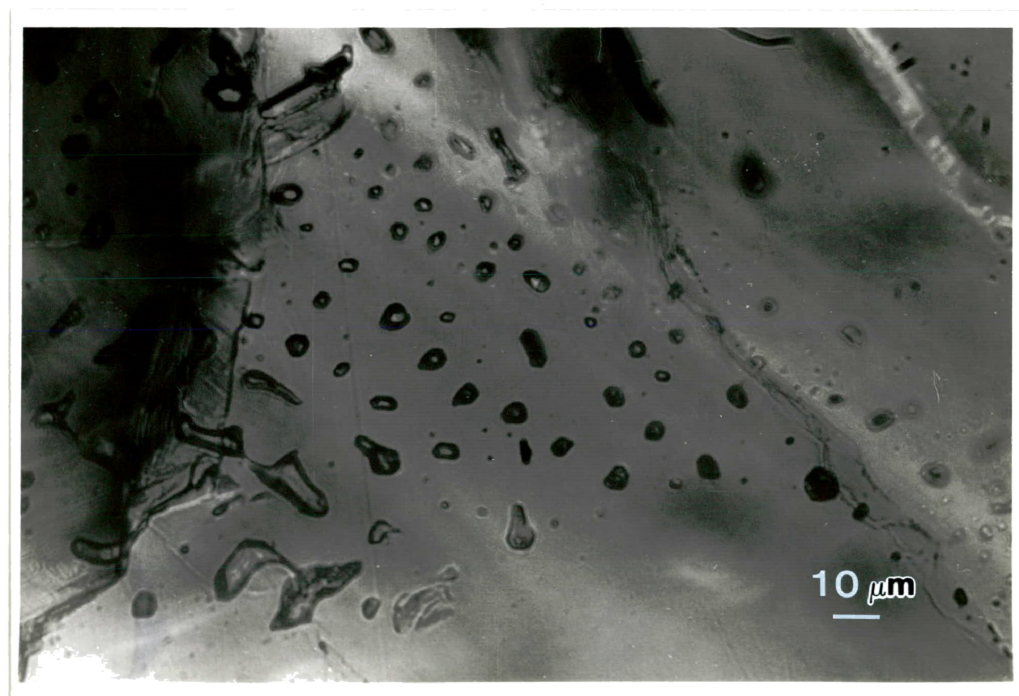
FIGURE 4.5 – PLANE OF SECONDARY INCLUSIONS IN SPHALERITE
ILLUSTRATING DIFFERENT STAGES OF NECKING.

scope at the Ecole Polytechnique, Montreal. The Chaixmeca stage utilizes an electrically heated metal pad for warming and dry air, cooled by liquid nitrogen in a Dewar flask, for cooling. A long working-distance lens was used (UMK 50/0.60) and when used with 25x oculars allowed observations on inclusions as small as 4 to 5 μm in diameter.

The accuracy of temperature measurements was determined when the system was installed using a series of synthetic organic standards manufactured by Merck. For calibration purposes, a small number of synthetic crystals were placed between two glass coverslips and heated until melting occurred. Actual melting of these standards occurred at temperatures slightly higher than their actual melting point due to problems in stage conductivity. This discrepancy increased with temperature in a regular fashion allowing the calculation of an equation for correction (L. Kheang, pers.comm.).

$\Delta T = -0.045$ (Tm-100) where ΔT is the correction to be subtracted from the observed homogenization temperature (Th). Three Merck standards were tested to check this calibration over the range 150° to 250°C and were found to be in good agreement with the established calibration curve.

Precision of heating and freezing experiments was determined by repeatedly heating and freezing several good quality inclusions. For freezing point determinations, the precision was less than ±0.5°C while for homogenization determinations the precision was in the order of ±3.0°C.

The major factors controlling the precision of the technique were observational. Most of the inclusions proved to be less than ideal. Condensation often fogged the field of view and the exact moment of the final melting of ice or of homogenization was often difficult to detect precisely. To account for these observational difficulties, inclusions were ranked from 1 to 3, representing good to poor quality observations, respectively. Fair to poor quality observations may contain an error in the determination of homogenization temperature of as much as $\pm 5°C$.

As is generally done, freezing determinations were made first to avoid problems with stretching due to over-heating. It was necessary to super-cool most inclusions to $-90°C$ to induce freezing, either because of problems in nucleating ice crystals or due to the presence of dissolved hydrocarbons. Once the inclusion was frozen, it was warmed at approximately $1.0°C/min$. During warming, the point of first melting (Te) and of the last melting (Tm) of ice were recorded. Due to observational restrictions, inclusions less than 10 μm in diameter were found unsuitable for freezing studies. Very little information on freezing behavior could be collected due to time constraints.

During heating studies the rate of heating was slowed to approximately $1.0°C/min$. below the estimated point of homogenization to allow the stage to equilibriate. The homogenization temperature (Th) was taken at the point where the vapor bubble was no longer visible. Where possible, numerous

inclusions in a section were homogenized consecutively.

4.3 Experimental Results

Homogenization Temperatures

Homogenization data are summarized in Table 4.1. In the majority of cases where discrete sub-populations are observed in individual hand samples, the sub-populations are readily apparent because they show no overlap. However, in one sample, 37-11#5, where there is overlap between sub-populations, a statistical t-test was used to compare the population means. Assuming a random sampling of normal populations having a common variance, the population means may be compared using the method described by Huntsburger and Billingsley (1977, p.225). All sub-populations from the same mineral in individual hand samples that are differentiated in Table 4.1 show either no overlap or may be distinguished at a 99.5% confidence level.

The homogenization data is also illustrated graphically for each of the units or zones. Histograms illustrate the distribution of homogenization temperature within individual units and zones. Bar diagrams for individual hand samples illustrate the range of data encountered in some samples for Units 1 through 4, and also differentiate the sub-populations distinguished in Table 4.1.

Eastern and Central Portions of the Upper Lens

Inclusion data for Unit 1 is presented graphically in

TABLE 4.1 - SUMMARY OF FLUID INCLUSION HOMOGENIZATION TEMPERATURES

SAMPLE	X̄	HOMOGENIZATION Range	TEMPERATURES (C) S	n	INCLUSION TYPE	HOST MINERAL
Eastern and central Upper Lens						
Unit 1						
37 - 11E #2	152.5	145 - 176	9.8	7	PS	Sp
37 - 11E #3	95.5	91 - 98	2.5	6	PS	Sp
	113.0	ND	ND	1	P	Dol(int)
35 - 11 #1	170.1	155 - 189	9.7	8	P	Dol(vein)
	133.5	121 - 138	5.5	7	P	Dol(int)
	99.2	75 - 113	11.5	9	P	Dol(vein)
35 - 11 #2	112.1	95 - 145	17.1	6	P	Dol(int)
	183.0	169 - 193	9.9	5	PS	Sp
35 - 11 #6	161.3	130 - 186	15.7	21	P	Dol(band)
21 - 09cc #1	94.0	74 - 106	14.2	3	P	Dol(int)
	176.0	144 - 196	20.4	5	P	Dol(int)
21 - 09N A	96.9	77 - 124	15.6	14	P; PS	Sp
21 - 11W	124.2	115 - 147	9.7	7	PS	Sp
13 - 09S A	185	172 - 202	7.4	12	P	Dol(int)
Unit 2						
37 - 11E #4	146.0	119 - 163	11.8	16	P; PS	Sp
37 - 11 #5	174.4	125 - 200	19.6	10	P; PS	Dol(band)
	131.3	106 - 168	20.3	6	P; PS	Dol(band)
	160.6	139 - 173	15.3	3	PS	Sp
21 - 09cc #2	179.2	166 - 216	13.2	13	P; PS	Dol(band,inter
	137.7	95 - 151	14.1	8	P; PS	Dol(band,inter
Unit 3						
37 - 11E #6	93.0	71 - 104	10.6	6	P	Dol(inter)
37 - 10W B	175.5	139 - 208	15.7	11	P; PS	Sp
35 - 11 #4	85.5	76 - 89	5.5	5	S	Sp
	152.7	145 - 163	6.9	4	P	Dol(band)

SAMPLE	HOMOGENIZATION TEMPERATURE (C)				INCLUSION TYPE	HOST MINERAL
	$\bar{X}$	Range	S	n		
21 - 09N B	119.5	98 - 131	11.9	7	P	Dol(inter)
	90.6	85 - 95	2.8	10	PS; P	Dol(band,inter)
21 - 09S #3	96.0	89 - 108	5.7	9	P	Dol(inter)
21 - 09cc #3	166.0	165 - 167	1.0	2	P	Sp
Unit 4						
35 - 11 #3	99.0	98 - 105	5.0	5	P	Dol(inter)
	85.4	77 - 93	8.2	5	P	Sp
21 - 09S #5	97.8	85 - 119	10.3	7	P; PS	Dol(inter)
	229.0	190 - 253	23.5	4	P	Dol(inter)
21 - 09S #6	163.0	150 - 206	14.5	14	PS	Sp
	114.0	101 - 133	10.9	6	PS	Sp
21 - 09cc #4	105.8	92 - 128	11.0	9	P	Dol(inter)
13 - 09S D	142.5	135 - 151	7.0	4	PS	SP
Unit 5						
2 1 - 09S #7	154.6	140 - 176	11.7	5	PS	Sp
37 - 11 #6	105.2	104 - 108	1.6	4	P	Dol(inter)
Unit 6						
3 7 - 11E #8	171.1	161 - 185	8.0	8	P	Dol(inter)
22 - 10W	98.0	80 - 116	13.3	6	S	Sp
	156.9	132 - 185	15.0	11	P	Dol(band,inter)
	100.4	83 - 117	13.0	10	P	Dol(band,inter)
13 - 09S E	127.6	118 - 133	5.3	6	PS	Sp
13 - 09S F	96.5	90 - 103	6.5	2	PS	Sp
Western Upper Lens						
6.5 - 08S B	109.1	90 - 129	16.6	7	PS	Sp
5.5 - 08S B	99.0	93 - 103	3.9	4	P	Dol(inter)
5.5 - 08S C	89.8	79 - 118	13.3	7	P	Dol(inter)

| SAMPLE | HOMOGENIZATION TEMPERATURE (C) | | | | INCLUSION TYPE | HOST MINERAL |
	X̄	Range	S	n		
Shale Zone						
09 - 07S	286.6	238 - 313	25.0	8	P	Sp
08 - 08N	267.8	181 - 295	33.2	20	PS	Sp
07 - 08S A	203.8	159 - 231	22.7	8	P; PS	Dol(inter)
Lower Lens						
LD 52S	380 +	ND	ND	7	P; PS	Sp
LD 54S	134.6	122 - 148	8.3	18	P	Dol(vein)
LD 60N B	153.0	131 - 164	14.5	12	P	Dol(vein)
Area 14 Orebody						
2 - 10N	132.6	110 - 174	20.9	6	P	Dol(inter)
3 - 10N B	141.7	134 - 150	6.5	3	PS	Sp
3 - 11 A	131.8	118 - 148	12.9	10	P	Dol(vein)
5SW A	101.3	81 - 117	13.7	6	PS	Sp
	135.0	122 - 146	8.3	5	P	Dol(inter)
4 - 11S	133.9	127 - 150	6.3	10	P	Dol(inter)

X̄ - sample mean
S - sample standard deviation
n - number of inclusions
P - primary inclusions
PS - pseudo-secondary inclusions
S - secondary inclusions
(vein) - late sparry dolomite vein
(inter) - sparry dolomite interstitial to sulfides
(band) - sparry dolomite interbanded with sulfides
ND - not determined

Figure 4.6. The data from Unit 1 are characterized by a wide range in homogenization temperature from 74°C to 202°C. Individual samples also display a wide range in temperature, but it can be demonstrated (Table 4.1) that much of the variation is due to the presence of discrete sub-populations in the data that may be related to textural features. For example, in sample 37-11#4, the wide range in homogenization temperature may be attributed to the presence of a number of late, crosscutting dolomite veinlets. Rarely, as in the case of sample 21-09cc#1, no textural explanation for the sub-populations can be found. A clear relationship between homogenization temperature and textural features, even among primary inclusions in dolomite, appears to be lacking. For example, the entire range in homogenization temperature from Unit 1 is expressed by interstitial dolomite alone. Data from dolomite in Unit 1 show a roughly trimodal distribution, with a main temperature grouping occurring at approximately 180°C. Data from sphalerite are skewed towards lower temperatures than dolomite, with a prominent grouping at 95°C. This low-temperature grouping in sphalerite may be a result of thermal stretching of very low temperature inclusions during section preparation, while the irregular nature of the homogenization temperature distribution suggests that some secondary inclusions have probably been analyzed. Therefore, any conclusions concerning the temperature of mineralization in Unit 1 should be based solely on data from dolomites.

As in the case of Unit 1, Unit 2 exhibits a wide
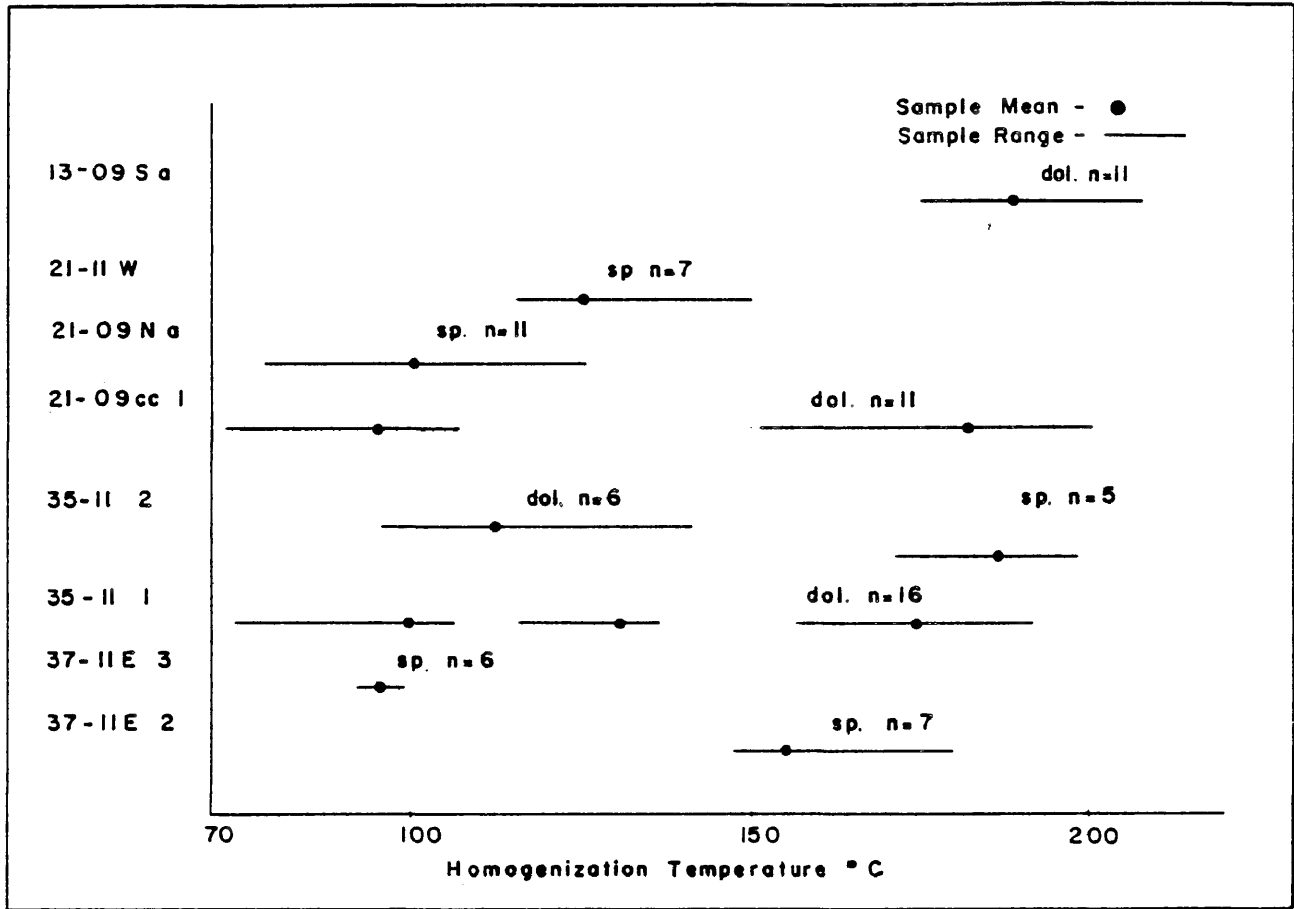
FIGURE 4.6a-SUMMARY OF FLUID INCLUSION DATA FOR UNIT I.
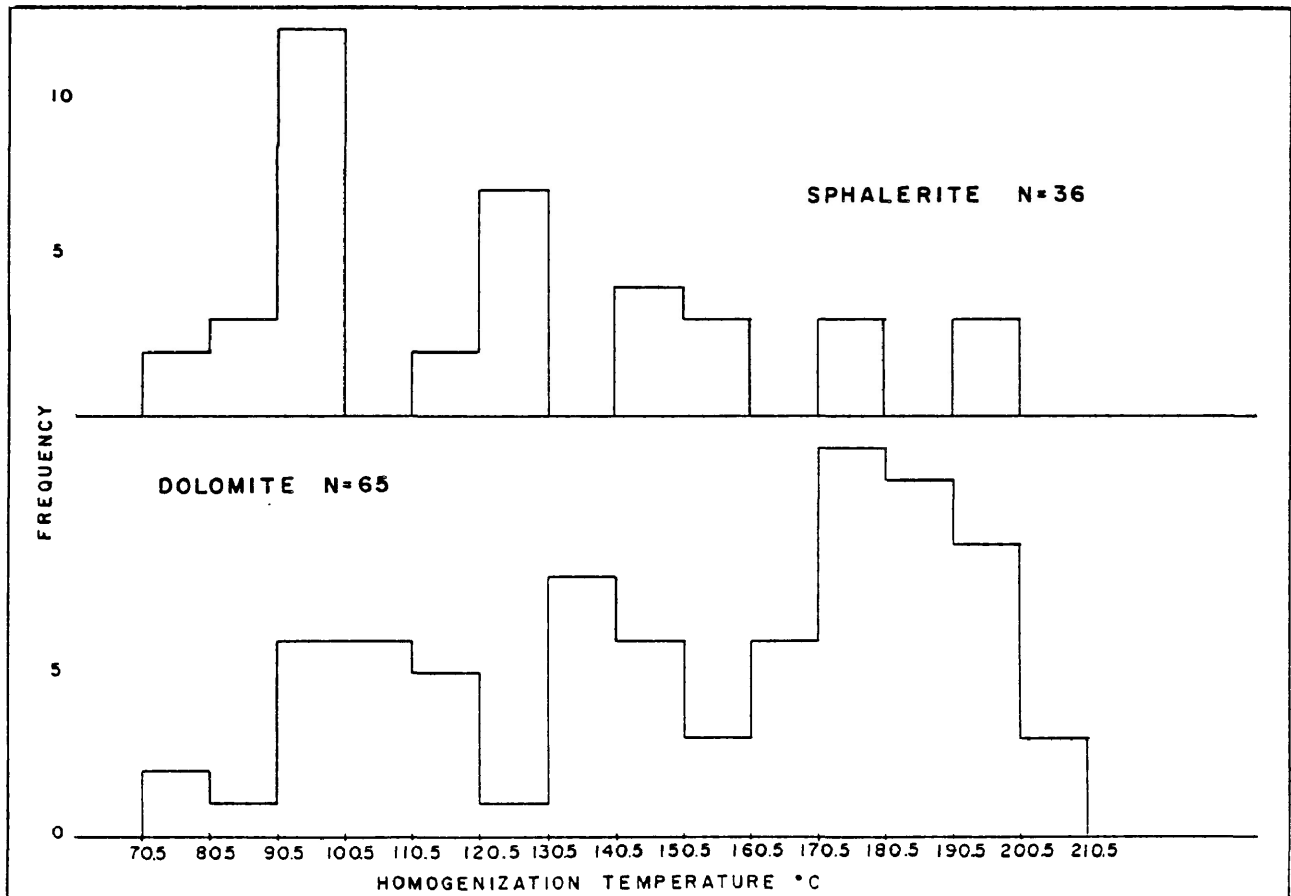
FIGURE 4.6b-DISTRIBUTION OF HOMOGENIZATION DATA FOR UNIT I.

range in homogenization temperature, although the range is less than that displayed by Unit 1 (Figure 4.7). Inclusions from sphalerite have a mean homogenization temperature of 148.3°C while inclusions from dolomite are characterized by two main groupings, one at 135.5°C and the other at 177.1°C. The two temperature groupings from dolomite have no apparent textural explanation. Good agreement between data from primary inclusions in dolomite and pseudo-secondary inclusions in sphalerite suggests that these pseudo-secondary inclusions relate to the main stage of mineralization.

Homogenization temperatures from Unit 3 are illustrated graphically in Figure 4.8. Again, a wide range in temperatures is apparent. However, two main populations are observed, a high-temperature population characterized by inclusions in sphalerite having a mean value of 174.0°C, and a low-temperature population in dolomite having a mean temperature of 98.9°C. Most of the low-temperature data occur in sparry dolomite interstitial to sulfides and therefore postdate the main period of mineralization. Homogenization data from sphalerite include both primary and pseudo-secondary inclusions and probably reflect the actual temperature of ore formation.

Homogenization temperature data from Unit 4 are illustrated in Figure 4.9. Inclusions in sphalerite form a high-temperature population having a mean temperature of 155°C, while dolomite tended to give homogenization temperatures around 100°C. As in the case of Unit 3, much of the
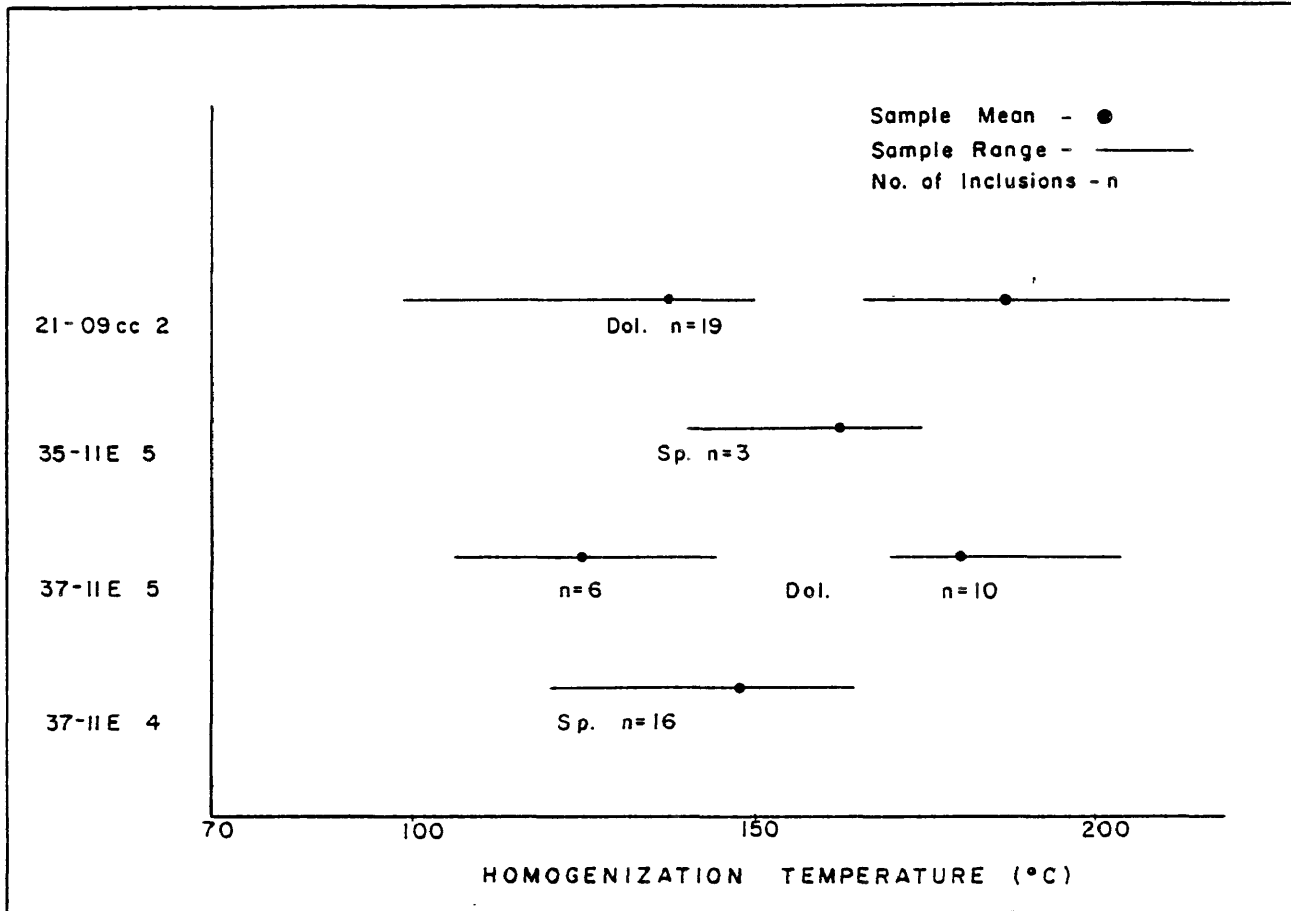
FIGURE 4.7a - SUMMARY OF FLUID INCLUSION DATA FOR UNIT 2.
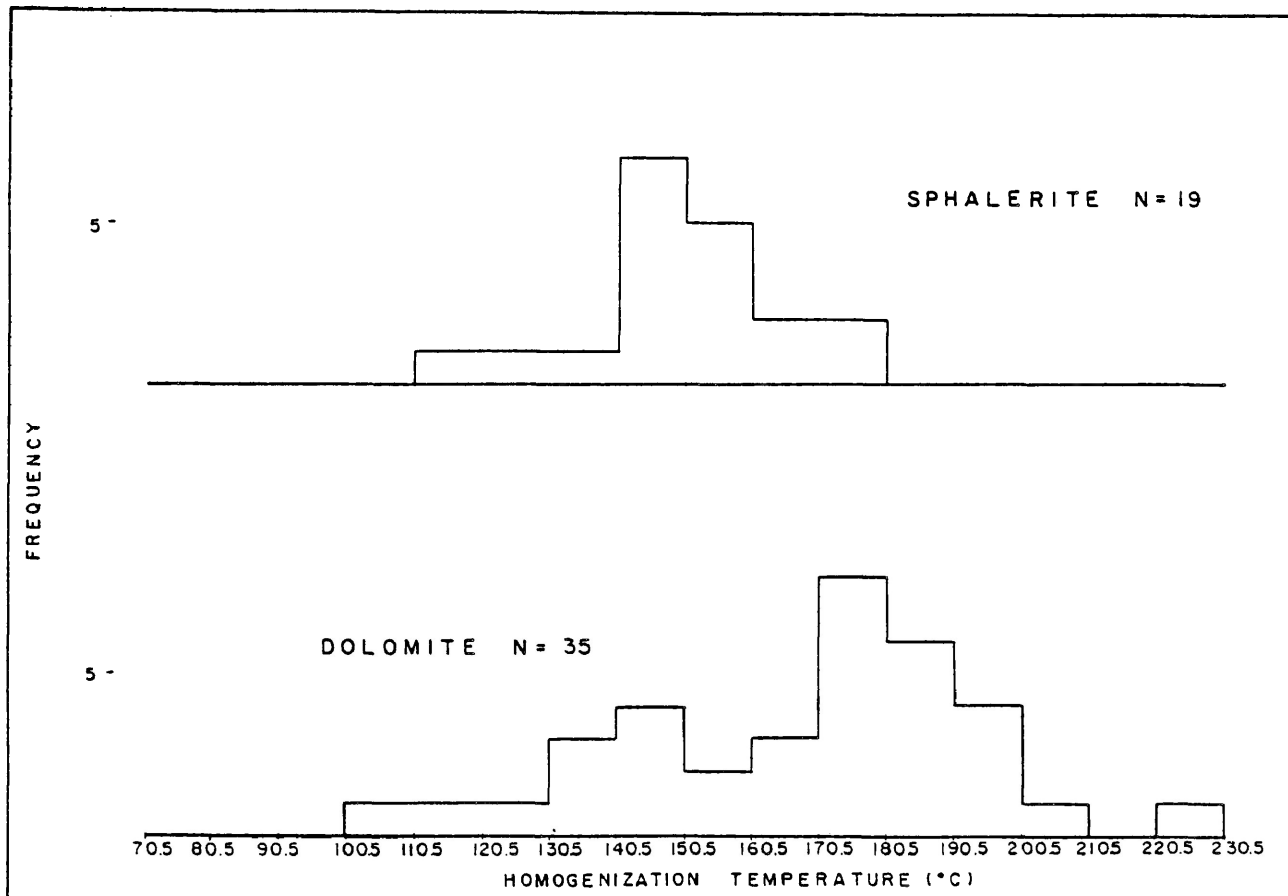
FIGURE 4.7b - DISTRIBUTION OF HOMOGENIZATION DATA FOR UNIT 2.
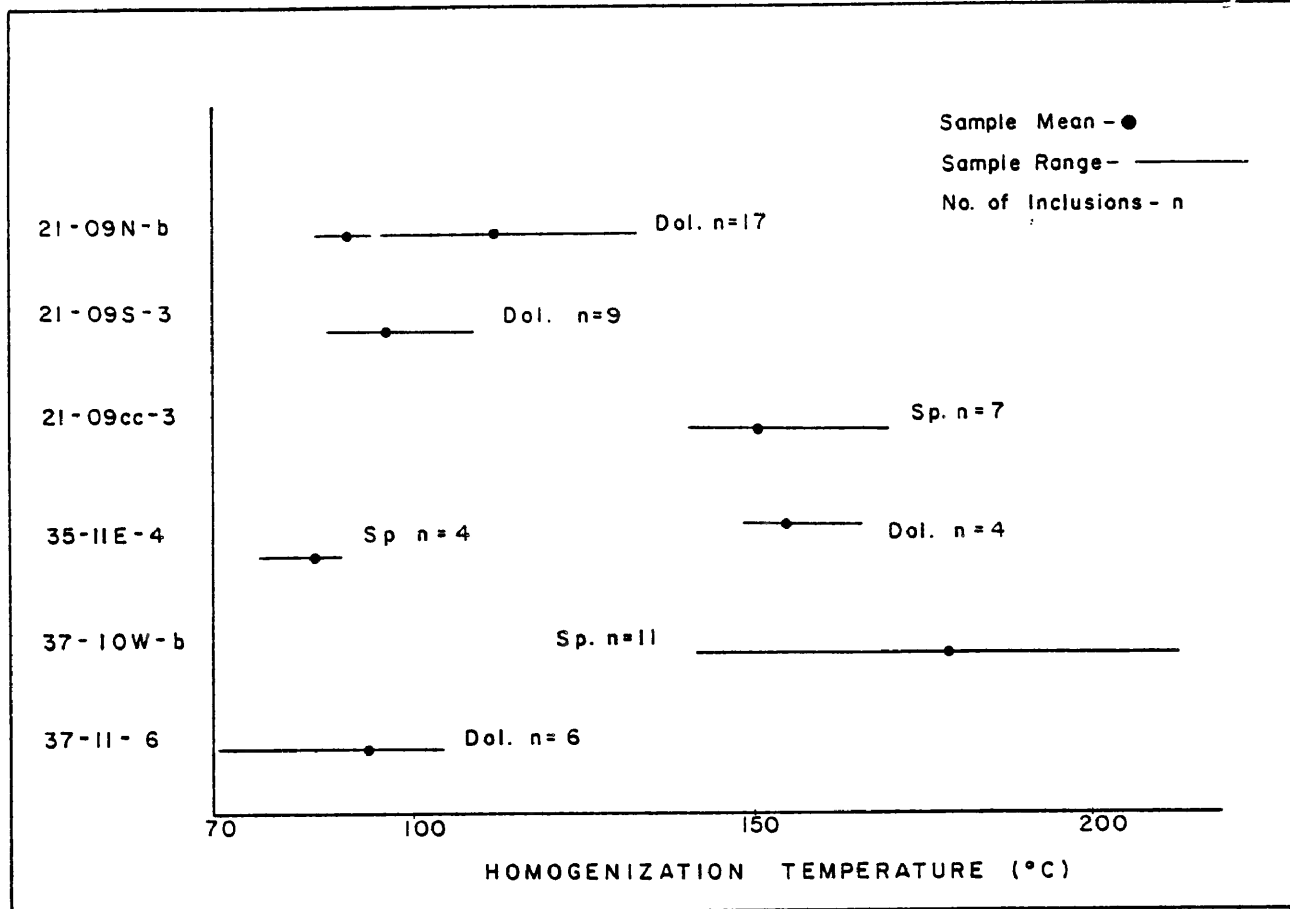
FIGURE 4.8a - SUMMARY OF FLUID INCLUSION DATA FOR UNIT 3.
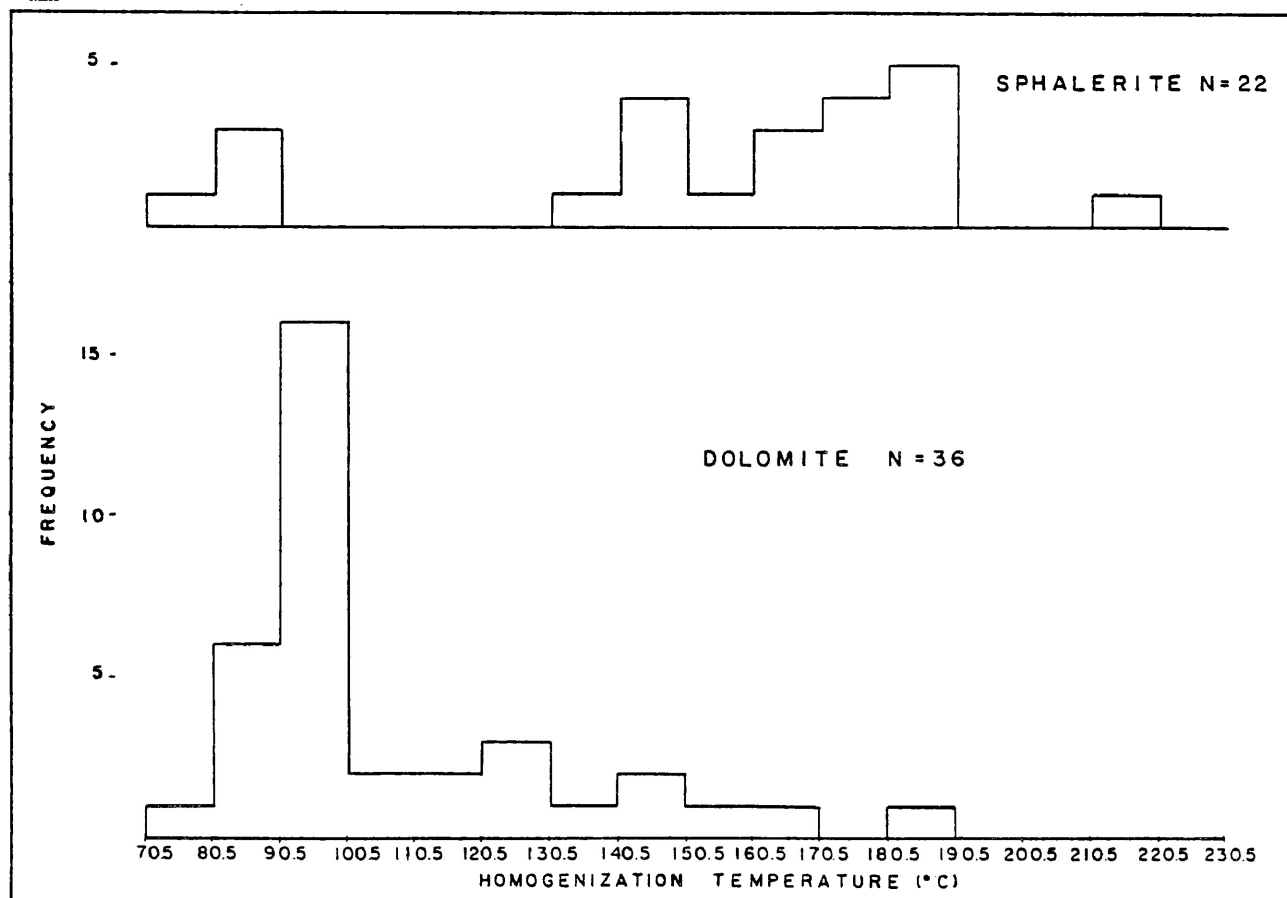
FIGURE 4.8b - DISTRIBUTION OF HOMOGENIZATION DATA FOR UNIT 3.
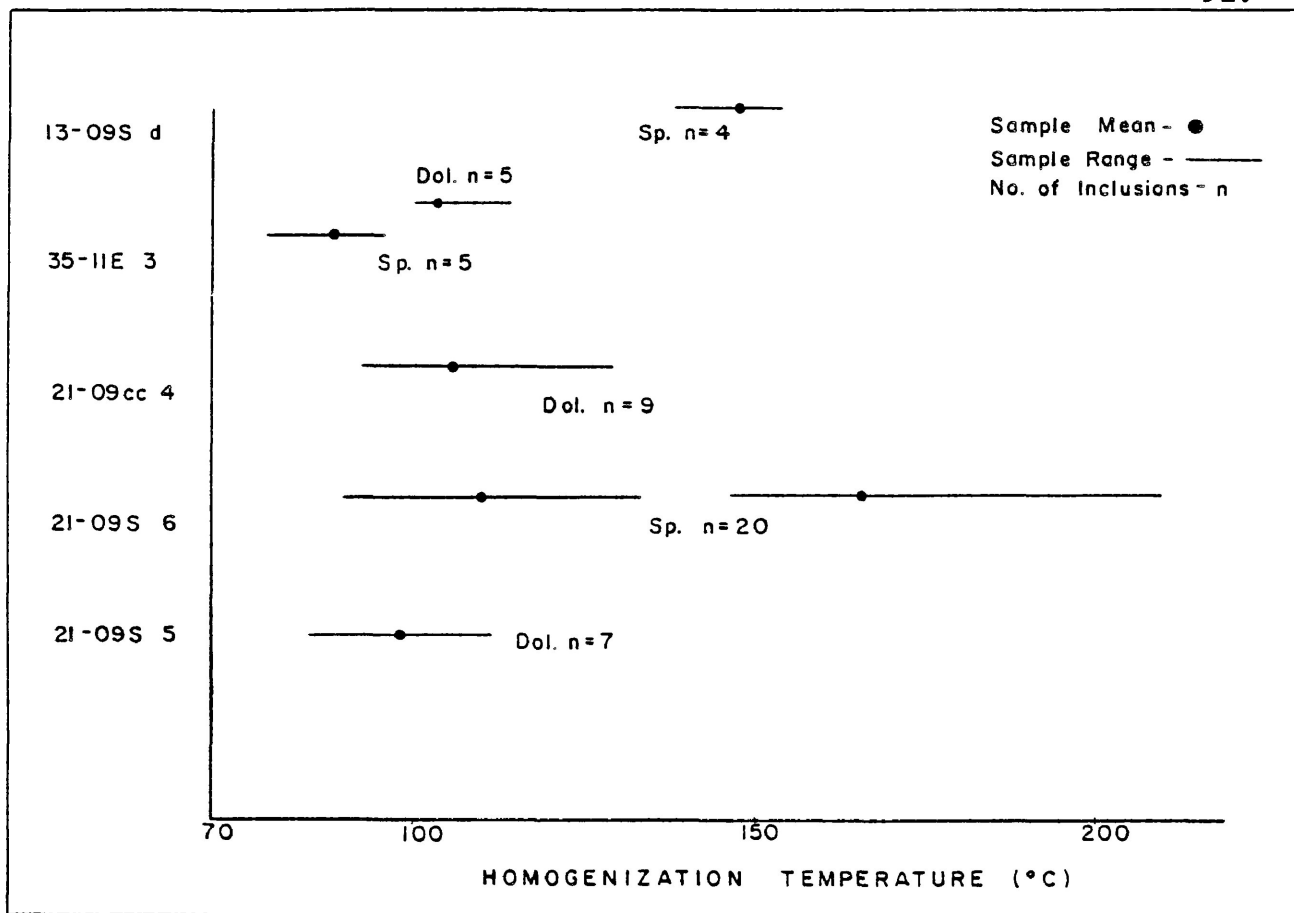
FIGURE 4.9a - SUMMARY OF FLUID INCLUSION DATA FOR UNIT 4.
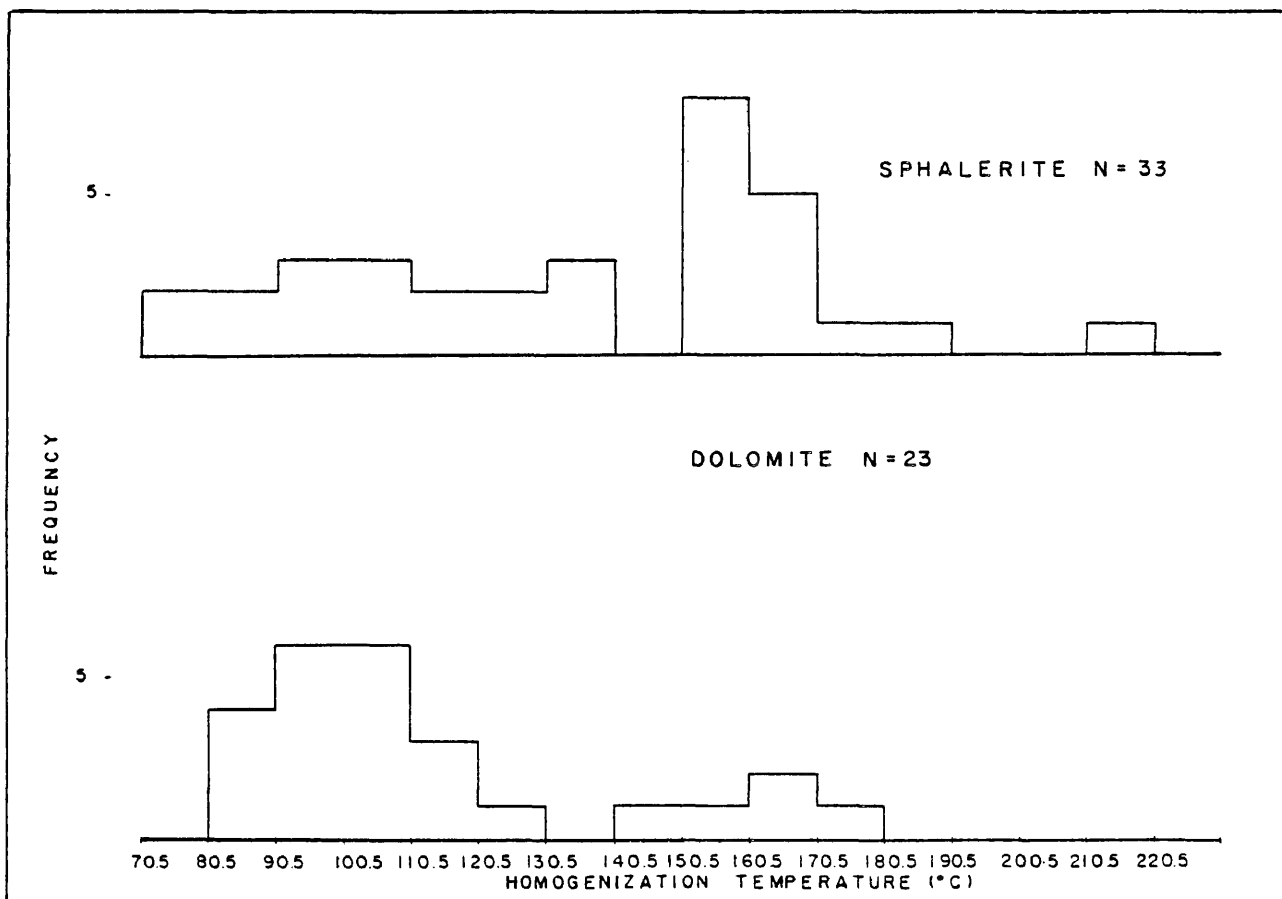
FIGURE 4.9b - DISTRIBUTION OF HOMOGENIZATION DATA FOR UNIT 4.

dolomite analyzed was interstitial to sulfides and therefore clearly postdates the main period of sulfide deposition. Although much of the data from sphalerite are from pseudo-secondary inclusions, the similarity of the high-temperature population to data from other mine units suggests that they may reflect the conditions of sphalerite formation. Primary inclusions from recrystallized interstitial dolomite in sample 21-09S#5 homogenized at anomalously high temperatures in excess of 200°C and may reflect the movement of a late, high-temperature fluid. Numerous other samples in the immediate area failed to share these high temperatures, suggesting that this high-temperature fluid was very localized.

Little information could be gathered on Unit 5 due to its poor exposure in the mine. The small amount of homogenization data collected came from two hand samples and suggests higher temperatures for pseudo-secondary inclusions from sphalerite than for primary inclusions from interstitial dolomite (Figure 4.10). Homogenization temperatures for four hand samples from Unit 6 are also illustrated in Figure 4.10. Interstitial and interbanded dolomite yielded homogenization temperatures primarily around 165°C, although a number of inclusions homogenized at temperatures less than 100°C. Primary inclusions in interstitial and interbanded sparry dolomite homogenized at both high and low temperatures, indicating that the bimodal distribution of homogenization data from Unit 6 is not related to different generations of sparry dolomite. Homogenization temperatures from secondary
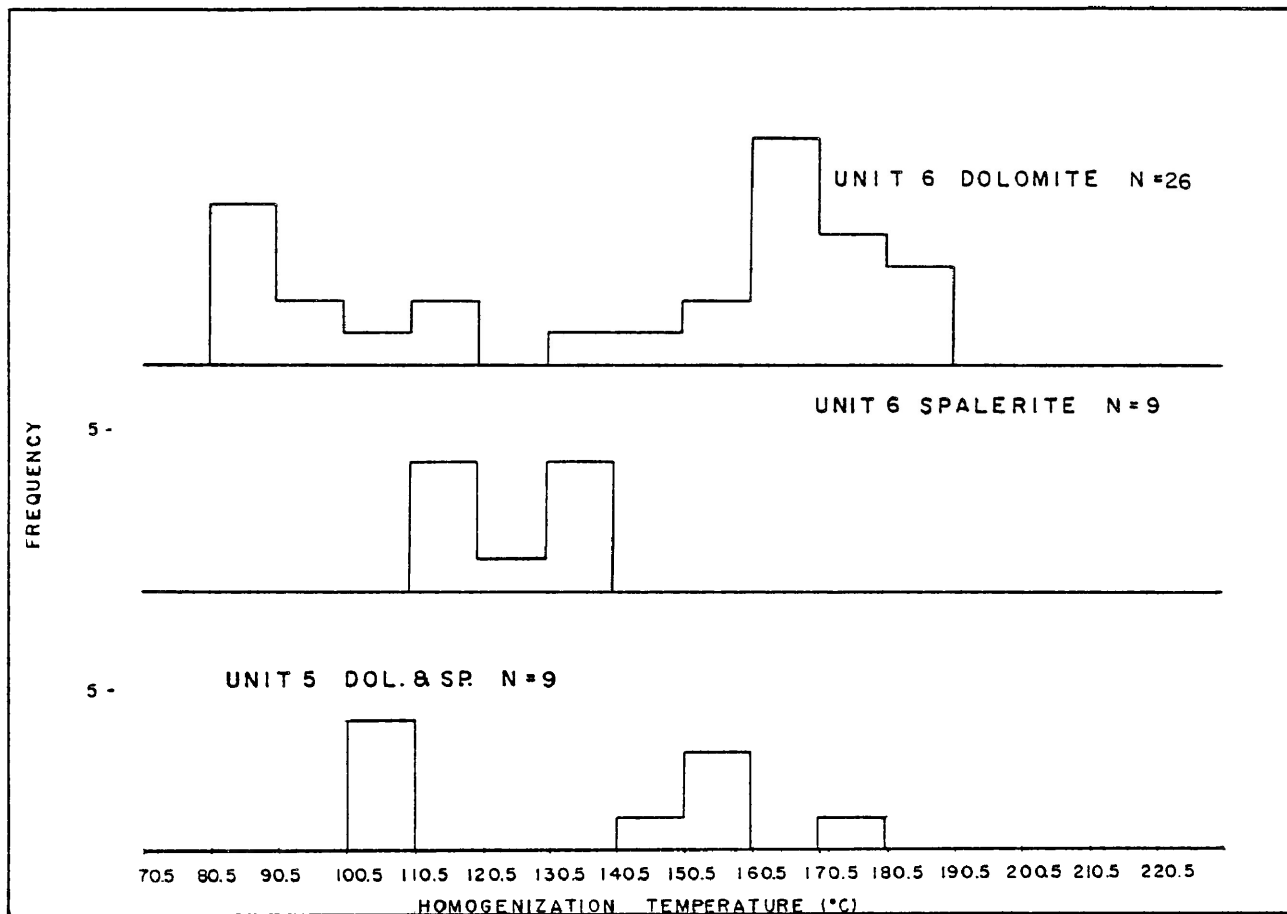
FIGURE 4.10 - SUMMARY OF FLUID INCLUSION DATA FOR UNITS 5 & 6.
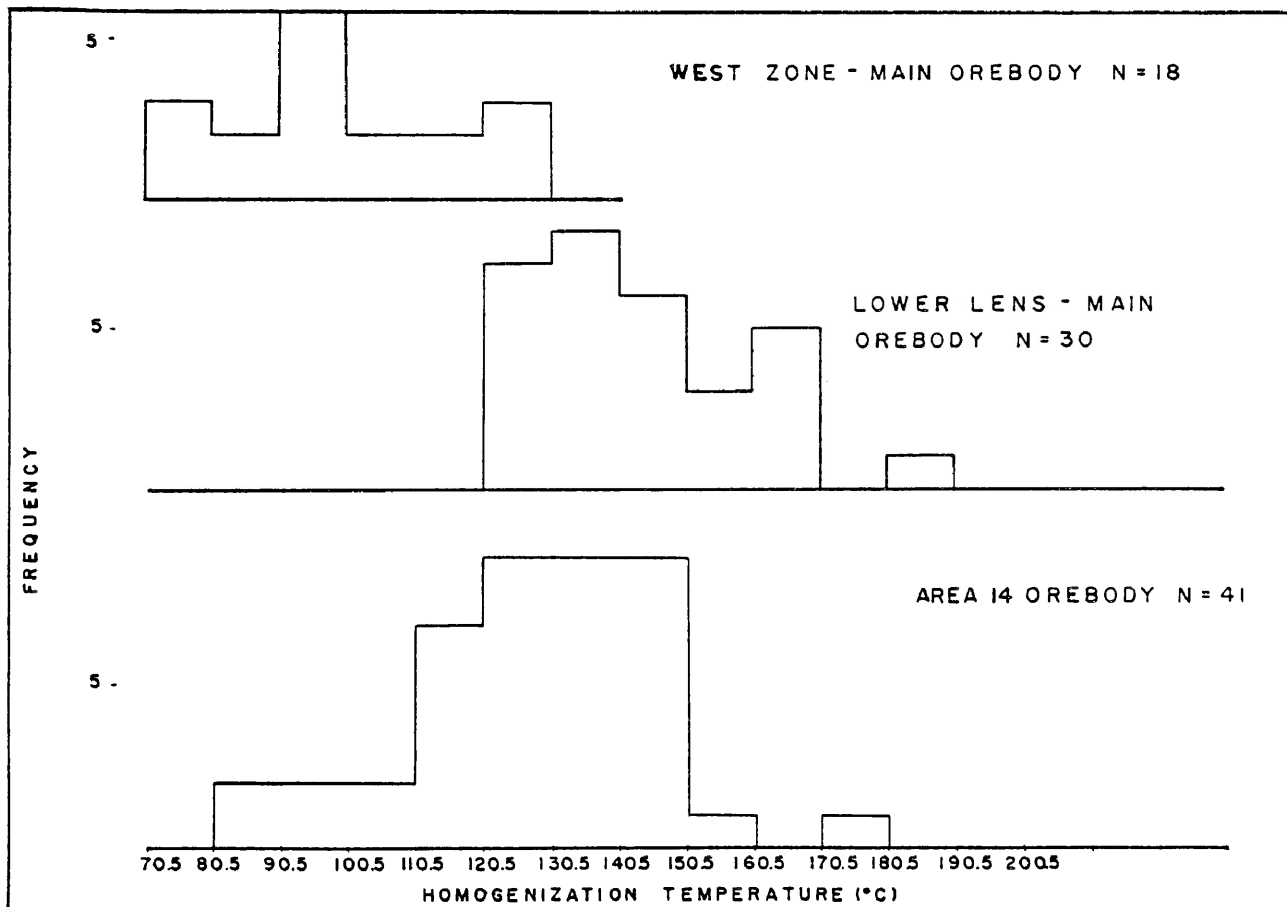
FIGURE 4.11 -DISTRIBUTION OF HOMOGENIZATION DATA FOR THE WEST ZONE, THE LOWER LENS, AND THE AREA 14 OREBODY.

and pseudo-secondary inclusions in sphalerite are typically less than 130°C and probably reflect a late ore fluid.

Due to the dark colour of sphalerite examined from the Keel Zone, no homogenization temperature data is available for this portion of the Main Orebody.

Western Portion of the Upper Lens

Results from 19 inclusions analyzed from the western Upper Lens between crosscuts 5 and 7 are listed in Table 4.1 and illustrated graphically in Figure 4.11. Homogenization temperatures from late, interstitial dolomite ranged from 79 to 118°C and are slightly lower than values obtained from pseudo-secondary inclusions in sphalerite. In general, homogenization temperatures are considerably lower than those from the central and eastern portions of the Upper Lens.

Shale Zone

Data from 33 inclusions in dolomite and sphalerite from the Shale Zone are presented in Table 4.1. As a group, the homogenization temperatures are anomalously high, with the highest values being found within approximately 30 m of the matic dike (sample 09-07S-A). Inclusions in sphalerite from sample 09-07S-A appear primary, but often have a negative crystal habit similar to that reported by Bending (1984) in sphalerite immediately adjacent to the dike.

Lower Lens

Suitable fluid inclusions for study occurred in only a few samples from the lower decline. No data was obtained from the drill hole samples (U21/20, U21/14, U37/4). Homo-

genization temperatures obtained from 30 primary inclusions in dolomite veins cutting ore are listed in Table 4.1 and illustrated graphically in Figure 4.11. Temperatures obtained from the lower decline are significantly lower than those obtained by McNaughton (1983) from drill core through the eastern portion of the Lower Lens, although they are similar to values generally found in the Upper Lens. One sample, LD 525, of very coarse-grained sphalerite rimming a vein of white rock in the lower decline contained primary and pseudo-secondary inclusions that failed to homogenize at temperatures in excess of 380°C. These anomalous temper-tures suggest that the sphalerite has been affected by a very high-temperature event related to the emplacement of white rock. As in the case of the Shale Zone, partial recrystal-lization rather than stretching would best explain the high homogenization temperatures because, as pointed out by Bodnar and Bethke (1984), brittle minerals such as sphalerite tend to decrepitate during overheating.

Area 14 Orebody

A total of 40 inclusions analyzed from the Area 14 Orebody included 9 pseudo-secondary inclusions in sphalerite and 31 primary inclusions from interstitial dolomite. The results are presented in Table 4.1 and Figure 4.11. Although the majority of inclusions are from the central sphalerite zone, data from sample 3-11-A do not suggest any drastic difference in temperature for the lower pyritic zone. Sample 5SW-A occurs where the sphalerite horizon downcuts through

the lower pyritic zone and passes beneath the crosscut floor. These downward extensions of the ore zone are also relatively rich in lead but appear to have formed at the same temperature as the rest of the Area 14 Orebody. The homogenization temperatures from dolomite agree well with the average temperature of 141.6°C obtained from dolomite associated with barren sulfide mineralization in Area 14 West (Bending, 1984).

Freezing Studies

Due to limited access on the heating/freezing microscope, only a small amount of information concerning freezing behavior was obtained. Freezing data are summarized in Table 4.2.

Table 4.2: Fluid Inclusion Freezing Point Depression (°C)

Sample	Tm	r	S	Te	N	Type	Mineral
21-09cc#3	-35.0	-21 to -41	10.0	ND	4	P	Sp
21-09S#5	-18.0	-16 to -21	2.6	-45	3	P	Dol
35-11E#1	-28.3	-28 to -28.5	ND	-46	2	P	Dol

Tm — Mean temperature of last melting of ice
r — Range in Tm
S — Standard deviation of Tm
Te — First melting of ice (eutectic)
N — Number of inclusions
P — Primary inclusions
ND — Not determined.

The salinity of the inclusion fluid may be calculated using the following equation from Potter et al (1978):

$$Ws = 1.76958 \; \theta - 4.2384 \times 10^{-2} \theta^2 + 5.2778 \times 10^{-4} \theta^3 \pm 0.0028$$

where θ = freezing point depressions (Tm) in °C and Ws is the salinity in weight percent NaCl equivalent. Measured freez-

ing point depressions indicate a range of salinity from 19.6 wt.% to 37.6 wt.% NaCl eq. However, eutectic melting points around $-45°C$ indicate the presence of cations other than Na^+, such as $Ca^{2+}$and Mg^{2+}. The eutectic point of the $CaCl_2-H_2O$ system occurs at $-49.8°C$ (Crawford, 1981), suggesting that the predominant salt present in inclusions at Nanisivik is $CaCl_2$, although appreciable Mg^{2+} is probably also present.

4.4   Pressure Correction

The presence of Ca^{2+}, and possibly Mg^{2+}, as the dominant cations in the inclusion fluids does not preclude the direct application of the pressure corrections calculated by Potter (1977) for inclusions of the $NaCl-H_2O$ system homogenizing to the liquid phase (Roedder, 1984). However, there is some uncertainty concerning the pressure of ore deposition. Olson (1977) estimated that the pressure of ore deposition may have varied between 300 and 900 bars corresponding to hydrostatic and lithostatic pressures, respectively. For a 25 wt.% NaCl eq. solution, this estimated pressure range corresponds to a range of pressure correction from $30°$ to $88°C$ at a homogenization temperature of $150°C$ (Potter, 1977). The presence of open-space filling textures at Nanisivik suggests that the pressure of ore formation was hydrostatic, in which case the estimated pressure correction to be applied would be on the order of $+30°C$. Given the uncertainties regarding the application of the pressure correction, inclusion data have been presented as homogenization temperatures

with the understanding that these values represent an absolute minimum for the temperature of trapping. However, in the discussion of the temperature of ore formation to come, the pressure correction will be taken into consideration.

As a range of salinity from 20 to 37 wt.% $CaCl_2$ eq. is indicated by the freezing studies, it is of interest to consider what effect a similar range of salinities has on the pressure correction to be applied to the $NaCl-H_2O$ system at 150°C and 300 bars pressure. For example, a 25 wt.% NaCl eq. solution requires a pressure correction of 30°C, while a 15% NaCl solution requires as much as 45°C. Assuming that the behavior of the Nanisivik fluid inclusions is approximated by the $NaCl-H_2O$ system at 150°C and 300 bars pressure, it is unlikely that the range in salinities encountered would account for more than a 15°C spread in homogenization temperatures.

CHAPTER 5: SULFUR ISOTOPIC COMPOSITION OF PYRITE

5.1   Introduction

Much information may be obtained from the sulfur isotopic composition of sulfides concerning fluid source and the physio-chemical conditions of ore formation. The isotopic composition of sulfides in hydrothermal ore deposits, in terms of $\delta^{34}S$‰., depends upon the initial isotopic composition of total dissolved sulfur in the ore fluid, the temperature, and the dominant sulfur species in the ore fluid. The latter is in turn related to total dissolved sulfur, oxygen fugacity, pH and temperature (Ohmoto, 1972; Rye and Ohmoto, 1974; Ohmoto and Rye, 1979). Once the parameters that influence isotopic fractionation are known, the composition of sulfides or sulfate in an ore deposit can be used to suggest a source for the sulfur. For example, the composition of seawater sulfate is generally indicated by highly positive $\delta^{34}S$ values, although its exact nature has varied throughout geologic time and is influenced by the amount of circulation that has occurred in the basin. A wide range of $\delta^{34}S$ values is suggestive of bacterial activity, while values near 0‰. suggest a mantle source (Brownlow, 1979).

Fractionation among co-existing sulfur phases is largely dependent upon temperature, allowing sulfide pairs

such as galena and sphalerite to be used as geothermometers where these minerals can be shown to have been deposited in equilibrium with no subsequent isotopic re-equilibriation between phases. Fractionation increases with decreasing temperature and is therefore more useful in the study of low temperature deposits. Rye (1974) evaluated the accuracy of sulfur isotope fractionation temperatures using the theoretical fractionation curve of Czamanske and Rye (1974) by comparison with fluid inclusion filling temperatures. Sulfur isotope fractionation temperatures were reported to be within 40°C of the pressure-corrected filling temperatures above 200°C. Inherent error in the use of sulfur isotope geothermometry, due to uncertainty concerning the calculated fractionation curves, is considered to be ±20°C for gn-sp pairs and ±25°C for py-gn pairs (Ohmoto and Rye, 1979).

Much of the error in sulfur isotope geothermometry involves assumptions concerning equilibrium, mutual crystal boundaries notwithstanding. However, for any given tempera-ture below approximately 800°C, whether it is known by other means or not, the relative fractionation between more than two co-existing sulfur phases should be constant if equilibrium was attained. Several recent sulfur isotope studies indicate that co-existing sulfides are often not deposited in equilibrium (Williams and Rye, 1974), a feature that may be characteristic of very low temperature hydro-thermal deposits (Rye, 1974; Ohmoto and Rye, 1979). Large variations in the isotopic values of co-existing sulfides

from southeast Missouri observed by Sverjensky *et al,* (1979) could not be attributed to the normal processes of fractionation. These differences probably reflect variations in the conditions of ore formation, a conclusion that is also indicated by variations of up to 8% in the $\delta^{34}S$ values of single crystals.

The sulfur isotopic composition of a single mineral phase may be used to study variations throughout an orebody (Williams and Rye, 1974; Willan and Coleman, 1983; Sverjensky *et al,* 1979). Observed variations may be related to temperature fluctuations, a variable source of sulfur and/or the mixing of several sources, or changes in the dominant sulfur species. For the purposes of this study pyrite was chosen for analysis because of its wide distribution in the paragenetic sequence and the large, pure crystals which it has formed. However, pyrite shows little fractionation relative to a H_2S source due to temperature (Figure 5.1) and will therefore not be very sensitive to temperature fluctuations. Also, there is some uncertainty concerning the fractionation of pyrite at temperatures less than 200°C as this information has been extrapolated from higher temperature experimental data.

5.2   Experimental Technique

Pyrite grains were hand picked from sixteen pyrite samples from the Main Orebody and the Area 14 Orebody. The
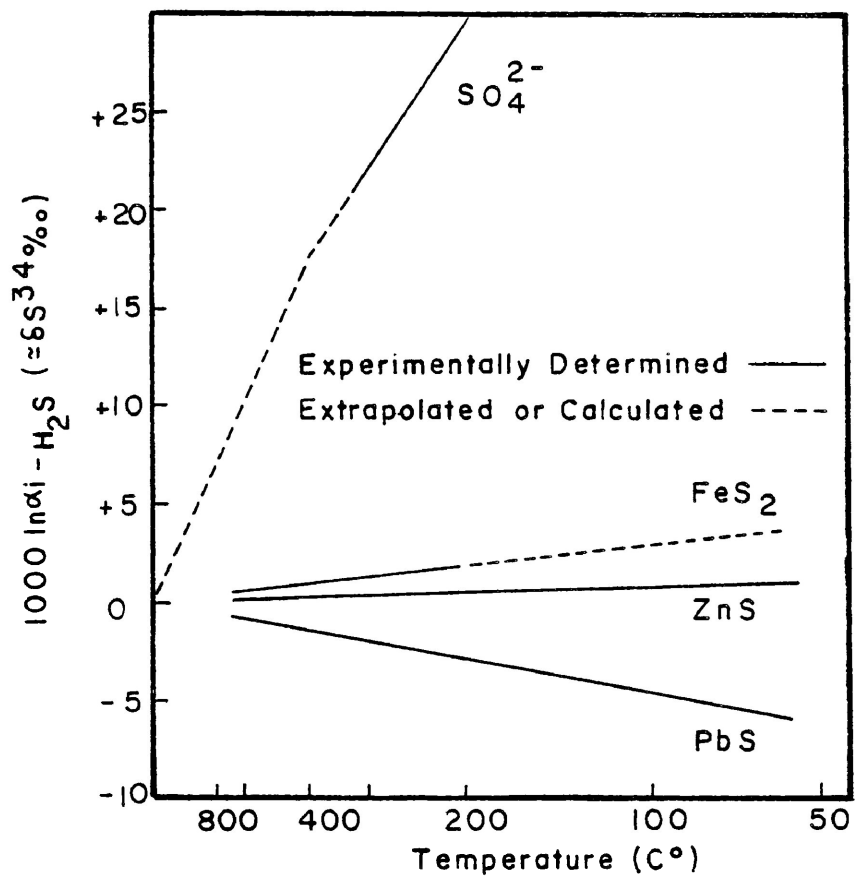
FIGURE 5.1 - FRACTIONATION OF BASE METAL
SULFIDES RELATIVE TO H_2S (AFTER OHMOTO
AND RYE, 1979).

pyrite samples were cleaned in warm, dilute HCL to remove any dolomite contamination. Material sampled included both cubic and bladed pyrite varieties from the main and late stages of ore mineralization. Analyses were performed by the Geochron Laboratories Division of Krueger Enterprises, Inc., Cambridge, Massachusetts. Canon Diablo troilite having an isotopic ratio of $^{34}S/^{32}S$ = 0.0450045 (Ault and Jensen, 1963) was used as a standard. Results are presented in Table 5.1. Duplicates of sample 2 analyzed to evaluate precision indicate excellent reproducibility. The typical level of un-certainty for sulfur isotope analysis is 0.2‰. (Ohmoto and Rye, 1979). The purity of samples having $\delta^{34}S$ > +28.0‰. or $\delta^{34}S$ < +27.0‰. was checked by examining polished mounts of material returned by the laboratory.

5.3   Experimental Results

Late, vug filling iron sulfide from the Main Orebody ranges in $\delta^{34}S$ from +27.4‰. to +28.0‰., giving a mean value of +27.76‰.. Iron sulfide from main-stage mineralization in the Upper Lens of the Main Orebody ranges from +27.4‰. to +27.9‰., giving a mean value of +27.72‰.. These analyses in-clude both inverted marcasite and cubic pyrite crystals. Pyrites from the Upper Lens are from different mine units and represent a vertical sequence through the orebody, but no trend in the isotopic composition of pyrite is apparent. A single sample of pyrite from the Keel Zone in the vicinity of

TABLE 5.1 - SULFUR ISOTOPE COMPOSITION OF PYRITE

SAMPLE	DESCRIPTION	^{34}S ‰
1	Late, vug-filling bladed pyrite	+ 27.4
2	Late, vug-filling bladed pyrite with stepped cubic habit	+ 27.4 + 27.4
3	Cubic pyrite from vug	+ 27.8
4	"Flaky" pyrite replacing dolostone	+ 27.6
5	Band of massive pyrite from which blades of pyrite project	+ 28.0
6	21 - 09cc #2; Coarse, tabular pyrite after marcasite in a sparry dolomite matrix	+ 27.9
	21 - 09cc #1; Tabular to massive pyrite with interstitial sparry dolomite (Unit 1)	+ 27.9
8	21 - 09cc #4; Minor cubic pyrite (Unit 4)	+ 27.4
9	21 - 09cc #5; Fine-grained pyrite interbanded with sphalerite and sparry dolomite (Unit 6)	+ 27.9
10	21 - 09S #3; Bladed pyrite interbanded with pyrite, sphalerite and sparry dolomite (Unit 3)	+ 27.5
11	21 - 09S #7; Massive pyrite band in coarsely banded ore (Unit 5)	+ 27.9
12	Keel Zone #1; Massive pyrite with trace pyrrhotite and sphalerite	+ 27.9
13	Area 14/ 3 - 11 A; Massive pyrite intergrown with sparry dolomite	+ 27.1
14	Lower Lens/ LD 60N; Massive pyrite interstitial to dolostone breccia fragments	+ 28.2
15	Lower Lens/ U21 - 14 (8m); Massive pyrite with interstitial sparry dolomite	+ 28.2
16	21 - 09S #6; Massive pyrite (Unit 4) * Contains 5 - 10% fine-grained sphalerite	+ 24.2 + 23.9

pillar 19 has a value of +27.9‰.. Two pyrite samples from the Lower Lens both give values of +28.2‰., suggesting that the Lower Lens is slightly enriched in ^{34}S relative to the Upper. A sample from the Area 14 Orebody yielded an isotopic composition of +27.1‰., slightly lower than the values obtained for the Main Orebody. The pyrite sample from Area 14 was examined for contamination and found to contain trace (<1 vol.%) sphalerite, but this is not considered to have greatly affected the analysis. Geochron Laboratories re-analyzed sample 16 to confirm the low value obtained. The duplicate analysis lies outside the expected level of uncertainty, reflecting inhomogenaity within the sample. Examination of the returned material indicates that sample 16 was contaminated with 5-10 vol.% sphalerite.

CHAPTER 6:   ORGANIC CHEMISTRY

6.1   Introduction

An association between organic matter and certain ore deposits has long been noted (Saxby, 1976), and an association with deposits of the Mississippi Valley Type appears to be quite common (Roedder, 1984). Hydrocarbons are present as: inclusions from the Cave-in-Rock Fluorspar District (Brecke, 1962) and Hansonburg, New Mexico (Norman, et al., 1985); petroleum globules at Pine Point (MacQueen and Powell, 1983) and the Tri-State District, U.S.A. (Dunsmore and Shearman, 1977); and solid bitumens at North Derbyshire, England (Pering, 1973), the Cave-in-Rock Fluorspar District, Illinois (Brecke, 1962), Robb Lake, British Columbia (MacQueen and Thompson, 1978), the Woodcutters Prospect, Australia (Saxby, 1976), the Polaris lead-zinc mine (Jowett, 1975), the Metaline District, Washington (McConnel and Anderson, 1968), the Viburnum Trend, Missouri (Sverjensky, 1981), Gays River, Nova Scotia (Akande and Zentilli, 1984) and Gayna River, N.W.T. (Hardy, 1979). A bitumen identified as grahamite is reported from the Illinois-Kentucky mining district (Grogan and Bradbury, 1981).

Organisms, particularly sulfate reducing bacteria, may be directly involved in the formation of certain syn-sedimentary and diagenetic ores (Trudinger, 1976). However,

the main significance of organic matter associated with epigenetic orebodies of the Mississippi Valley Type is as a potential reducer of sulfate (Barton, 1967). The possible role of organic matter has recently received much attention, particularly following the Orr experiments (1975, 1982) in which the processes of sulfate reduction were examined. The exact timing of sulfate reduction may vary (Anderson, 1979) and, as pointed out by Anderson (1983, 1984) and Barnes (1983), whether or not sulfate reduction occurs at the point of ore deposition should have a profound effect on ore textures.

In addition to the visible solid bitumen associated with ore at Nanisivik noted by Olson (1977), several microscopic occurrences also appear to be present. Dark brown to colourless suspected hydrocarbons occur in pseudo-secondary inclusions in sphalerite, where they may either completely fill the inclusion or accompany the normal fluid phases (Figures 6.1, 6.2). Some of these inclusions fluoresce under ultraviolet light (Dave Bending, pers.comm., 1984), suggesting the presence of aromatic compounds. As previously discussed, the presence of H_2S and CH_4 in inclusions might also explain the unusual freezing behavior noted by Bending (1984). Hanor (1980) reported that dissolved organic material in fluid inclusions may evolve CH_4 after trapping, resulting in abnormally high inclusion homogenization temperatures. Microscopic globules of suspected organic material were also observed intergrown with sparry dolomite gangue
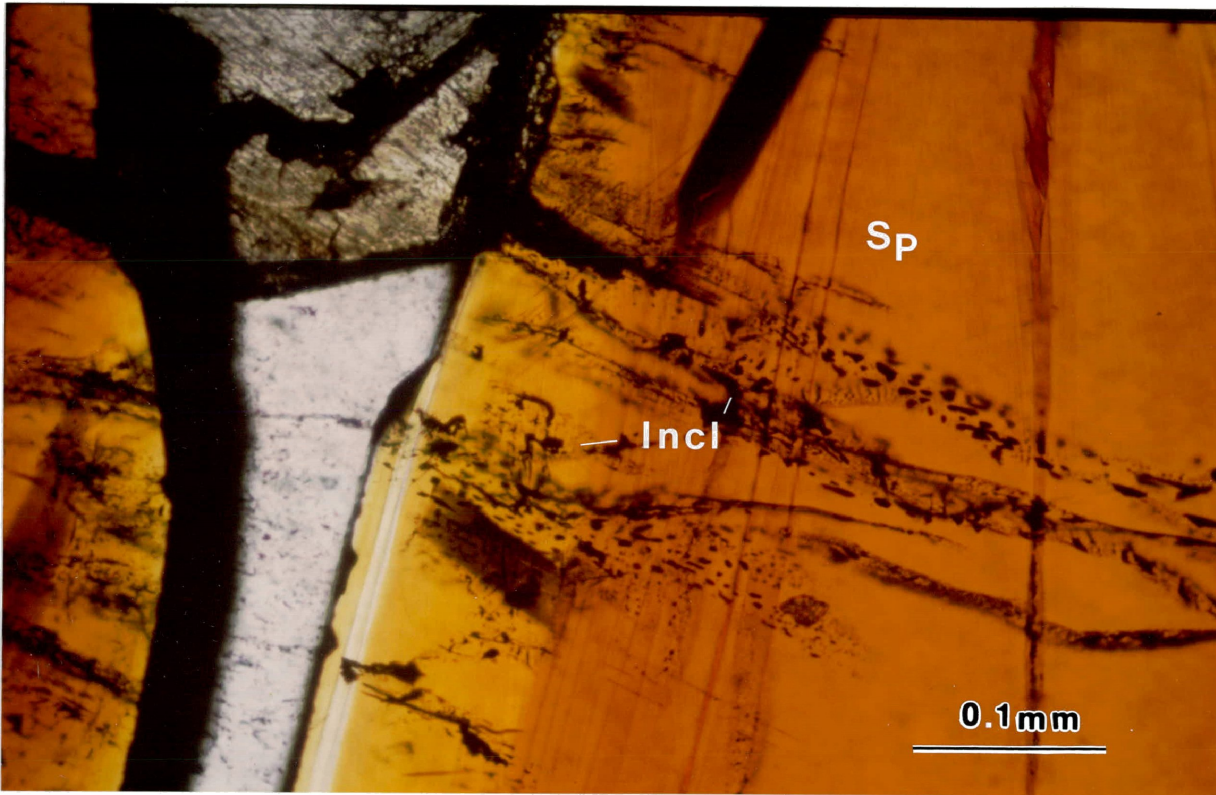
FIGURE 6.1 — SECONDARY PLANES OF POSSIBLE HYDROCARBON — BEARING INCLUSIONS.
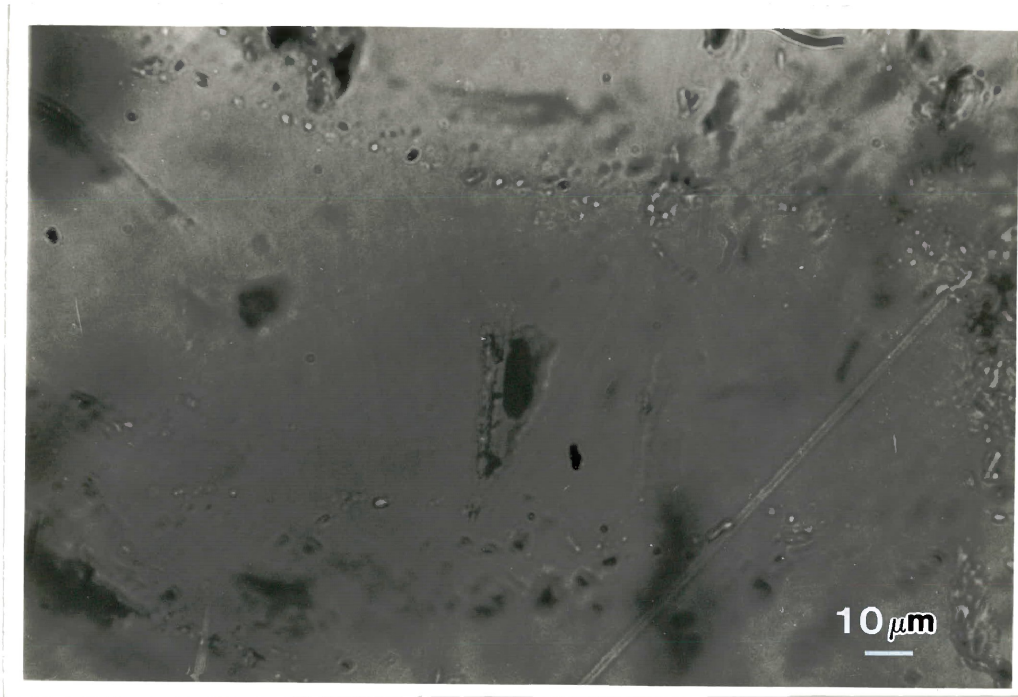
FIGURE 6.2 – HYDROCARBON (?) GLOBULE IN A PRIMARY FLUID INCLUSION IN SPHALERITE.
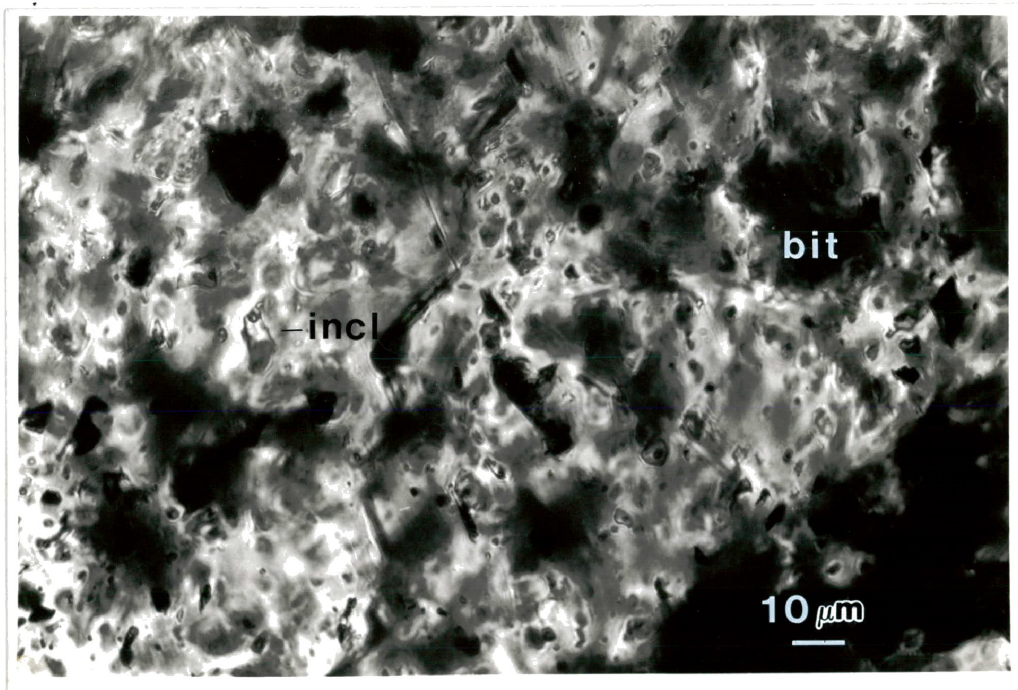
FIGURE 6.3 – SOLID INCLUSIONS OF A BLACK BITUMINOUS (bit) MATERIAL IN DOLOMITE. TWO – PHASE FLUID INCLUSIONS (incl) ALSO INDICATED.

(Figure 6.3). Cathodoluminescence indicates that the hydro-carbons in dolomite often occur along growth bands (Dave Bending, pers.comm., 1984). Occasionally, partings in dolo-mite contain a light brown film of possible organic material.

Bituminous substances may be differentiated by their solubility in organic solvents. Those organics that are soluble may be further characterized by infrared absorption, mass spectrometry and gas chromatography. Insoluble organics are characterized by infrared absorption, X-ray diffraction and elemental analysis (Saxby, 1970; Kwiatkowski, 1975). Thermal degradation releases CH_4 and H_2S from bitumen (Saxby, 1976) so the H/C ratio may be used to indicate the degree of maturation (Jiamo, 1979).

6.2   Experimental Technique

Extraction of Soluble Hydrocarbons

An attempt was made to extract and identify hydro-carbons using a solvent extraction technique described by Powell (1978) and MacQueen and Powell (1983). Four samples were crushed to -100 mesh and extraction attempted on a 10 g sample in a Soxhlet apparatus for approximately 24 hrs. Three of the four samples used were from the Main Orebody and represented the microscopic occurrences mentioned previously. A sample of Society Cliffs dolostone was also examined so that a comparison could be made with the Main Orebody. The organic solvent used as an 85/15% mixture of chloroform and

methanol, although pure benzene was used in one attempt. An attempt was also made to dissolve organics in CCL_4 by mixing a small amount of solvent with crushed ore material and waiting overnight. After completion of each extraction experiment, the solvents were scanned on an Infrared Beckman 4250 Spectrometer using halite cells to detect any volatile hydrocarbons present. The remaining solvent was concentrated by evaporation and again scanned on the spectrometer.

Extraction of Insoluble Hydrocarbons

Given the possibility that any bituminous material present might be insoluble in the solvents used, an extraction following the technique of Saxby (1970) was attempted on a sample of Society Cliffs dolostone from near the Main Orebody. For the extraction of insoluble kerogens Saxby (1970) recommended treatment of finely crushed material in 5N HCL to remove carbonates, followed by treatment in 40% HF to remove silicates. Sulfides may be removed using either a strong oxidant (1 part concentrated HNO_3 to 7 parts H_2O) or a strong reductant ($LiAlH_4$). However, due to the presence of sphalerite, it was found that concentrated HCL had to be used for its removal. Nitric acid was chosen to remove pyrite. Although treatment with a strong oxidant will affect the oxygen content of the bituminous material, it should not affect the H/C ratio or the X-ray diffraction pattern (Saxby, 1970). After completion of the acid treatments, the remaining residue was washed with benzene in a sonic bath to remove any sulfur produced by the acid.

Following treatment with concentrated HCL, the residue was dried and a solvent extraction in CCL_4 performed to remove any soluble hydrocarbons. The presence of hydrocarbons in the solvent was detected by infrared spectrometry. The residue remaining after complete acid/benzene treatment was analyzed by infrared spectrometry using a KBr disc preparation technique. The organic residue was also analyzed by X-ray powder diffractometry using $CuK\alpha$ radiation both before and after treatment with HNO_3 to test for the presence of ordered graphite structure. Elemental composition of the organic residue was determined on a Perkin-Elmer 240 Elemental Analyzer. A sample of black bitumen from a sparry dolomite vein in drill core from the Lower Lens was analyzed in a similar fashion for comparative purposes.

Volatiles

An attempt was made to detect the volatile component of fluid inclusions on a Hitachi RM-60 Mass Spectrometer by several different methods. Initial attempts involved crushing sample material in an evacuated syringe attached to the gas intake and heating previously crushed material to thermally decrepitate inclusions. These early attempts were unsuccessful due to the small sample size and atmospheric contamination. A more refined technique involved crushing sparry dolomite in a sealed container with a nitrogen atmosphere. Such a method removes much of the interference on the mass spectrometer resulting from H_2O and O_2 in the atmosphere. Water vapor masks the CH_4 peak, while O_2 interferes with the

H_2S peak due to their similar molecular weights.

6.3   Experimental Results

Extraction of Soluble Hydrocarbons

Analyses of solvents following the organic solvent extraction of the four crushed samples failed to conclusively indicate the presence of hydrocarbon bonding. However, in the concentrated chloroform/methanol extracts from samples 21-09cc#2 and 37-11E#8, minor infrared absorption peaks occurred at 1710-1720 cm and at 2390-2400 cm. The former is in the region of C=O bonding, and probably resultsfrom carboxyl bonds in carbonate-contaminated solvent. No absorption was observed in the region around 3000 cm , which is the area indicative of C-H stretching characteristic of hydrocarbons. Infrared analyses of the CCL_4 solvents after mixing with a small amount of crushed ore also failed to indicate the presence of any hydrocarbon bonding.

Bitumen from the Lower Lens and insoluble residue from the dissolution of Society Cliffs dolostone in HCL show minor infrared absorption in CCL_4 (Figure 6.4). A broad peak at 1550 cm is not characteristic of hydrocarbons and may result from NO_2 bonding. However, a broad peak which is best developed in the insoluble residue, occurs in the region 2800-3000 cm and is indicative of C-H bonding. This hydrocarbon peak is almost negligible in bitumen from the Lower Lens, suggesting that light hydrocarbons have been stripped from

% Transmission

1550

2900
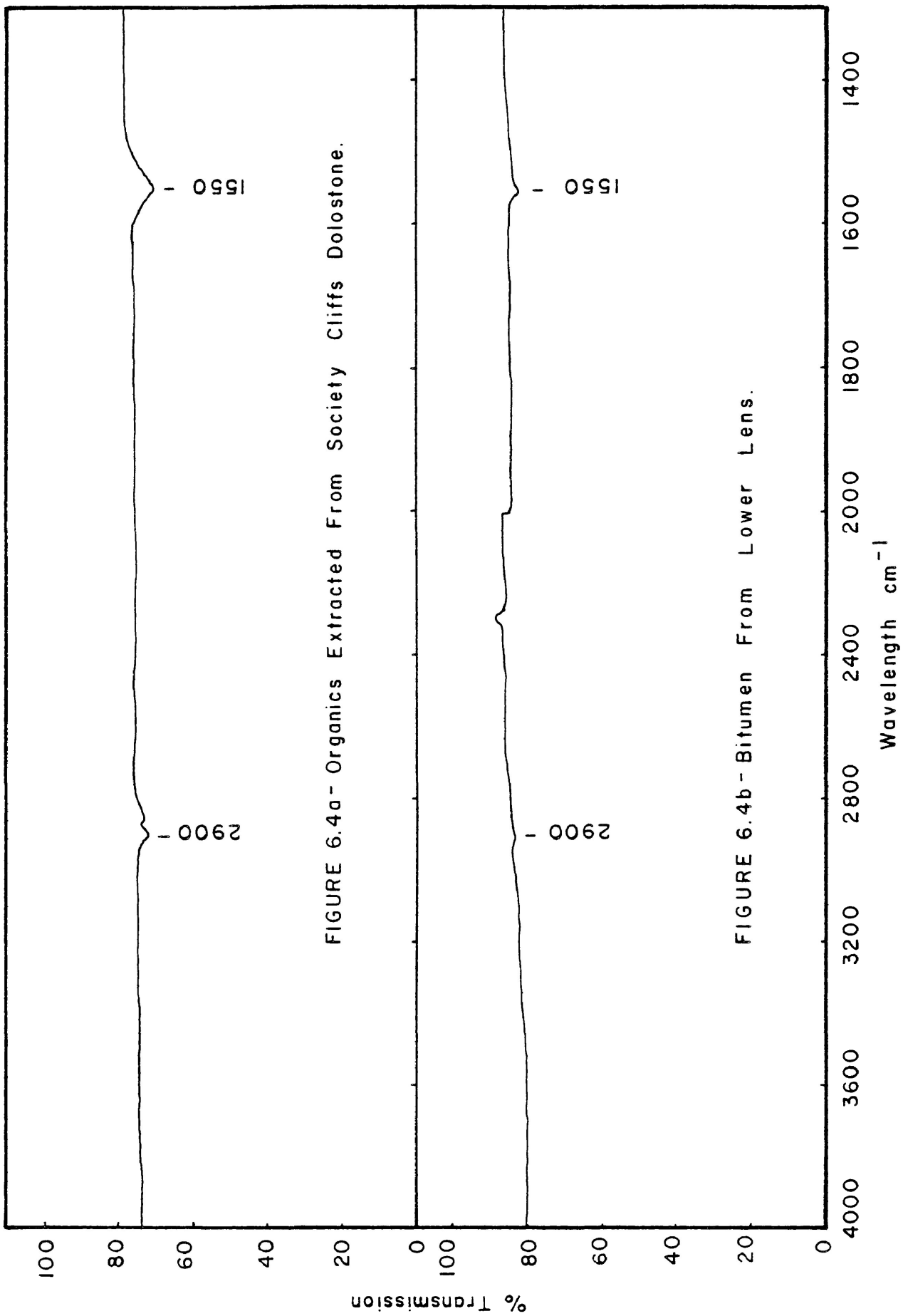
FIGURE 6.4a - Organics Extracted From Society Cliffs Dolostone.

1550

2900

FIGURE 6.4b - Bitumen From Lower Lens.

Wavelength cm^{-1}

FIGURE 6.4 - INFRARED SPECTRA OF CCL$_4$- SOLUBLE HYDROCARBONS IN NANISIVK ORGANICS.

115.

organics associated with ore.

Extraction of Insoluble Hydrocarbons

X-ray powder diffraction patterns from bitumen associated with mineralization and from insoluble residue following complete acid-benzene treatment of Society Cliffs dolostone are illustrated in Figure 6.5. Both patterns are characterized by broad peaks in the 25° to 27° 2θ range and an absence of ordered graphite structure. A broad peak in the 26° 2θ area is characteristic of bituminous coal. A similar diffraction pattern is reported from insoluble kerogen associated with the McArther River Deposit (Saxby, 1970).

Infrared absorption spectra obtained using a KBr disc preparation technique for bitumen associated with mineralization and for the insoluble residue obtained from the acid/benzene extraction of wall rock are presented in Figure 6.6. Both spectra are fairly flat, with steadily decreasing transmission at lower wavelengths. The Lower Lens bitumen sample shows some absorption around 3400 cm while the Society Cliffs bitumen shows little absorption in this region. Comparison with infrared spectra obtained by Kinney and Doucette (1958) for a coalification series indicates that the Nanisivik bitumen has an infrared absorption pattern similar to that of anthracite. Both spectra are consistent with organic material having a very high carbon content (Saxby, 1970).

The bitumen sample from the Lower Lens contains, on average, 74.6 wt.% C, 2.9 wt.% H and 0.6 wt.% N, yielding a H/C atomic ratio of 0.46. Comparison with Table VI from King
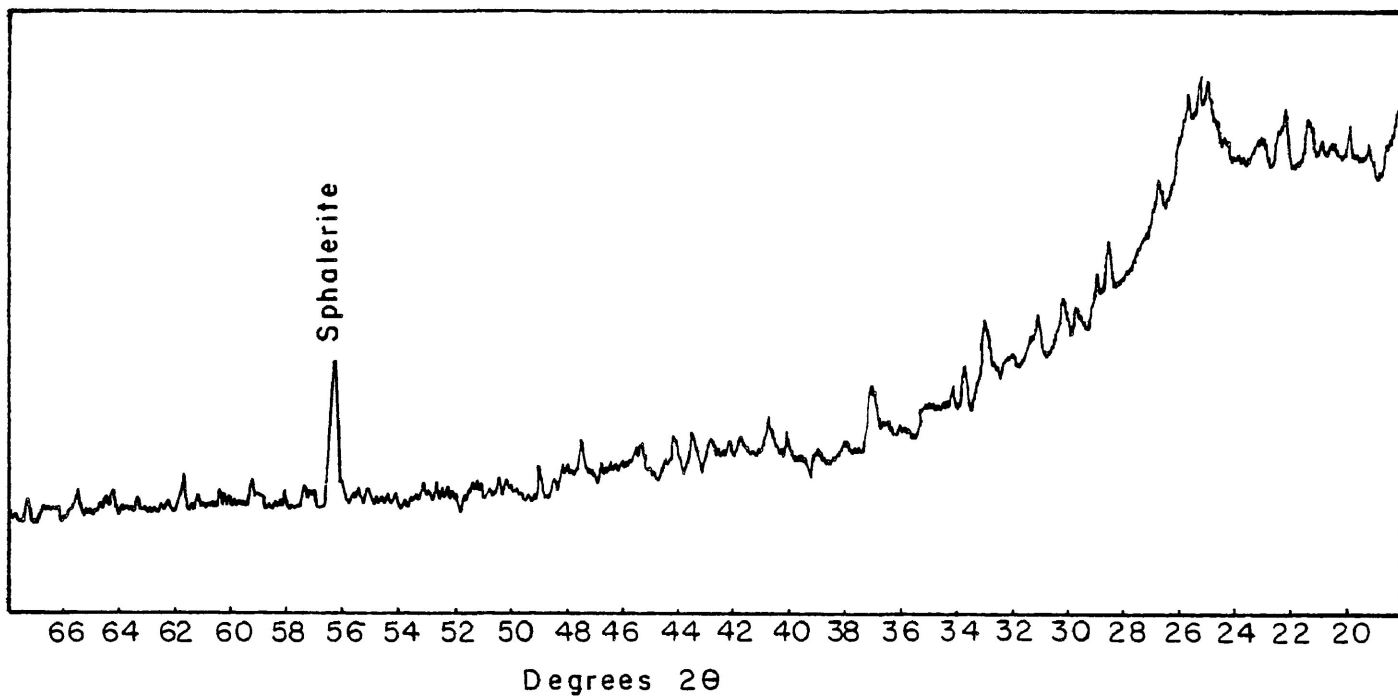
FIGURE 6.5a - X-RAY DIFFRACTION PATTERN OF ORGANICS EXTRACTED FROM SOCIETY CLIFFS DOLOSTONE.
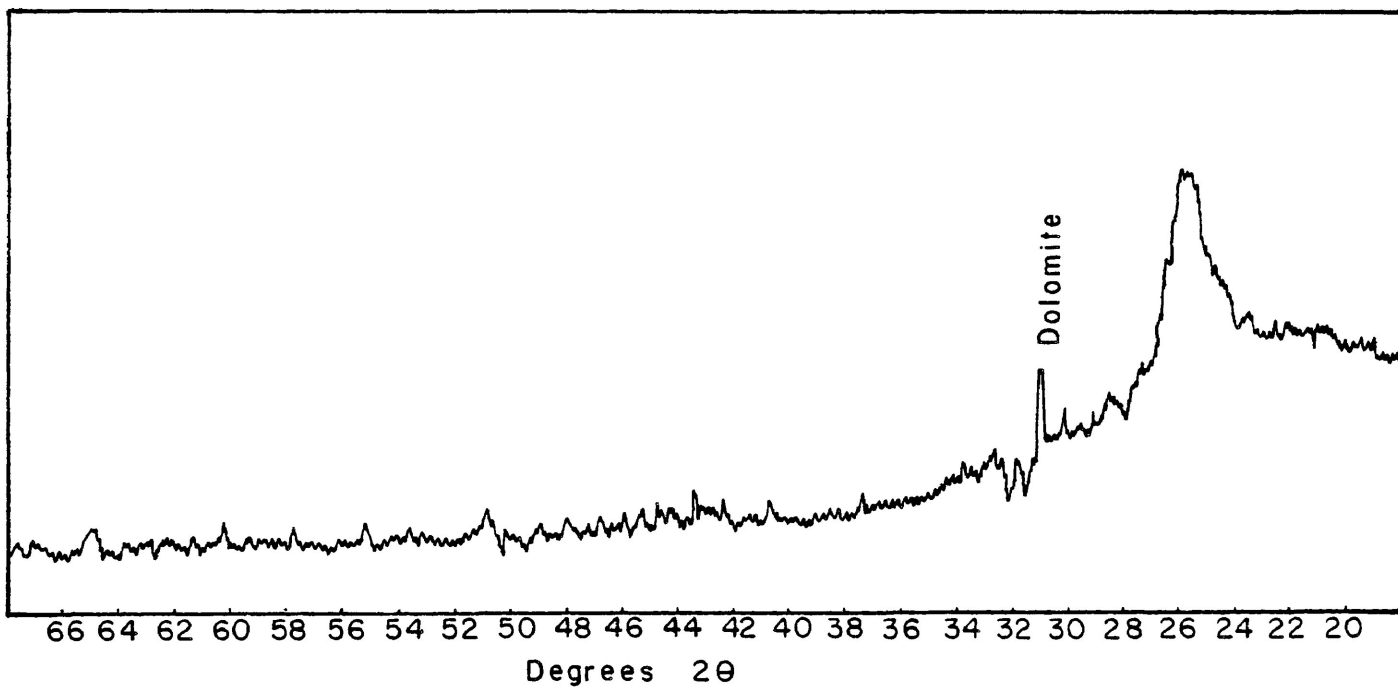
FIGURE 6.5b - X-RAY DIFFRACTION PATTERN OF BITUMEN FROM THE LOWER LENS.

FIGURE 6.6a - Organics Extracted From Society Cliffs Dolostone.

FIGURE 6.6b - Bitumen From Lower Lens.
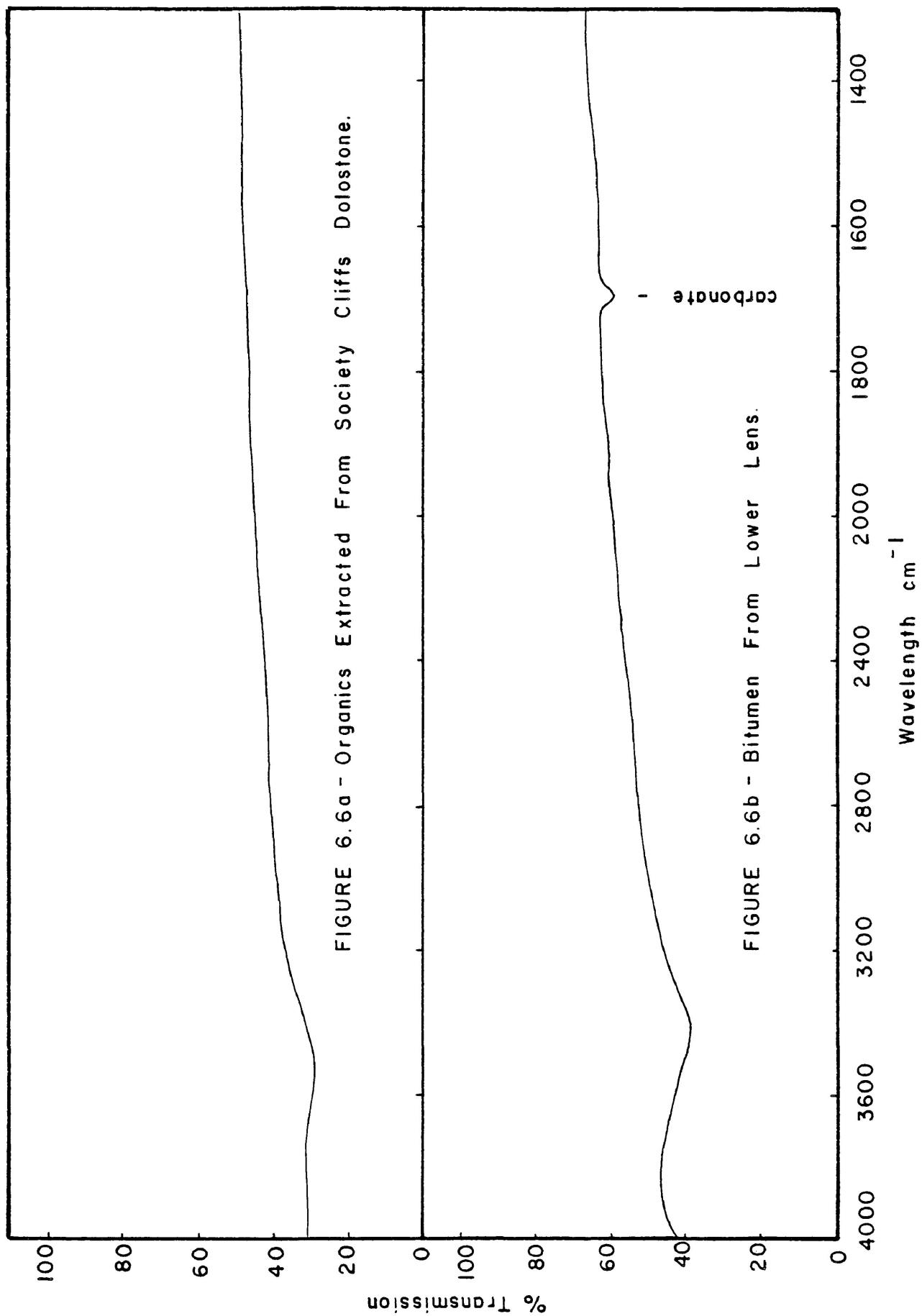
FIGURE 6.6 - INFRARED SPECTRA OF INSOLUBLE HYDROCARBONS (KBr DISC PREPARATION).

et al suggests that this bitumen is most similar to thucholite. Insoluble residue from the Society Cliffs dolostone extraction has an average composition of 59.0 wt.% C, 2.6 wt.% H and 2.4 wt.% N giving a H/C atomic ratio of 0.52. Although not detectable on the Perkin-Elmer 240 Elemental Analyzer, large amounts of sulfur interfere with operation of the apparatus (Keith Pringnitz, pers.comm.). Therefore it is unlikely that more than several percent sulfur is present. The H/C atomic ratios from bitumen associated with ore and the extracted organics are very similar. However, the bitumen from the Lower Lens has a slightly lower H/C atomic ratio, suggesting that it might be slightly more mature. Bitumen from the Lower Lens also differs from the extracted organics in containing less nitrogen, although this is probably an artifact of treatment with nitric acid.

Volatiles

Attempts to detect volatiles in fluid inclusions met with little success, probably due to the small quantities involved and the crude techniques employed. However, during fine crushing of sparry dolomite gangue and Society Cliffs dolostone, H_2S could be detected by its odor. Roedder (1984) quoted an average minimum detectability of 0.025 ppm for the human nose so that the smell of H_2S may be used as a reliable qualitative indicator. However, this method is not totally infallible as sphalerite may produce a H_2S odor when scratched. Mineral separates between -35 and -65 mesh were finely crushed under water in a mortar while being observed

under a binocular microscope to check for noncondensable gases. When sphalerite was finely crushed, gas bubbles were observed on the bottom of the mortar indicating the presence of a noncondensable phase within sphalerite inclusions. Sphalerite grains were also crushed while submersed in acetone and no vapor bubbles were observed, suggesting that the noncondensable phase present is more soluble in acetone than in water. Sparry dolomite was finely crushed while submersed in water but no noncondensable gas bubbles were observed.

CHAPTER 7:   THE PHYSICAL AND CHEMICAL CONDITIONS

OF ORE FORMATION

7.1   Introduction

Although Olson (1984) discussed the physical and chemical conditions of ore deposition and the evolution of the ore fluid with time, no geochemical model presently exists for the formation of the different types of minerali- zation encountered at Nanisivik. The mine units described by Curtis (1984) are based on variations in mineralogy and texture that should reflect changes in the physical and chemical conditions of ore deposition. In addition to the contrasts between mine units in the central and eastern portions of the Upper Lens, significant changes occur along strike in the Upper Lens of the Main Orebody and between satellite sulfide bodies. The latter may in part be associated with changes in the temperature of ore deposition. Recent studies concerning the formation of marcasite, the structure of ZnS, the significance of metal ratios and the chemistry of carbonate-hosted ore deposition allow a more detailed examination of ore formation at Nanisivik.

7.2   Temperature of Ore Formation

Homogenization temperatures obtained for the Main Orebody range from less than 100°C to more than 250°C. Many

of the homogenization temperatures less than 100°C in the central and eastern portions of the Upper Lens may be attributed to late stage dolomite veining and secondary inclusions. Homogenization temperatures in excess of 250°C may be attributed to the following post-ore events: emplacement of the gabbro dike, emplacement of white rock and the localized passage of a hot fluid through the area of crosscut 21. Therefore, the majority of inclusions probably representative of ore stage mineralization homogenized over the range of 100 - 200°C.

Interpretation of the inclusion data is complicated by the uncertainty concerning the relationship of sphalerite inclusions to their host mineral. Definite primary inclusions in sphalerite were rare, and the majority of inclusions analyzed were thought to be pseudo-secondary. Although pseudo-secondary inclusions are useful indicators of the temperature of ore deposition, they cannot always be distinguished from secondary inclusions. However, data from pseudo-secondary inclusions in sphalerite from the western portion of the Upper Lens and in the Area 14 Orebody agreed well with data from primary inclusions in dolomite. Furthermore, primary inclusions in dolomite showed as much range in homogenization temperature as pseudo-secondary inclusions in sphalerite. Homogenization temperature data from pseudo-secondary inclusions in sphalerite probably provide a reasonable minimum estimate of the temperature of sphalerite formation in most cases.

Homogenization data from individual mine units for the central and eastern portions of the Upper Lens are characterized by distinct temperature groupings that are somewhat lower than temperatures reported by McNaughton (1983) for the Main Orebody. Temperature groupings around 100°C must be viewed with suspicion because of the possibility that they are artifacts of stretching during sample preparation. Homogenization temperature groupings for dolomite generally fall within the range 135° - 180°C, with a well-developed grouping at 180°C and a less well-developed grouping at approximately 150°C. This characteristic distribution for data from dolomite is well illustrated in data from Unit 1. The highest temperature groupings for dolomite occur within the lower units 1 and 2, while the lowest temperature groupings occur within Units 3 and 4. Homogenization temperatures from sphalerite also tend to reflect a roughly bimodal distribution, with a well developed grouping at approximately 180°C and a less well defined grouping at 150°C. The highest temperature grouping for sphalerite occurs in Unit 3, while the lowest occurs in Unit 1. Even disregarding data from sphalerite as unreliable, the conclusions regarding the temperature of ore formation in the central and eastern portions of the Upper Lens remain the same. If the homogenization temperatures are corrected for pressure using an estimate of 30°C as discussed in Chapter 4, then ore formation in the eastern portion of the Upper Lens would be estimated to lie between 155 - 210°C. There does

not appear to be any appreciable difference in the temperature of ore formation between the mine units described by Curtis (1984).

Homogenization temperatures from the western portion of the Upper Lens are significantly lower than those found elsewhere in the Main Orebody and support McNaughton's (1983) observation that a thermal low exists in this area of the mine. Inclusion data from the eastern and central portions of the Upper Lens do not show a consistent decrease in temperature from east to west when homogenization data are plotted on the basis of sample location alone. However, the lateral extent of the Upper Lens examined during the course of this study is much smaller than that studied by McNaughton (1983). As previously discussed, McNaughton's trends of decreasing homogenization temperature and salinity toward the gabbro dike appear to be real. The limited amount of homogenization data obtained from late, dolomite veinlets in the Lower Lens as exposed along the lower decline failed to confirm McNaughton's (1983) observation that temperature increases with depth. However, failure to confirm this observation may be due to the nature of the material sampled, or due to the position of those samples studied relative to those analyzed by McNaughton (1983).

Homogenization data from the Area 14 Orebody indicate temperatures of ore formation similar to those estimated for the Main Orebody. However, homogenization data from Area 14 show less variation than data from the Main Orebody.

Compared to the satellite sulfide bodies examined by Bending (1984), homogenization temperatures from massive ore are typically 50°C higher, suggesting that temperatures well in excess of 100°C are generally associated with economic mineralization. However, low-temperature mineralization of the western Upper Lens provides an exception to this trend.

Pyrrhotite occurs as trace amounts in samples from the Keel Zone, where it is totally surrounded by pyrite. The average atomic percent iron content calculated from micro-probe data is 47.4%, although there is an appreciable range in the results. A pyrrhotite composition of 47.4 At.% is consistent with either hexagonal pyrrhotite at temperatures greater than 254°C, or a mixture of hexagonal and monoclinic pyrrhotite below 254°C (Kissin and Scott, 1982). However, hexagonal pyrrhotite is only in equilibrium with pyrite above 254°C, although the hexagonal pyrrhotite + monoclinic pyrrhotite + pyrite assemblage is a common disequilibrium assemblage below 254°C (Kissin and Scott, 1982), as metastable phase relations are common in the Fe-S system below 300°C (Barton and Skinner, 1979). From the preceding discussion of temperature, it appears unlikely that tempera-tures in excess of 254°C were attained in the Main Orebody, so that the pyrrhotite + pyrite assemblage of the Keel Zone is probably not representative of equilibrium conditions.

7.3   **Chemical Conditions of Ore Formation**

Although marcasite was initially very common in Units 1, 3 and 5 of the central and eastern Upper Lens, reflected light petrography and X-ray diffraction studies indicate that it has been entirely replaced by pyrite. According to the experimental work of Murowchick (1984), the formation of marcasite at 75°C requires a pH < 5 and the presence of H_2S_2 and $S_2O_3^{-2}$. The activity of thiosulfate ($S_2O_3^{-2}$) is primarily dependent upon the oxygen activity (aO_2) and has a maximum value approximated by the lower boundary of the SO_4^{-2} field shown in Figures 7.1 and 7.2 (Barnes and Kullerud, 1961). The position of the boundaries on these diagrams is affected mainly by temperature and, to a lesser extent, by total sulfur content. It can be seen from these diagrams that the maximum activity of $S_2O_3^{-2}$ occurs at increasing aO_2 with increasing temperature. For example, at a pH = 5, which is significant for marcasite formation according to the criteria stated by Murowchick (1984), log aO_2 at maximum $S_2O_3^{-2}$ activity varies from -52 at 100°C to -38 at 200°C. These two temperatures represent the maximum range of primary depositional temperatures which probably existed in the western and eastern portions of the Upper Lens, respectively.

The iron content of sphalerite may be used to further constrain the aO_2 during ore formation (Giordano and Barnes, 1981; Barnes, 1983). Sphalerite iron content is dependent upon the sulfur activity (aS_2) of the co-existing sulfide
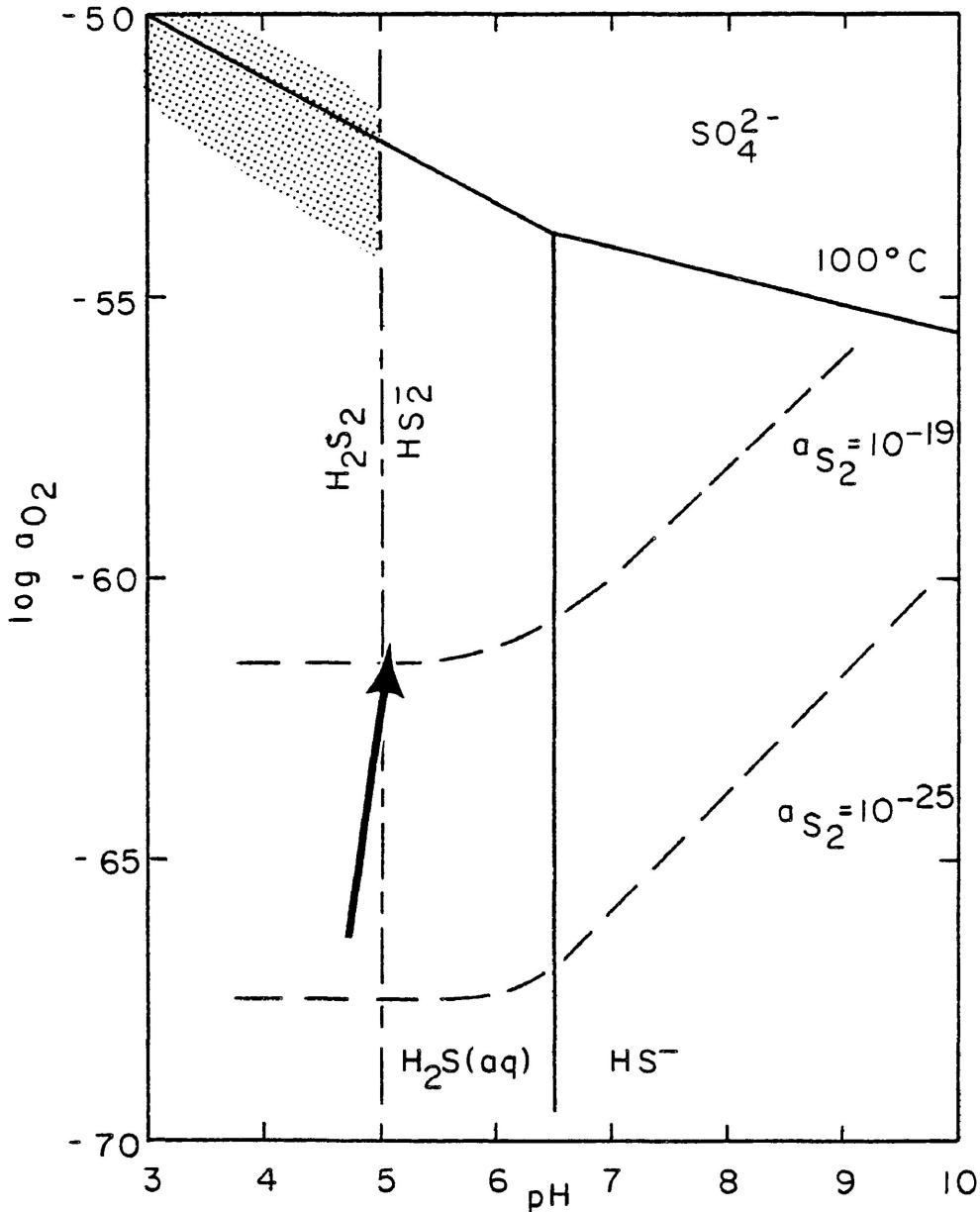
FIGURE 7.1 - Log aO_2 - pH DIAGRAM AT 100 °C FOR THE
WESTERN UPPER LENS. ░░░ - AREA FAVORABLE FOR MARCASITE
PRECIPITATION; ———·—— H_2S_2 STABILITY (AFTER MUROWCHICK,
1984); ———— SULFUR ACTIVITY CONTOURS FOR TOTAL SULFUR
= 0.01 moles AND SPHALERITE FeS = 16 mole % (aS_2= 10^{-25})
AND 0.3 mole % (aS_2= 10^{-19}), (AFTER GIORDANO AND BARNES,
1981); ➤ EVOLUTION OF ORE FLUID IN A SINGLE
SULFIDE BAND.
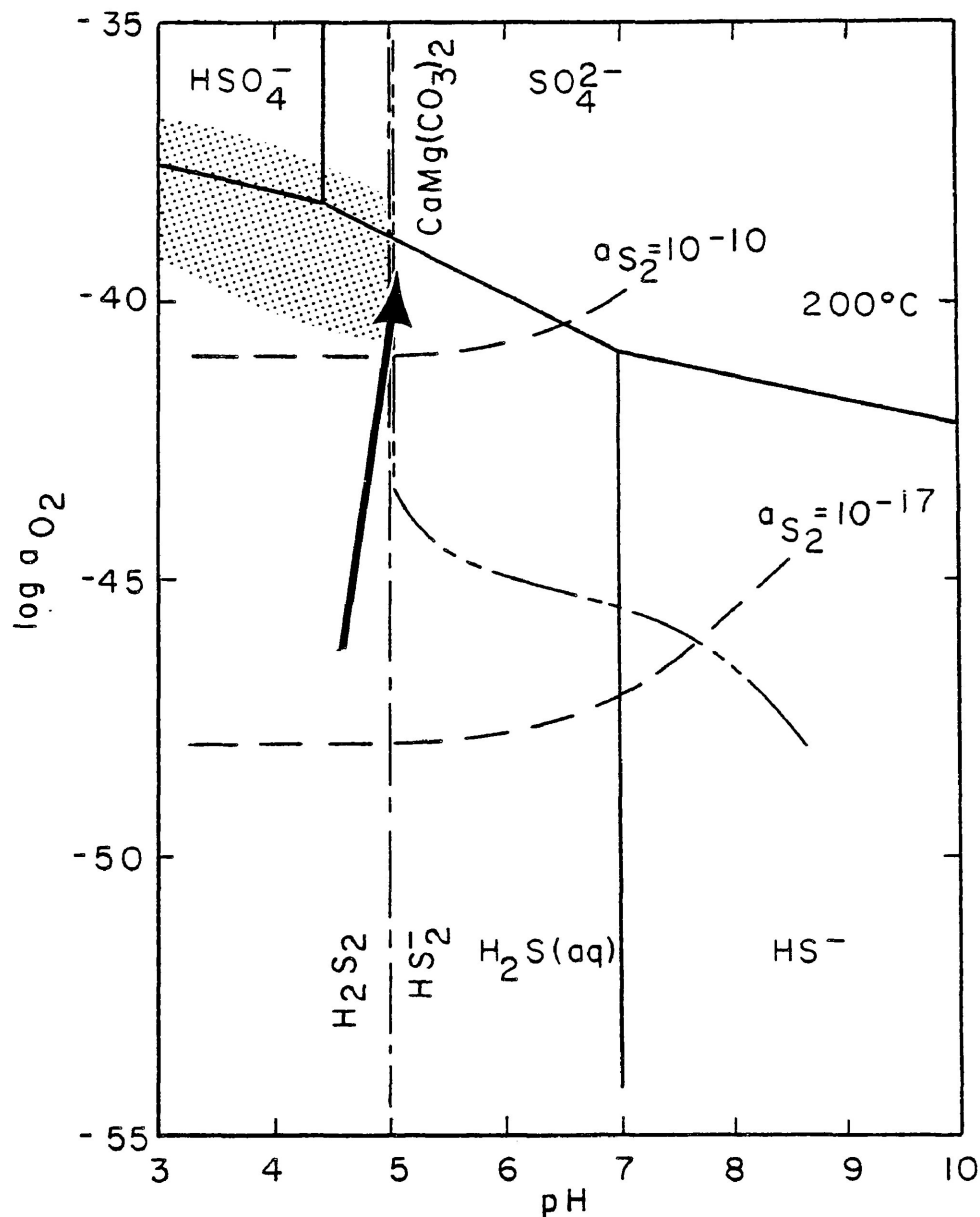
FIGURE 7.2 - Log aO_2 - pH DIAGRAM AT 200 °C FOR THE
CENTRAL AND EASTERN UPPER LENS. ░░░ - AREA FAVORABLE
FOR MARCASITE PRECIPITATION; —··— DOLOMITE STABILITY
FOR TOTAL C = 0.1 moles (AFTER OLSON, 1984); —·—— H_2S_2
STABILITY (AFTER MUROWCHICK, 1984); ———— SULFUR ACTIVITY
CONTOURS FOR TOTAL S = 0.01 moles AND SPHALERITE FeS =
16 mole % ($aS_2= 10^{-17}$) AND 0.3 mole % ($aS_2= 10^{-10}$) (AFTER
GIORDANO AND BARNES, 1981); ➞ EVOLUTION OF ORE
FLUID IN A SINGLE SULFIDE BAND.

assemblage at high temperature (Barton and Skinner, 1979), and this relationship is believed to persist to temperatures below 300°C (Scott and Kissin, 1973). Sulfur activity contours calculated for sphalerite iron contents of interest are also shown on Figures 7.1 and 7.2. A trend of decreasing iron content during sphalerite mineralization reflects a progressive increase in the aO_2 during mineralization in the eastern and central portions of the Upper Lens. Only at high temperatures does the aO_2 field defined by the iron content of sphalerite overlap with the maximum activity of $S_2O_3^-$ near the $SO_4^{2-} - H_2S$ boundary. As a result, marcasite is best developed in the high temperature central and eastern Upper Lens.

The precipitation of marcasite rather than pyrite in hydrothermal solutions at 75°C appears to depend upon the availability of sulfanes (Murowchick, 1984). Sulfanes, or polysulfides as they are sometimes referred to, have the general formula HxSx where x > 1. Sulfanes may form in ore solutions from sulfate through reactions (1) and (2), which involve thiosulfate as an intermediary (Murowchick, 1984).

$$2SO_4^{2-} + 2H^+ \longleftrightarrow H_2O + 2O_2 + S_2O_3^{-2} \tag{1}$$

$$H^+ + H_2S \text{ (aq)} + S_2O_3^- \longleftrightarrow H_2S_2 + HSO_3^- \tag{2}$$
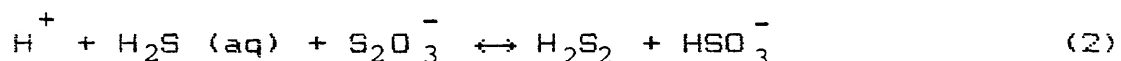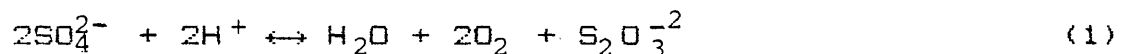
Alternatively, sulfanes may be produced by the oxidation of H_2S (Murowchick, 1984) as indicated by equation (3).

$$2H_2S \text{ (aq)} + 1/2 \, O_2 \longleftrightarrow H_2S_2 + H_2O \tag{3}$$
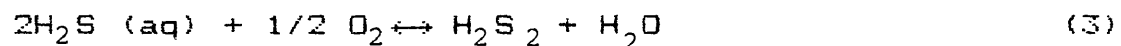
The stability of sulfanes is in turn dependent upon the pH at which they ionize. For example, the stability of

the simplest sulfane H_2S_2 is controlled by the reaction:

$$H_2S_2 \leftrightarrow HS_2^- + H^+ \qquad pk = 5.0 \text{ at } 20°C \qquad (4)$$
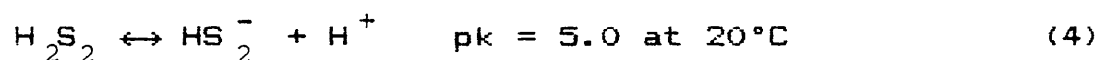
where the pk of the reaction sets the maximum pH for which the sulfane is stable. The maximum pH at which marcasite is stable is 5.0 because more complex sulfanes ionize at lower pH (Murowchick, 1984). Giggenbach (1974) demonstrated that, in slightly alkaline solutions, the equilibrium constants governing the relative proportions of nonprotonated poly-sulfides (SxS_2^-) do not change appreciably with temperature up to 240°C. Furthermore, the ionization of H_2S to HS^- does not vary greatly with pH at elevated temperatures (Barnes, 1979). Therefore, the assumption that the pk of reaction (4), and thus the maximum pH of marcasite stability, does not vary greatly up to 200°C is considered to be reasonable. On the basis of this assumption, the stability fields for marcasite at 100° and 200°C are shown in Figures 7.1 and 7.2 respectively. The presence of sparry dolomite interbanded with bladed marcasite pseudomorphs indicates that the pH of the ore fluid must have exceeded 5.0 immediately following marcasite precipitation. Under these conditions it is not surprising that marcasite inverted entirely to pyrite.

From Figure 7.2 it can be seen that the best overlap of conditions interpreted as being most favorable for marcasite precipitation with the oxygen activities indicated by the iron contents of sphalerite occurs at total sulfur concentrations equal to 10^{-2} m or less. Marcasite formation could not have occurred too close to the H_2S (aq)$-SO_4^{-2}$ bound-

ary, however, because an ore fluid of this composition would be expected to carry enough SO_4^{-2} to affect sulfide fractionation (Ohmoto, 1972), something that is not indicated by the sulfur isotopic results. Although isotopic re-equilibriation may have occurred during the marcasite-pyrite transition, it is suggested that this transition was initiated immediately following marcasite precipitation. Therefore, the sulfur isotopic data from bladed pyrite probably reflects the initial isotopic composition. If the marcasite-pyrite inversion resulted from a pH increase too close to the $H_2S(aq)-SO_4^{-2}$ field boundary, noticeable fractionation between precipitated sulfides and the ore fluid would be expected, given the slope of the $H_2S(aq)-SO_4^{-2}$ boundary. The dominant sulfur species was probably H_2S throughout the mineralizing process at both high and low temperatures.

Several possible explanations for the non-precipitation of marcasite in certain mine units and regions of the Main Orebody have been mentioned in the preceding discussion. In the case of the western portion of the Upper Lens, a temperature drop resulting in lower oxygen fugacities is the most likely explanation, if it is assumed that the iron content is similar to that found in the eastern Upper Lens. A restricted range in the sulfur isotope data and, to a certain extent, the fluid inclusion data limit any major fluctuations in temperature, as well as any significant changes in the dominant sulfur species or the sulfur source between the mine units.

Although changes in pH have a profound effect given the pH dependence of H_2S stability, the banded textures and sulfide to gangue ratios suggest that the pH continued to fluctuate near neutrality. Dissolution textures suggest that the pH of the ore fluid may have occasionally dropped well below 5. A drop in the oxygen activity may also have been significant, as relatively high oxygen activities appear to favor marcasite precipitation. Evidence for a minor drop in the oxygen activity in Units 2 and 4 is indicated by the slightly higher average iron contents of sphalerite from these units and their poorly developed colour zoning relative to Units 1, 3, 5 and 6.

Unit 6, however, is problematic. Colour zoning is well developed in sphalerite, and very low iron contents at crystal margins indicate that aO_2 sufficiently high to precipitate marcasite was attained near the end of sphalerite precipitation. As in the case of Units 2 and 4, neither a drastic drop in temperature or a dramatic rise in pH seems likely. The limiting factor in the case of this unit may lie in the availability of sulfanes.

Although marcasite is detectable in the Lower Lens, it appears restricted to an early generation of finely laminated iron sulfide, which has been disrupted by later mineralization similar in terms of metal ratios to that found in units of the Upper Lens. Although nothing definite can be said concerning aO_2, an early generation of marcasite, which has been partially replaced by pyrite, suggests high initial

aO_2 that decreased with time. Metal to gangue ratios similar to those from the eastern and central portions of the Upper Lens suggest a pH that fluctuated around 5.

The significance of wurtzite at Nanisivik remains unclear. Although not identified during this study, reports by other workers indicate its presence. According to Scott and Barnes (1972), below 200°C wurtzite is favored by a log $fS_2 > 20$atm under highly reducing conditions and at pH near neutrality. The position of reported wurtzite occurrences late in the paragenetic sequence is consistent with high aS_2 at this time and a pH near neutrality appears to have been prevalent throughout most of the mine during ore deposition. However, highly reducing conditions are not consistent with the presence of marcasite and might explain the elusiveness of wurtzite. Although it is uncertain as to whether anisotropic zones in sphalerite are the result of trace elements or inversion from wurtzite, had wurtzite initially been extensive, it probably would have been unstable under the general conditions of ore formation outlined above.

As previously discussed in the section concerning temperature, the hexagonal ± monoclinic pyrrhotite + pyrite assemblage of the Keel Zone is probably not in equilibrium. Metastability in the Keel Zone is also indicated by the low iron content of sphalerite (< 0.2 wt.% FeS) from this portion of the mine. According to the phase diagram of Scott and Kissin (1973), sphalerite having such low iron contents will not co-exist stably with an equilibrium pyrrhotite + pyrite

assemblage at any temperature because the iron content of sphalerite is ultimately dependent upon the sulfur activity of the iron sulfide assemblage. However, because of the small amount of pyrrhotite present and because sphalerite is not observed in contact with pyrrhotite, the pyrrhotite + pyrite assemblage probably had negligible control on the iron content of sphalerite from the Keel Zone. Furthermore, the low iron content of sphalerite, which was generally the last mineral formed in the Keel Zone, suggests the late passage of a relatively oxidized fluid.

The cause of regular fluctuations in aO_2 and aS_2 reflected by internal zonation in the Main Orebody is difficult to assess due to the number of variables involved. However, in the case of the western Upper Lens, low aO_2 and hence a corresponding predominance of pyrite over marcasite may be attributed to the effect of temperature. Elsewhere, fluid inclusion and sulfur isotopic results negate radical fluctuations in the temperature of the ore fluid. Sulfur isotopic results and mineralogoy also preclude drastic variations in pH. Undoubtedly variations in the activities of various gaseous species among the different mine units reflects their concentration in the ore fluid at that point in time, as well as changes in the bulk chemical composition of the ore fluid.

CONCLUSIONS

The various mine units described by Curtis (1984) for the central and eastern portions of the Upper Lens, and the different ore zones within the Main Orebody may be distinguished on the basis of a number of physical and chemical criteria.

The central and eastern portions of the Upper Lens, Main Orebody are characterized by a number of well-banded to chaotic mine units exhibiting both replacement and open space filling textures. Mineral paragenesis of individual sulfide bands in this portion of the Main Orebody is relatively simple, consisting of: sphalerite → iron sulfide → galena → sparry dolomite. Compared to the rest of the Upper Lens, the eastern portion is enriched in sparry dolomite and galena. Coarse, bladed crystals of anomalously anisotropic, porous pyrite are best developed in this portion of the mine. Although the textures are indicative of initial marcasite precipitation, single crystal X-ray diffraction studies indicate that the iron sulfide has inverted entirely to pyrite. Fluid inclusion homogenization temperatures generally vary from 100 to 200°C, but evaluation of the data and correction for the estimated pressure of ore formation suggests that, in this part of the Main Orebody, most ore precipitation took place between 155 - 210°C. Limited freezing data from sphalerite and dolomite inclusions indicate that the ore

fluid was a hyper-saline brine containing 20 - 37 wt.% $CaCl_2$. The iron content of sphalerite from the central and eastern Upper Lens varies from 0 to 14 mole % FeS indicating a range of log aO_2 from -41 to -46 for a total dissolved sulfur concentration of 10^{-2} moles at pH = 5 and 200°C. Under these conditions marcasite is considered to have formed at pH < 5 and at the highest oxygen activities.

Mine Units 1, 3 and 5 are characterized by replacement textures and the presence of pyrite pseudomorphs after marcasite in coarsely bladed ore. Sphalerite iron contents suggest that these units were formed under conditions of slightly higher aO_2 than Units 2 and 4, and thus were most favorable for marcasite formation. Sphalerite from banded Units 2 and 4 has slightly higher iron contents reflecting higher aS_2 and thus lower aFeS levels at the time of ore formation. Chaotic Unit 6 is characterized by open space filling textures and appears to have formed under aO_2 conditions similar to those prevailing during formation of the replacement units. No reason for the formation of pyrite rather than marcasite in Unit 6 is apparent.

Sulfur isotopic compositions of pyrite vary from +27.4 to +28.0 %, indicating that temperature, the dominant dissolved sulfur species in solution, and the source of sulfur did not vary drastically throughout main and late-stage mineralization. Fluid inclusion homogenization temperatures, although highly variable, also indicate relatively consistent temperatures of ore formation for the mine units.

Consistent sulfide to gangue ratios suggest that the pH of the ore fluid was relatively constant for most the mine units. The precipitation of both marcasite and dolomite indicates that the ore fluid fluctuated around a pH = 5.0. Sulfide ratios indicate that Units 1, 3 and 5 are iron rich with respect to Units 2, 4 and 6.

Fluid inclusion homogenization temperatures from a small region of the western Upper Lens indicate temperatures of ore formation from 100 to 150°C after correction for pressure. At these temperatures conditions of aO_2 would not have been favorable for the precipitation of marcasite. Lower temperatures also result in greater dolomite solubility and a decrease in galena solubility.

The paragenesis of the Lower Lens is similar to that of the Upper with the addition of early, finely laminated iron sulfide consisting of a mixture of pyrite and minor marcasite. Mineralization of the Lower Lens is irregular although minor rhythmically banded ore is present in the western portion. Sulfide content and sulfide to gangue ratios are similar to those of the eastern and central Upper Lens, suggesting similar conditions of ore formation. The sulfur isotopic composition of pyrite from the Lower Lens is slightly higher than that encountered in the Upper Lens. The small number of fluid inclusions analyzed indicate temperatures of ore formation similar to those of the eastern and central Upper Lens. Near the matic dike contact, Lower Lens ore has been affected by white rock emplacement involving

temperatures in excess of 250°C. An early generation of marcasite suggests an initially high a_{O_2} that fell during the bulk of Lower Lens mineralization.

Detailed examination of ore from the Shale Zone indicates that recrystallization and remobilization has occurred in this portion of the Main Orebody, resulting in ore that is relatively enriched in metal sulfides. Fluid inclusion homogenization temperatures are elevated and increase towards the matic dike that cuts the Main Orebody, suggesting that perhaps dike emplacement was responsible for remobilization.

Keel Zone mineralization is characterized by trace amounts of pyrrhotite and minor, late sphalerite having a very low iron content. Iron contents of pyrrhotite and sphalerite indicate that the Keel Zone is not an equilibrium assemblage, precluding any conclusions concerning the conditions of sulfide deposition.

The Area 14 Orebody is similar to the Lower Lens in terms of ore paragenesis, with the addition of a late generation of colourless sphalerite. Gross textural relations are much simpler than in the Main Orebody. The presence of marcasite was not confirmed by single crystal X-ray diffraction. Fluid inclusion homogenization temperatures are similar to those encountered in the Main Orebody, although not as variable. A single isotopic value from pyrite suggests that the Area 14 Orebody has a slightly lighter sulfur isotopic composition than the Main Orebody. Sulfide contents and sulfide to gangue ratios are similar to those

found in the Shale Zone and in Unit 6, although sampling was biased towards the central sphalerite unit.

The presence of wurtzite could not be confirmed by single crystal and powder X-ray diffraction studies. Evaluation of the physical and chemical conditions of ore formation suggests that the ore fluid was probably too oxidized in the eastern and central portions of the Upper Lens for wurtzite to be stable. Anisotropic domains in sphalerite probably reflect zones of disordered hexagonal packing which result from either trace element distortion of the cubic sphalerite structure, or partial inversion of primary, metastable wurtzite to sphalerite. Trace elements Cu, Mn, and Ga occur within sphalerite, in addition to the previously reported Cd and Ag. These trace elements are probably responsible for the red-orange fluorescence along clear sphalerite rims from Units 1, 3, 5 and 6 observed under ultraviolet light.

A very limited study of organics associated with Lower Lens mineralization and organics extracted from Society Cliffs dolostone indicates that the two are similar in terms of solubility in organic solvents, X-ray diffraction patterns and infrared absorption. The two bitumens probably have a similar origin. Bitumen from the Lower Lens has a slightly lower H/C ratio suggesting that it has been preferentially depleted in hydrogen.

MODEL OF ORE FORMATION

To be acceptable, any proposed model of primary ore formation must attempt to explain the observed textural and mineralogical variations under the constraints imposed by the physical and chemical conditions of ore formation. A model of ore formation must also explain variations in sulfide content and sulfide to gangue ratios and the nature of wall rock - orebody contacts. Two major schools of thought prevail concerning theories of ore deposition for deposits of the Mississippi Valley Type: 1) reduction of an oxidized ore fluid at the site of ore precipitation; 2) precipitation from a reduced ore fluid in response to physical changes. At Nanisivik, the *in situ* reduction of a single ore solution best explains inferred changes in ore solution chemistry and precipitation of marcasite. An *in situ* reduction model is also consistent with replacement of organic-rich carbonate wall rock and the presence of organics in ore.

General Model

Oxidized ore fluid is considered to have entered the Nanisivik area along karst passageways and faults. A hydrostatic control, perhaps along a fluid interface, at the site of ore formation is inferred from the horizontal nature of most suflide bodies. Reduced sulfur may have already been present at the site of ore formation or may have been generated through thermal maturation of more complex hydro-

carbons. Hot, metal-bearing brine probably entered the eastern Upper Lens resulting in a high aO_2 favorable for marcasite precipitation.

A preliminary investigation of organics at Nanisivik suggests that bitumen, and possibly other hydrocarbons associated with the ore, were derived from the Society Cliffs dolostone. Thermal degradation of bitumen is known to liberate CH_4 as well as H_2S (Bailey, 1977; Saxby, 1977) resulting in lower H/C ratios in the remaining residue. In a study of the evolution of organic matter in carbonate strata, Jiamo (1979) concluded that a H/C ratio from 0.3 to 0.4 is the lowermost limit for methane generation. A H/C ratio of 0.52 for bitumen extracted from the Society Cliffs dolostone indicates that it is capable of generating CH_4, while bitumen from the Lower Lens having a H/C ratio of 0.46 suggests thermal degradation has occurred. On the basis of experimental work, Orr (1982) concluded that thermochemical sulfate reduction is viable in the temperature range 175 - 250°C provided H_2S is present initially. The Society Cliffs Formation is widely reported to be petroliferous, so initial H_2S is not unlikely. The karst system which was considered by Olson (1977, 1984) and Clayton and Thorpe (1982) to have controlled mineralization may have acted as a hydrogen sulfide reservoir.

Involvement of hydrocarbons from the Society Cliffs Formation in sulfate reduction requires the dissolution or replacement of a significant quantity of dolostone by the ore

fluid. Ford (1981) concluded that as much as 95% of the orebody volume was generated at the time of ore deposition, a conclusion supported by evidence of considerable replacement in the central and eastern Upper Lens (Curtis, 1984), and by the presence of blocks of dolostone "floating" in ore (Kissin, 1983).

Development of Ore Textures

Although much of the banding in the Main Orebody is nearly horizontal, the presence of inclined banding in Unit 2 indicates that ore deposition did not occur by simple precipitation from solution with gravity settling. Banding is best developed along the margins of the Upper Lens where replacement textures are observed, suggesting that banding and wall rock replacement are intimately related processes. Bubela and McDonald (1964) demonstrated experimentally the ability of diffusional processes to produce banding during sulfide precipitation by both inorganic and microbial sulfate reductants. The amount of replacement texture in Units 1, 3 and 5 suggests that diffusional processes predominated in these areas of the mine. Present wall rock - orebody contacts are therefore best thought of as diffusional replacement fronts along which processes of sulfate reduction and sulfide precipitation were concentrated. The wall rock - orebody contacts are considered to have migrated outward from an initial karst system that channelled fluid flow. The present orientation of banding in the ore probably reflects former wall rock - orebody contacts.

Chemical reactions involving sulfate reduction, sulfide precipitation, dolostone dissolution and dolomite precipitation (recrystallization?) that occurred along the migrating replacement front are summarized below from Kissin (1983).

$$CH_4 + SO_4^{2-} + 2H^+ = H_2S + CO_2 + 2H_2O \qquad (5)$$

$$Zn^{2+} + H_2S = ZnS + 2H^+ \qquad (6)$$

$$4H^+ + CaMg(CO_2)_3 = Ca^{2+} + Mg^{2+} + 2CO_2 + 2H_2O \qquad (7)$$

$$CO_2 + H_2O = H_2CO_3 \qquad (8)$$

$$Ca^{2+} + Mg^{2+} + 2HCO_3^- = CaMg(CO_2)_3 + 2H^+ \qquad (9)$$
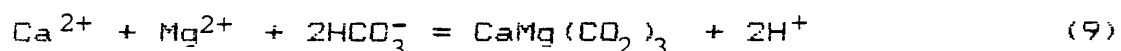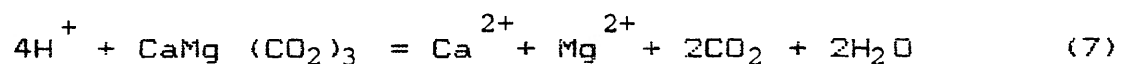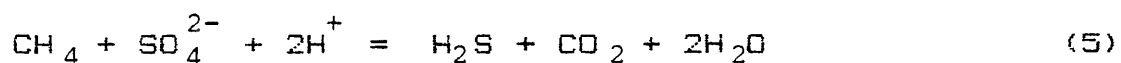
When sulfate reduction and sulfide precipitation both occur at the site of ore formation, carbonic acid is produced according to equation (10), and little carbonate dissolution would be expected (Anderson, 1983, 1984; Barnes, 1983).

$$SO_4^{2-} + CH_4 + Zn^{2+} = ZnS + H_2CO_3 + H_2O \qquad (10)$$
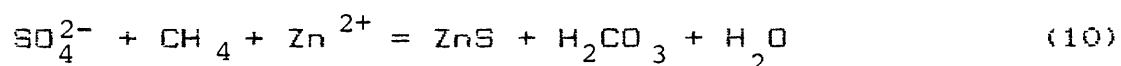
The amount of banded ore in the Upper Lens of the Main Orebody suggests that equal volume replacement processes predominated and that there was no net production of acid in those portions of the mine where banding is well developed.

Repetitively banded ore is considered to have formed during the pulsatory influx of ore fluid in the following way. During precipitation of sulfide bands, the release of acid would momentarily lower the pH of the ore fluid allowing it to react with the carbonate wall rock. Reaction of the hot, slightly acidic ore solution with organic-rich wall rock would liberate CH_4 and H_2S produced by the thermal degradation of bitumen. Increasing a_{O_2} during sphalerite precipita-

tion suggests that H_2S was being depleted in the ore fluid so that by the time iron sulfides began to precipitate, conditions were favorable for the precipitation of marcasite in the main replacement units. Meanwhile, CH_4 and H_2S liberated by wall rock interaction with the ore fluid was available to react with a new influx of oxidized brine according to equation (5). Reaction (5) is acid consuming so that during sulfate reduction the pH of the ore fluid would be expected to rise, allowing the precipitation or recrystallization of sparry dolomite from a solution saturated with respect to carbonate. A replenished supply of metal ion and continued hydrogen sulfide generation would initiate another cycle of sulfide precipitation at the new wall rock - orebody contact.

Although ore from Units 2 and 4 generally lacks replacement textures, finely banded ore from these units is also considered to have formed through the progressive replacement of wall rock. Slightly higher sphalerite FeS contents than those found in Units 1, 3, 5 and 6 indicate lower aS_2 and aO_2 during ore formation. Pyrite, rather than marcasite precipitation probably reflects the lower aO_2 in Units 2 and 4, while higher Sp/Py ratios relative to Units 1, 3 and 5 may reflect lower aS_2. Fluid inclusion homogenization temperatures and sulfur isotopes suggest that lower aS_2 and aO_2 are not simply a result of lower temperatures.

A mechanism for the production of lower aS_2 and aO_2 in the absence of a significant temperature drop is problematic. If the limiting factor on sulfide precipitation

is considered to be metal supply rather than the availability of reduced sulfur, then a surplus of H_2S might be expected in certain portions of the mine. Upon arrival of sufficient metal at the site of ore formation, metal precipitation might be expected to predominate over sulfate reduction with a corresponding decrease in ore fluid pH. Sulfide to dolomite ratios for Units 2 and 4 indicate that the pH of the ore fluid continued to fluctuate around pH = 5.0, suggesting that lower aS_2 and aO_2 in these units was not a result of an H_2S surplus. Lower aS_2 and aO_2 in Units 2 and 4 may reflect poor circulation of fresh, oxidized ore fluid to the wall rock — orebody interface.

The presence of pyrite "ribs" floating in ore from Unit 6, and downcutting contacts between Unit 6 and the underlying well banded units indicate dissolution of previously deposited ore. Dolostone breccia cemented by sparry dolomite gangue in the Lower Lens suggests carbonate dissolution during mineralization in this portion of the Main Orebody as well. One of the most likely causes of dis- solution would be a sharp drop in pH. Precipitation of sulfides from a solution already saturated with reduced sulfur is the most likely mechanism for an increase in acid- ity, as previously discussed. Excess H_2S may have accumu- lated from sulfate reduction occurring elsewhere in the Main Orebody, or may have been introduced from outside the system. Uneconomic mineralization of the Keel Zone may have developed during sulfide precipitation from a previously reduced ore

fluid, resulting in excess acid.

Mineralization of the Keel Zone may have continued until the immediate supply of metal was consumed. Dissolution of carbonate wall rock in the Lower Lens and previously deposited ore in the Upper Lens in response to excess acid produced during Keel Zone mineralization might have eventually buffered the ore fluid until it returned to a pH = 5. Mixing of a new influx of oxidized ore fluid with any remaining H_2S in cavities created during Keel Zone mineralization would explain the chaotic mineralization of Unit 6 and the irregular ore of the Lower Lens. FeS contents of sphalerite, sulfide contents, sulfide to gangue ratios and fluid inclusion homogenization temperatures indicate conditions of ore formation for Unit 6 and the Lower Lens similar to those that occurred during formation of the banded units in the Upper Lens. The presence of local rhythmically banded ore in the Lower Lens indicates that minor replacement has also occurred.

By the time the ore fluid had reached the western portion of the Upper Lens, it had cooled to less than 150°C. Assuming a sphalerite FeS content similar to that occurring farther east, the aO_2 of the ore fluid would have been too low for the widespread precipitation of marcasite. Given the low content of sparry dolomite gangue in the western Upper Lens and the scarcity of pyrite pseudomorphing marcasite, few constraints may be placed on the pH of the ore fluid. Nearly equal volume replacement of dolostone by massive sulfides and

the lack of extensive dissolution features attributable to acid generation suggest that H_2S supply and sulfide precipitation occurred at similar rates in the western Upper Lens.

The zinc/lead ratio tends to increase from east to west in the Upper Lens (Olson, 1984; Neumann, 1984) and high Pb contents are related to apparent zones of upwelling (?) in the Area 14 Orebody. Examination of fluid inclusion data in samples containing galena from both the Main Orebody and the Area 14 Orebody fails to indicate any conclusive relationship between temperature and galena mineralization. Although a drop in temperature from 200° to 100°C would adequately explain a decrease in galena solubility under the conditions of ore formation at Nanisivik (Giordano and Barnes, 1981; Figures 3 & 4), the fluid inclusion and sulfur isotope data preclude such drastic fluctuations in temperature in the eastern and central Upper Lens. Perhaps a more significant relation is the preference of galena for replacement units along the margins of the Upper Lens. Galena is much less soluble than sphalerite in hydrothermal chloride solutions containing stoichiometric proportions of reduced sulfur (Sverjensky, 1981). Therefore galena is likely to be preferentially precipitated at the point of initial sulfate reduction, thus explaining its distribution in both the Main and Area 14 Orebodies.

DISCUSSION

The rhythmically banded ore common to the Upper Lens of the Main Orebody often exhibits a strong bipolarity to mineral growth. Similar ore textures were described by Fontebote and Amstutz (1983) and Levin and Amstutz (1976). Although Fontebote and Amstutz (1983) proposed a diagenetic crystallization process for the formation of rhythmically banded ore, the epigenetic nature and high temperatures of mineralization preclude such an explanation at Nanisivik. As previously discussed, a diffusional replacement process is considered to have resulted in banded ore textures at Nanisivik, although it is difficult to envision how such a process would produce a bipolarity to crystal growth.

Repetitive ore sequences and ore rhythms displaying textures similar to those at Nanisivik were reported in the Zn-Pb sulfide ores of Upper Silesia, Poland, by Sass-Gustkiewicz et al., (1982). Banded "metasomatic sphalerite ores" were considered to result from replacement processes. The development of "disaggregated dolomite" during replacement of carbonate wall rock was suggested to explain the unhindered growth of crystals. Although there is no evidence for the development of a "disaggregated dolomite" phase during wall rock replacement at Nanisivik, unhindered crystal growth probably occurred under conditions of simultaneous carbonate dissolution, dolomite recrystallization and sulfide

precipitation prevalent along replacement fronts.

In an examination of data from oil field brines Lydon (1983) discussed the effect of various chemical parameters on metal ratios in sediment-hosted stratiform Pb-Zn deposits. The three parameters considered most important were reduced sulfur content, pH and fO_2. Decreasing pH, fO_2 and reduced sulfur content were thought to increase the Fe/(Fe+Zn) ratio in ore precipitated from metal saturated solutions. According to Lydon's (1983) model, a Fe/(Fe+Zn) ratio near 1.0 such as that found in the Keel Zone and the barren satellite bodies, may be explained by a decrease in all three parameters. As previously discussed, a drop in pH is considered to have been most significant for the Keel Zone while the reduced sulfur content is thought to have actually increased. Units 1, 3 and 5 have Fe/(Fe+Zn) ratios approximately equal to 0.5 indicating intermediate pH, fO_2 and reduced sulfur content. Units 2, 4 and 6 are characterized by Fe/(Fe+Zn) less than 0.5, which would indicate an increase in pH, fO_2 and reduced sulfur content. However, pH is not considered to have varied greatly between mine units, while fO_2 is considered to have dropped slightly in Units 2 and 4. An increase in the reduced sulfur content is most consistent with the model already presented. Iron to zinc ratios for the Lower Lens are similar to those from Units 1, 3 and 5 suggesting similar chemical conditions of ore formation. Ore from the western Upper Lens has Fe/(Zn+Fe) ratios similar to Units 2 and 4.

The model of ore formation proposed here favors transport of metals to the site of ore deposition with sulfate in order to explain the presence of thiosulfate and sulfanes required for the precipitation of marcasite. In addition to satisfying the conditions of ore formation, oxidized sulfur is favored over reduced sulfur because transport of sufficient metal with reduced sulfur seems improbable under the pH conditions indicated at Nanisivik (Anderson, 1977; Giordano and Barnes, 1981; Sverjensky, 1984). On the basis of experimental work by Drean (1978), which suggested a kinetic barrier to sulfate reduction by organic matter, Spirakis (1983) proposed a partially oxidized ore fluid for deposits of the Mississippi Valley Type. Partial oxidation of an initially reduced fluid might be brought about by reaction with iron oxides and would greatly enhance the metal-carrying capacity of the ore fluid (Spirakis, 1983). Partially oxidized sulfur species are thought to be stable for sufficiently long periods of time and are easily reduced by organic matter. Such a model would also provide for the transport of metals and the presence of thiosulfate and sulfanes at the site of ore deposition.

The model of ore deposition outlined above is similar in many respects to that proposed by Olson (1984). On the basis of carbon and oxygen isotope data, Olson (1984) calculated a range of log aO_2 from -41 to -44. Olson's range of aO_2 is in good agreement with the range suggested for the central and eastern Upper Lens by this study on the basis of

sphalerite iron content and marcasite precipitation. Olson (1984) also suggested that the ore fluid became progressively more reduced in the later stages of mineralization, which would correspond to movement of the ore fluid from the eastern to the western portions of the Upper Lens. However, a major point of departure from Olson's (1984) model involves the significance of wall rock interaction proposed here. Olson (1984) did not recognize the importance of replacement and dissolution of dolostone during mineralization and proposed the existence of a hydrocarbon reservoir at the site of ore deposition in order to explain reduction of the ore fluid. However, an ore deposition model involving mixing seems inadequate to explain the laterally extensive banding developed along the margins of the deposit, the coarse-grain size of the ore and the lack of colloform textures.

Significant wall rock interaction with the ore fluid should be reflected by the carbon and oxygen isotopes. Carbon dioxide generated by dissolution of wall rock should be isotopically similar to the initial carbonate, while the oxidation of reduced carbon within the wall rock could produce negative $\delta^{13}CO_2$ values (Ohmoto and Rye, 1979). Olson (1984) reported $\delta^{13}CO_2$ values from calcite and dolomite of the Main Orebody in the range 0‰ to -10‰, suggesting involvement of normal marine carbonate and oxidized organic material. Compared to carbon isotope data from other deposits, data from Nanisivik is most similar to epithermal vein and replacement deposits, deposits of the Upper Mississippi

Valley District, and the early stages of Pine Point (Ohmoto and Rye, 1979).

The δ^{18}O values reported by Olson (1984) are quite high (21‰ to 34‰) relative to connate brines (Taylor, 1979; Figure 6.4) but are slightly less than values for Society Cliffs dolostone. These oxygen isotopic values might be explained if the main source of oxygen was dolostone, although involvement of connate brines might produce values slightly less than those measured for the wall rock. Although the isotopic results presented by Olson (1984) are very preliminary, they are not incompatible with a model involving wall rock interaction. Murowchick (1984) proposed mixing of meteoric water with ore fluid to produce the sulfanes required for marcasite precipitation in the Upper Mississippi Valley District. However, Olson (1984) considered meteoric water to have had very little involvement at Nanisivik.

Using the fractionation factors given by Ohmoto and Rye (1979), the isotopic composition of H_2S in the ore fluid would be approximately +26‰ on the basis of sp-gn fractionation reported by Olson (1984) and between +26 and +27‰ on the basis of py-gn fractionation reported by Ghazban (1984) for Unit 1. Given the small amount of fractionation between ZnS and H_2S under equilibrium conditions, the measured composition of sphalerite should approximate the composition of sulfur in the ore fluid. The average of five values reported by Olson (1984) for sphalerite is +26.48‰ while the average

of seventeen analyses reported by Ghazban (1984) is +26.82‰..
Assuming an intial isotopic composition of +26‰. , the
expected fractionation of pyrite in the range 150 to 200°C
would be between 1 - 2‰. under equilibrium conditions. There-
fore an estimated isotopic composition for the ore fluid of
+26‰. would be in agreement with the isotopic compositions
determined for pyrite in this study.

Orr (1975) suggested three possible mechanisms for
the production of H_2S in petroleum reservoirs. Microbial
sulfate reduction and thermal decomposition of sulfur-bearing
organic compounds generally produces H_2S 15±5‰. lighter than
associated sulfate, while thermochemical sulfate reduction is
considered to result in similar isotopic compositions. Given
the heavy nature of sulfur at Nanisivik, a source 15±5‰.
heavier is considered unlikely. Thermochemical sulfate reduc-
tion with minor isotopic fractionation appears to have been
the important process at Nanisivik.

According to Claypool *et al.,* (1980), Middle Protero-
zoic evaporites have an average $\delta^{34}S$ composition of 17‰. , al-
though values up to 25‰. are reported in the literature. The
most likely source of sea water sulfate at Nanisivik are
evaporite horizons in the Society Cliffs Formation, although
this sulfate is reported to be isotopically lighter than
sulfides at Nanisivik (Olson, 1984).

A graph of salinity versus homogenization temperature
for paired inclusion data (McNaughton, 1983) shows a good
positive correlation (Figure 8.1), with the highest tempera-

tures and salinities associated with sparry dolomite inclusions. In contrast, the detailed hand sample work of Bending (1984) suggested sparry dolomite precipitation was associated with lower temperatures and salinities, although carbonate precipitation is unlikely to be triggered by simple cooling (Holland and Malinin, 1979). A trend of decreasing salinity and temperature from east to west is hard to reconcile with the observed distribution of sparry dolomite in the Upper Lens. Although conditions of high temperature and salinity should be conducive to dolomite precipitation in the eastern Upper Lens, at lower temperatures in the western portion dolomite would be expected to be more soluble, resulting in even higher salinities.

The solubility of carbonates in a hydrothermal solution is dependent upon a number of variables, including temperature, the ionic strength and composition of the ore fluid, the partial pressure of CO_2 and the pH (Holland and Malinin, 1979). Although it has been suggested that the positive correlation between temperature and salinity observed in McNaughton's (1983) data might be explained by simple cooling, given the behavior of carbonate solubility products with temperature, this is unlikely. Recent studies by Taylor *et al.* (1983), Zimmerman and Kesler (1981), and Samson and Russell (1983) utilized paired salinity-homogenization data to evaluate fluid mixing models. A negative correlation between salinity and homogenization temperature was reported in each of these studies, although this is not necessarily
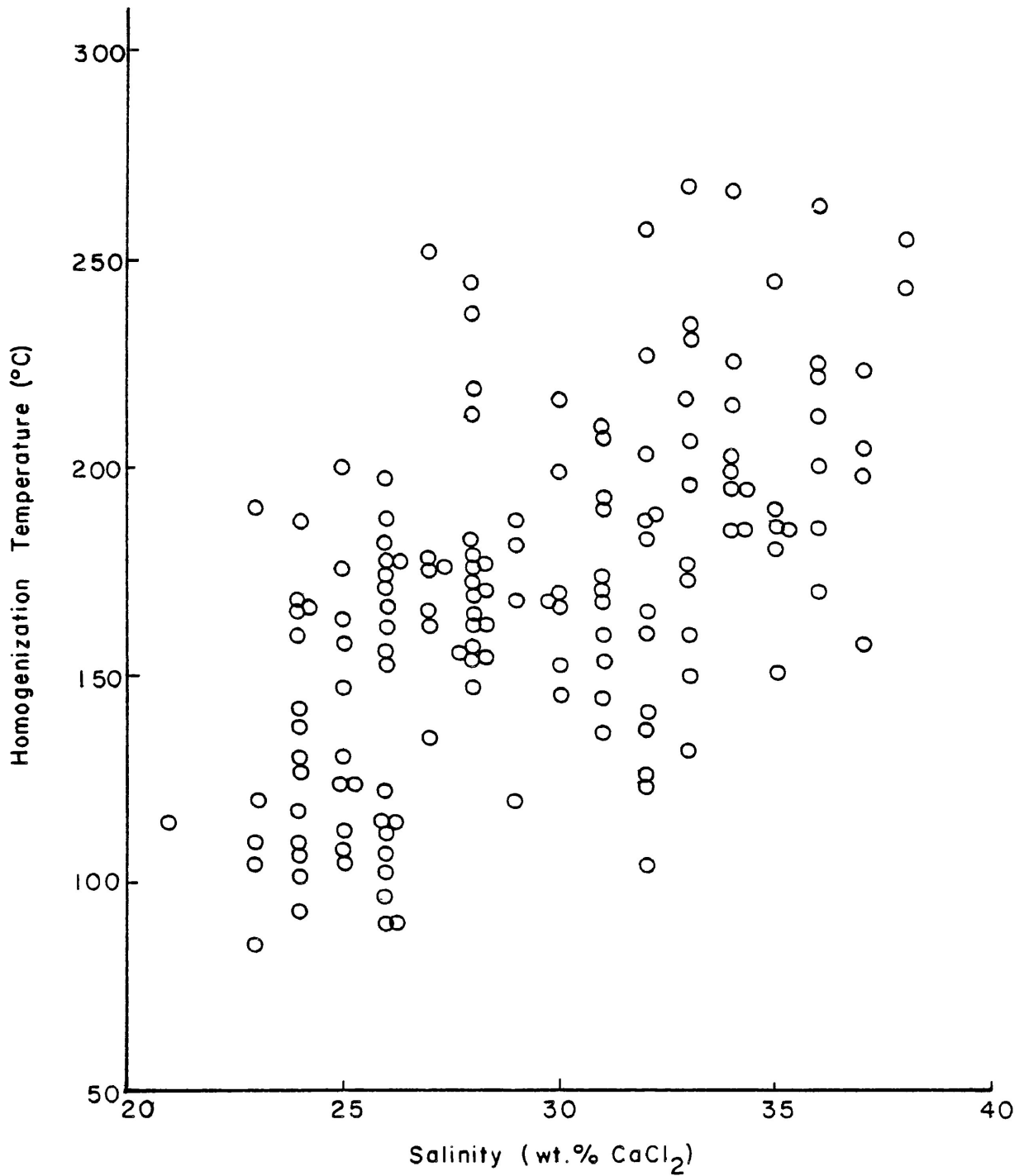
FIGURE 8.1 – PAIRED FLUID INCLUSION DATA FROM McNAUGHTON (1983) FOR THE MAIN OREBODY, NANISIVIK. SECONDARY INCLUSIONS AND THOSE AFFECTED BY DIKE EMPLACEMENT EXCLUDED.

indicative of fluid mixing (S.E. Kesler, pers.comm., 1985).

Based on the calculations of Rising (1973) and the observations of McKibben and Elders (1985), Murowchick and Barnes (1984) concluded that marcasite forms only below 160°C. Radke and Mathis (1980) consider saddle dolomite to form in the temperature range 60 - 150°C in association with hydrocarbon reservoirs, epigenetic base metal deposits, and sulfate-rich carbonates. Although sparry dolomite at Nanisivik generally lacks the curved crystal faces characteristic of saddle dolomite, the sweeping extinction it does exhibit reflects some deformation of the crystal lattice. Therefore, the question that arises is whether or not inclusion homogenization temperatures reflect the original temperature of ore formation.

Evaluation of isotopic fractionation amongst co-existing sulfides presented by Olson (1984) using the fractionation factors given by Ohmoto and Rye (1979) indicates that pyrite, sphalerite and galena were seldom all deposited in isotopic equilibrium. However, Olson's (1984) temperature estimates based on sp-gn fractionation are in good agreement with fluid inclusion results from the eastern and central Upper Lens, although the exact location of Olson's samples is unknown. Also, the fact that a graph of salinity versus homogenization temperature shows a recognizable correlation (Figure 8.1) suggests that inclusions from the Main Orebody do reflect the actual ore-forming event.

McKibbens and Elders (1985) reported the replacement

of marcasite by pyrite at T > 160°C in boreholes from the Salton sea geothermal area. On the basis of experiments involving the breakdown of marcasite, Rising (1973) concluded that marcasite was metastable at high oxygen activities and low sulfur activities at all temperatures. Both studies consider the breakdown of marcasite, rather than its formation, under conditions of ore formation probably dissimilar to those at Nanisivik. Fluid inclusion homogenization temperatures and sulfur isotope fractionation results from Nanisivik suggest that metastable marcasite can form at T > 160°C under conditions of high aO_2. Radke and Mathis (1980) based their conclusions concerning the temperature stability of saddle dolomite on a review of natural occurrences. However, mineralization at Nanisivik indicates that sparry dolomite having some characteristics similar to the saddle dolomite described by Radke and Mathis (1980) does occur at T > 150°C in association with epigenetic base metal deposits.

A characteristic of this and previous inclusion studies involving ore from Nanisivik has been the wide range of homogenization temperatures encountered, even within a single hand sample. As discussed previously, analytical error may account for as much as ±5°C variance in the observed homogenization temperatures. From the discussion of the salinity data and its possible effect on pressure corrections, a further range in homogenization temperature of 15°C might be expected. Section preparation involved heating to 100°C but this is unlikely to have had any effect on the bulk

of the inclusions. Some, but not all, of the variation in homogenization temperatures from dolomite may be related to features such as late veining, while some of the variation in sphalerite temperatures may be attributed to uncertainty surrounding inclusion origin. Good grouping of homogenization data from Area 14, the Lower Lens and the western portion of the Upper Lens suggests that there is something unusual about inclusions from the central and eastern portions of the Upper Lens.

Bending (1984) suggested the presence of CH_4 and H_2S in inclusions from Nanisivik on the basis of their unusual freezing behavior. Fine crushing of dolomite gangue suggests the presence of H_2S within the inclusions but, due to inadequate analytical methods, the presence of methane could not be confirmed. The presence of observable hydrocarbons within some inclusions suggest that an *in situ* generation of methane may have occurred as suggested by Hanor (1980). If the *in situ* generation of methane did occur, it would result in an artificial spread of homogenization temperatures towards higher values. Methane produced by the thermal degradation of organics, either prior to entrappment or by *in situ* generation, would also affect the pressure correction to be applied (Hanor, 1980).

A possibility exists that the Nanisivik area has also been subjected to regional rewarming given its tectonic setting. Unusually young K-Ar ages from diabase dikes on Borden Peninsula and a disagreement between K-Ar and Rb-Sr ages for

the Nauyat volcanics suggests that regional rewarming has occurred. Armstrong (1966) suggested that a minimum temperature of 200°C, corresponding to argon loss from biotite, is needed to reset K-Ar age determinations. Regional rewarming to at least 200°C might be expected to have an effect on fluid inclusions (Bodnar and Bethke, 1984), particularily those formed at low temperatures. However, the relatively uniform distribution of data from Area 14, the western Upper Lens and the Lower Lens are not suggestive of stretching. If hydrocarbons were preferentially concentrated in the central and eastern Upper Lens, the breakdown of complex hydrocarbons within the inclusions during mild regional rewarming to produce methane would only affect homogenization temperatures in this portion of the mine. Detailed regional studies of hydrocarbon maturity and/or illite crystallinity might help to resolve the question of regional rewarming. Analysis of inclusion contents by destructive or non-destructive techniques would also elucidate the role of hydrocarbons in the ore fluid.

Mineralization at Nanisivik has been compared favorably to that of the Mississippi Valley Type (Olson, 1977, 1984; McNaughton, 1983) with which it shares low temperature-high salinity fluids, dolomitic host rock, simple mineralogy, epigenetic mode of emplacement, and heavy sulfur isotopes. There are also significant dissimilarities. Coarse-grain size, replacement textures, banding parallel to wall rock contacts, a complex overall paragenesis and well zoned

sphalerite crystals are features more common to epithermal base metal vein and replacement deposits (Craig and Vaughn, 1981). However, Nanisivik does lack the very high temperatures, high sphalerite iron contents, and silicate gangue common to some epithermal vein deposits (Ohmoto and Rye, 1970). A high iron sulfide content relative to base metals, recoverable Ag, and a tectonic setting in a rifted basin are features more commonly associated with sedimentary exhalative base metal deposits (Large, 1983; Lydon, 1983). Clearly mineralization at Nanisivik is unusual and probably represents a hybrid of several deposit types.

SUMMARY

Ore mineralization of the Main Orebody at Nanisivik is characterized by lateral and vertical variations in ore texture and mineralogy. Horizontally banded ore of the Upper Lens, Main Orebody exhibits a relative increase in pyrite and sphalerite content from east to west with a corresponding decrease in galena and sparry dolomite content. Eastern and central Upper Lens mineralization is further distinguished from the western Upper Lens by the presence of texturally and mineralogically distinct mine units developed along the margins of the ore body. Mine Units 1, 3 and 5 are in contact with dolostone wall rock of the Society Cliffs Formation, and are characterized by replacement textures and the presence of bladed pyrite. Mine Units 2 and 4 are well banded and less commonly display evidence of replacement. Banded ore of Unit 2 is often inclined at a high angle parallel to the termination of dolostone fins that project a considerable distance into the Upper Lens. Unit 6 is characterized by chaotic, "selvage" textured ore which truncates banding in other mine units. Irregular, chaotic ore of the Lower Lens underlies the Upper and is in contact with brecciated dolostone. Locally, the Upper and Lower Lens are connected by a vertical section of massive pyrite mineralization known as the Keel Zone. Mineralization of the Shale Zone is massive and irregular. The Area 14 Orebody is

similar mineralogically to the Main Orebody but is texturally much simpler.

Examination of hand samples, and polished and doubly polished thin sections indicates that the paragenetic sequence of individual sulfide bands usually consists of sphalerite → pyrite (marcasite) → galena → sparry dolomite. Evidence of an early, finely laminated iron sulfide occurs in both the Lower Lens and in the Area 14 Orebody. Both the Shale Zone and the Area 14 Orebody contain a late, cross-cutting generation of colourless sphalerite. Pyrite of the Shale Zone also shows evidence of annealing. Bladed iron sulfide crystals of the main replacement units 1, 3 and 5 are anisotropic and porous, indicating inversion of marcasite to pyrite. Single crystal X-ray diffraction patterns failed to indicate the presence of remnant marcasite structure. Finely laminated, early iron sulfide from the Lower Lens consists predominantly of pyrite, although minor marcasite is present. Sphalerite of the eastern and central Upper Lens is typically well zoned, varying from dark coloured centers to light rims. Zoning with colourless sphalerite rims is best developed in the main replacement units and these rims often fluoresce under ultraviolet light. Fluorescence probably results from a number of trace element impurities. Microprobe analyses indicate that colour zoning in sphalerite crystals is related to iron content. Dark red crystal cores contain up to 14 mole % FeS, decreasing to 0 mole % FeS at colourless rims. Although wurtzite has been reported to occur at Nanisivik as

late stage mineralization, single crystal X-ray diffraction studies failed to confirm its presence.

Homogenization temperature data from primary inclusions in dolomite and pseudo-secondary and primary inclusions in sphalerite indicate temperatures ranging from 70°C to over 300°C for the Main Orebody. Evaluation of the homogenization data and correction for pressure indicate that mineralization in the eastern portion of the Upper Lens predominantly took place in the more restricted range 150 - 210°C. Although complicated by the wide range of homogenization data and by some uncertainty surrounding the use of pseudo-secondary inclusions, temperature probably did not vary greatly between mine Units 1 to 6. A small number of freezing experiments indicate that inclusions contain a brine consisting of 20 - 37 wt.% $CaCl_2$ eq.

Sulfur isotope analyses of both bladed and cubic, main to late stage pyrite crystals show a remarkably narrow range of $\delta^{34}S$ values from +27.4‰ to +28.0‰., suggesting little variation in temperature, fluid source or the dominant sulfur species in solution, provided no subsequent re-equilibriation of sulfur isotopes has occurred. A single sample from the Area 14 Orebody has a slightly lower $\delta^{34}S$ value of +27.1‰ while two samples from the Lower Lens are slightly heavier, having $\delta^{34}S$ compositions of +28.0‰.

A brief comparison of bitumen associated with Lower Lens mineralization and solid organics extracted from a sample of Society Cliffs dolostone indicates that the two

types of organics are similar with respect to their organic solvent-soluble fraction, their infrared absorption, and their X-ray diffraction patterns. The two types of bitumen differ in their C/H ratio, but this may be explained by the preferential depletion of hydrogen in bitumen associated with mineralization.

The iron content of sphalerite in equilibrium with pyrite may be used to constrain the sulfur activity at the time of sphalerite deposition as well as the oxygen activity of the ore solution. Decreasing iron contents towards the edges of crystals indicate that the oxygen activity increased from 10^{-46} to 10^{-41} for a $\Sigma mS = 10^{-2}$ at 200°C. An oxygen activity of 10^{-41} at 200°C is close to the SO_4^{-2}/H_2S boundary where the activity of thiosulfate ($S_2O_3^-$) is at its highest, being the main intermediary in sulfate reduction. Reaction of thiosulfate to produce sulfane (H_2S_2) is considered necessary to precipitate marcasite. Maximum oxygen activities (i.e.: lowest FeS content in sphalerite) occurred in the main replacement units 1, 3 and 5, and it is in these units that marcasite is most common. The stability of sulfanes is pH dependent over the temperature range of interest and, therefore, the presence of marcasite may be used to indicate a pH < 5.0 at the time of precipitation, as this is the upper stability limited of H_2S_2. Dolomite precipitation is also extremely pH dependent and occurs at pH > 5.0 at 200°C for a $\Sigma mC = 10^{-1}$. The occurrence of interbanded bladed pyrite and sparry dolomite indicates that the pH of the ore fluid

fluctuated around pH = 5. At 100°C, assuming a similar range of sphalerite compositions, the oxygen activity and thiosulfate activities are lower. Therefore, in the lower temperature western portion of the Upper Lens marcasite would not be expected to be widespread. Also at lower temperatures and oxygen activities, dolomite would become more soluble. Although the solubility of galena decreases by nearly an order of magnitude from 200°C to 100°C, temperature does not appear to have played a significant role in the distribution of lead.

The model of ore formation proposed is similar to that suggested by Curtis (1984) and agrees with the isotopic evidence of Olson (1977, 1984). A schematic illustration of the mineralizing event is presented in Figure 8.2. A hot, saline solution carrying sulfate and metals is envisioned to have entered the area of the Main Orebody in the central and eastern portions of the Upper Lens. Although the Main Orebody is considered primarily to be a replacement phenomenon, initial fluid flow may have been channeled by karstic features. On encountering H_2S and CH_4 at the site of ore deposition, sulfate was reduced and sulfides precipitated to produce acid. Interaction of the warm acid solution with the carbonate country rock liberated more hydrocarbons which continued to reduce sulfate in the presence of H_2S. Carbonate replacement and sulfate reduction were concentrated along wall rock — orebody contacts and it is near these regions that thiosulfate activities were at their highest. The

FIGURE 8.2 - SCHEMATIC DIAGRAMS SUMMARIZING ORE FORMATION IN THE EASTERN MAIN OREBODY
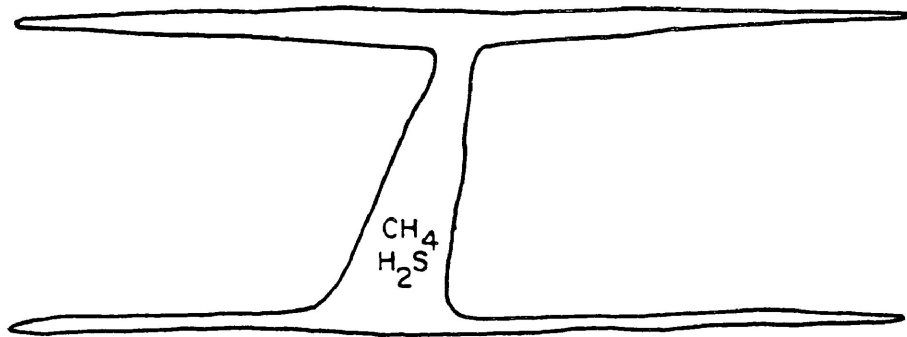
POSSIBLE CONFIGURATION OF ORIGINAL KARST OPENING.

⇒ MIGRATION OF REPLACEMENT FRONTS
→ MOVEMENT OF CHEMICAL SPECIES
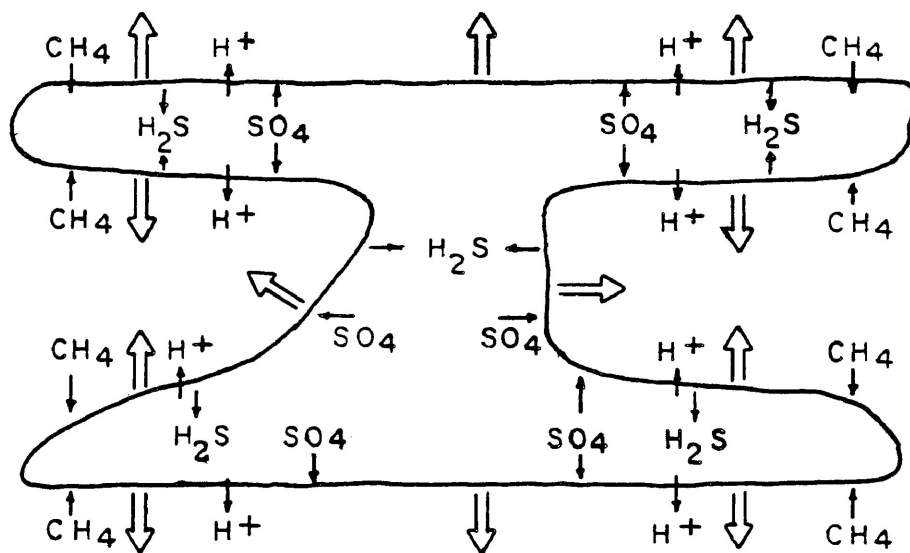
ENLARGEMENT OF THE INITIAL OPENING BY REPLACEMENT
TO PRODUCE BANDED MINE UNITS I THROUGH 5.
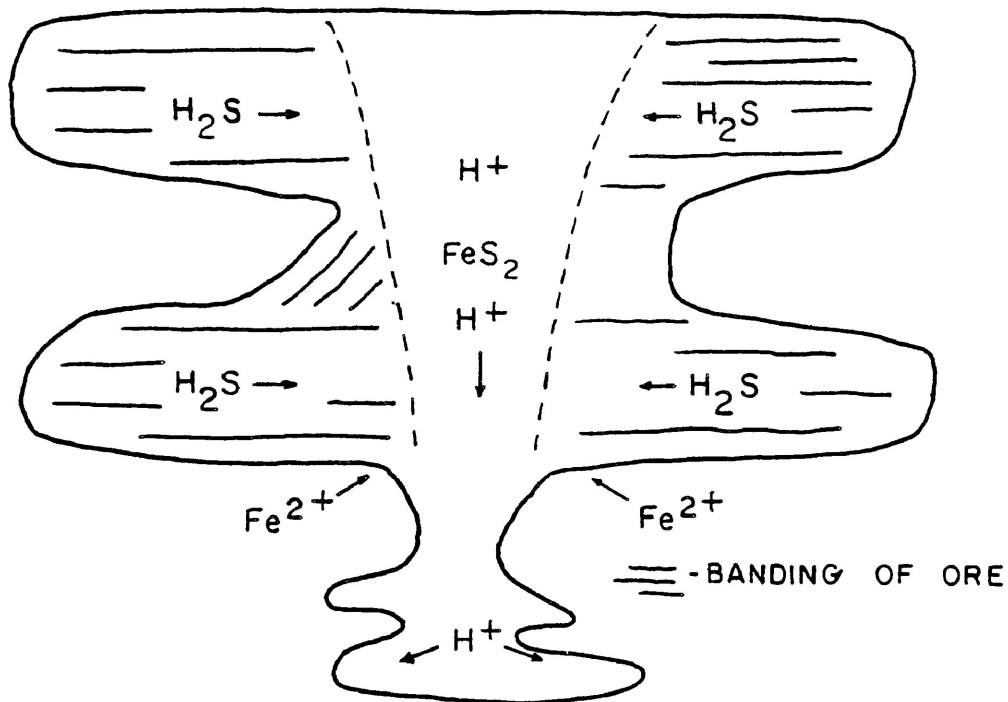
STAGE 2: DEVELOPMENT OF THE KEEL ZONE ACCOMPANIED BY DOWNCUTTING AND DISSOLUTION IN THE LOWER LENS.
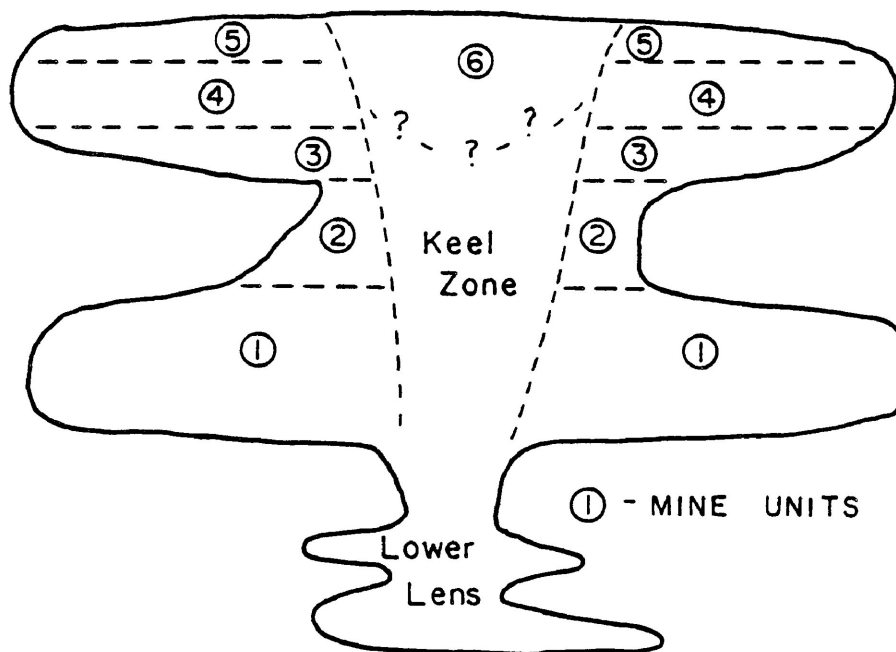
STAGE 3: MINERALIZATION OF UNIT 6 AND THE LOWER LENS TO COMPLETE FORMATION OF THE MAIN OREBODY.

interaction of thiosulfate in an acidic solution with sulfides produced the sulfane necessary for marcasite precipitation in the replacement units 1, 3 and 5. Once the immediate supply of metals was exhausted, interaction of the ore fluid with carbonate wall rock buffered the solution until dolomite precipitated. Banding of ore is probably the result of repetitive sulfate reduction, metal precipitation and wall rock dissolution in response to the continued influx of ore fluid (Figure 8.3). The present orientation of banding is probably a manifestation of initial wall rock contacts. Nearly equal volume replacement of wall rock by sulfides and sparry dolomite gangue allows for the *in situ* reduction of the ore fluid. An excess of H_2S may have led to the production of acid during the formation of the Keel Zone under more reduced conditions. Excess acid production resulted in downcutting of the Keel Zone through banded units and the dissolution and brecciation of wall rock in the Lower Lens. Mineralization of Unit 6 and the Lower Lens consequently filled open spaces and therefore lacks the banding of replacement units. As the ore fluid migrated from east to west, it was already partially reduced and much cooler resulting in sulfide precipitation dominated by pyrite and sphalerite. Once the ore fluid exited the immediate region of the Main Orebody it was probably reduced, low temperature and depleted in economic metals. This "exhausted" ore fluid may have been responsible for many of the low temperature barren pyritic bodies to be found in the Nanisivik area.
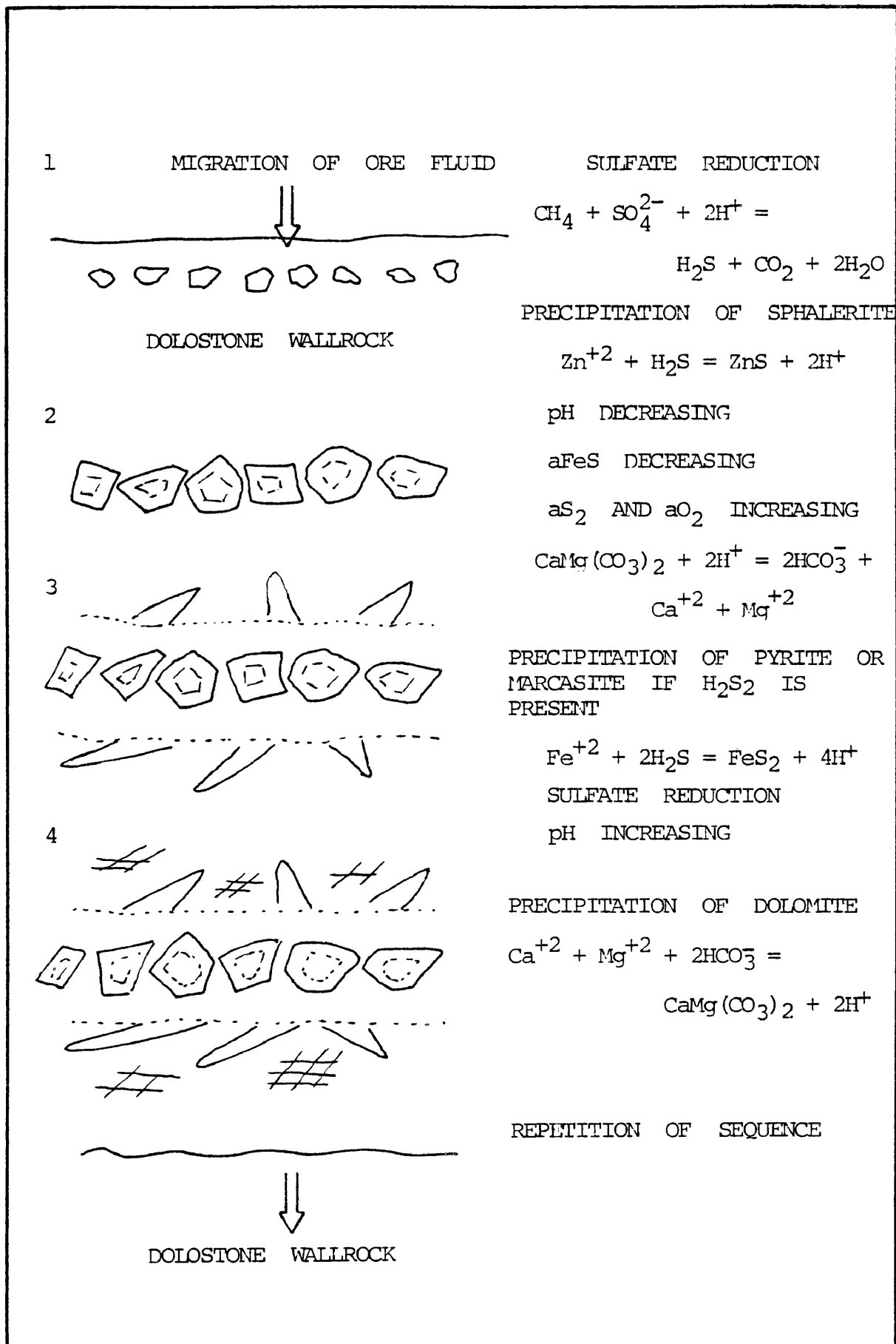
REFERENCES

AKANDE, S.O. and ZENTILLI, M. (1984); Geologic, fluid inclusion, and stable isotope studies of the Gays River lead-zinc deposit, Canada: *Econ. Geol.* vol. 79, p. 1187-1211

AKIZUKI, M. (1981); Investigation of phase transition of natural ZnS minerals by high resolution electron microscopy: *Amer. Mineral.* vol. 66, p. 1006-1012

ANDERSON, G.M. (1984); Sulfate reduction and sulfide precipitation in carbonate rocks: in *Recent Advances in the Geochemistry of Ore Deposits*, Mineral Exploration Research Institute Symposium, Montreal, p. 3-7

ANDERSON, G.M. (1983); Some geochemical aspects of sulfide precipitation in carbonate rocks: in *International Conference on Mississippi Valley Type Lead-Zinc Deposits, Proceedings Volume;* G. Kisvarsanyi, S.K. Grant, W.P. Pratt and J.W. Koenig (eds.), Univ. of Missouri-Rolla, p. 61-76

ANDERSON, G.M. (1979); Mississippi Valley - type ores: in *Ore Deposit Workshop Volume,* Univ. of Toronto, p. 11-35

ANDERSON, G.M. (1977); Thermodynamics and sulfide solubilities: in *Application of Thermodynamics to Petrology and Ore Deposits,* Mineral. Assoc. Can. Short Course Notes, Vancouver, p. 136-150

ANDERSON, G.M. and MACQUEEN, R.W. (1982); Ore deposit models - 6. Mississippi Valley - type lead-zinc deposits: *Geoscience Canada,* vol. 9, p. 108-117

ARMSTRONG, R.L. (1966); K - Ar dating of plutonic and volcanic rocks in orogenic belts: in *Potassium Argon Dating;* O.A. Schaeffer and J. Zahringer (eds.), Springer- Verlag, p. 117-133.

AULT, W.V. and JENSEN, M.L. (1963); Summary of sulfur isotope standards: in *Biogeochemistry of Sulfur Isotopes;* M.L. Jensen (ed.), Natl. Sci. Found. Symposium Proc. Yale Univ.

BAILEY, N.J. (1977); Hydrocarbon and hydrogen sulphide generation in early diagenesis by thermal maturation: in *Proceedings of the Forum on Oil and Ore in Sediments*, Imperial College, London, England, 1975, p. 93-107.

BARNES, H.L. (1983); Ore-depositing reactions in Mississippi Valley type deposits: in *International Conference on Mississippi Valley Type Lead-Zinc Deposits, Proceedings Volume;* G. Kisvarsanyi, S.K. Grant, W.P. Walden and J.W. Koenig (eds.), Univ. of Missouri-Rolla, p. 77-85

BARNES, H.L. (1979); Solubilities of ore minerals: in *Geochemistry of Hydrothermal Ore Deposits*, 2nd edition, H.L. Barnes (ed.), John Wiley and Sons, p. 404-460.

BARNES, H.L. and KULLERUD, G. (1961); Equilibria in sulfur-containing aqueous solutions, in the system Fe-S-O, and their correlation during ore deposition : *Econ. Geol.* vol. 56, p. 648-688

BARTON, P.B. (1967); Possible role of organic matter in the precipitation of the Mississippi Valley ores: in *Genesis of Stratiform Galena - Zinc - Barite - Fluorite Deposits*, J.S. Brown (ed.), Econ. Geol. Mono. 3, p. 371-379

BARTON, P.B. and SKINNER, B.J. (1979); Sulfide mineral stabilities: in *Geochemistry of Hydrothermal Ore Deposits*; H.L. Barnes (ed.), John Wiley and Sons, p. 278-403

BENDING, D. (1984); *Report on Cathodoluminescence of Carbonates in the Nanisivik Region*: Report to Nanisivik Mines Ltd.

BENDING, D. (1984); Report on fluid inclusion studies at the University of Toronto Fluid Inclusion Laboratory: in *Report on Investigations of the Nanisivik FeZnPbAg Deposits*; L. Curtis, Final Report to Nanisivik Mines Ltd., p. 121-133

BODNAR, R.J. and BETHKE, P.M. (1984); Systematics of stretching of fluid inclusions I: fluorite and sphalerite at 1 atmosphere confining pressure: *Econ. Geol.* vol.79, p.141-161

BRECKE, E.A. (1962); Ore genesis of the Cave-in-Rock fluorspar district, Hardin County, Illinois: *Econ. Geol.* vol. 57, p. 499-535

BROWNLOW, A.H. (1979); *Geochemistry*: Prentice-Hall, Englewood Cliffs, N.J., 498 p

BUBELA, B. and McDONALD, J.A. (1969); Formation of banded sulphides: metal ion separation and precipitation by inorganic and microbial sulphide sources: *Nature*, vol.221, p. 465-466.

BURRUSS, R.C. (1981); Analysis of phase equilibria in C-OH-S fluid inclusions: in *Fluid Inclusions: Applications to Petrology*; Mineral. Assoc. Can. Short Course Notes, Calgary, p. 39-74

CABRI, L., CAMPBELL, J., LAFLAMME, J.H., LEIGH,R., MAXWELL,J. and SCOTT, J. (1985); Proton - microprobe analysis of trace elements in sulfides from some massive - sulfide deposits: *Can. Mineral.*, vol. 23, p. 133-148

CHRISTIE, K.W. and FAHRIG, W.F. (1983); Paleomagnetism of the Borden dykes of Baffin Island and its bearing on the Grenville loop: *Can. Jour. Earth Sci.*, vol. 20, p. 275-298

CHURNET, H.G. (1979); *The Relationship between Dolomitization and Sphalerite Mineralization in the Lower Ordovician Upper Knox Carbonate Rocks of the Copper Ridge District, East Tennessee:* Unpub. PhD thesis, Univ. of Tennessee, Knoxville, 237 p

CLAYPOOL, G.E., HOSLER, W.T., KAPLAN, I.R., SAKA, H. and ZAK,I. (1980); The age curves of sulfur and oxygen isotopes in marine sulfate and their mutual interpretation: *Chem. Geol.*, vol. 28, p. 199-260

CLAYTON, R.H. and THORPE, L. (1982); Geology of the Nanisivik zinc-lead deposit: in *Precambrian Sulfide Deposits;* R.W. Hutchinson, C.D. Spence and J.M. Franklin (eds.), Geol. Assoc. Can. Spec. Pap. 25, p. 739-758

CRAIG, J.R., SOLBERG, T.N. and VAUGHAN, D.J. (1983); Growth characteristics of sphalerites in Appalachin zinc deposits: in *International Conference on Mississippi Valley Type Lead-Zinc Deposits, Proceedings Volume;* G. Kisvarsanyi, S.K. Grant, W.P. Pratt and J.W. Koenig (eds.), Univ. of Missouri-Rolla, p.317-327

CRAIG, J.R. and VAUGHAN, D.J. (1981); *Ore Microscopy and Ore Petrography:* John Wiley and Sons, 406 p

CRAWFORD, M.L. (1981); Phase equilibria in aqueous fluid in-clusions: in *Fluid Inclusions: Applications to Petrology,* Mineral. Assoc. Can. Short Course Notes, Calgary, p. 75-100

CURIE, D. (1963); *Luminescence in Crystals:* G.F.J. Garlick (trans.), John Wiley and Sons, New York, 332 p

CURTIS, L.W. (1984); *Report on Investigations of the Nanisivik Fe Zn Pb Ag Deposits:* Final Report to Nanisivik Mines Ltd.

CZAMANSKE, G.K. and RYE, R.O. (1974); Experimentally determined sulfur isotope fractionations between sphalerite and galena in the temperature range 600°C to 275°C: *Econ. Geol.* vol. 69, p. 17-25

DREAN, T. (1978); *Experimental Study on Sulfate Reduction by Methane, Xylene and Iron in a Temperature Range 175 – 350:* Unpub. MSc thesis, Penn. State Univ.

DUNSMORE, H.E. and SHEARMAN, D.J. (1977); Mississippi Valley – type lead-zinc orebodies: a sedimentary and diagenetic origin: in *Proceedings of the Forum on Oil and Ore in Sedi-ments,* Imperial College, London, England, 1975, p.189-205

FAHRIG, W.F., CHRISTIE, K.W. and JONES, D.L. (1981); Paleomagne-tism of the Bylot basins: evidence for McKenzie continental tension tectonics: *Can. Geol. Surv. Pap. 81-10,* p. 303-312

FLEET, ME. (1977); The birefringence – structural state relation in natural zinc sulfides and its application to a schalenblende from Primbram: *Can. Mineral,* vol. 15, p. 303-308

FONTBOTE, L. and ANSTUTZ, G.C. (1983); Diagenetic crystallization rhythmites in Mississippi Valley type lead-zinc deposits: *Inter-national Conference on Mississippi Valley Type Lead-Zinc Deposits, Proc. Volume;* G. Kisvarsanyi, S.K. Grant, W.P. Walden and J.W. Koenig (eds.), Univ. of Missouri-Rolla, p. 328-337

FORD, D.C. (1981); *Report upon Karstic Features of Sulphide Deposition at Nanisivik*: Report to Nanisivik Mines Ltd.

FRIEDMAN, G.M. (1959); Identification of carbonate minerals by staining methods: *Jour. of Sed. Pet.*, vol. 29, p. 87-97

GAIT, R.I. (1985); The morphology and habit of pyrite crystals from the Nanisivik mine, Baffin Island, NWT. (abs.): *Geol. Assoc. Can./Min. Assoc. Can. Annual Meeting*, Halifax.

GEILKMAN, M.B. (1982); Mechanisms of polytype stabilization during the wurtzite – sphalerite transition: *Phys. Chem. Minerals*, vol. 8, p. 2-7

GELDSETZER, H. (1973); The tectono – sedimentary development of an algal dominated Helikian succession on north Baffin Island, NWT: in *Arctic Geology*; M.G. Pitcher (ed.), Am. Assoc. Petrol. Geol. Mem. 19, p. 101-127.

GHAZBAN, F. (1984); PhD progress reports on sulfur isotopes to Nanisivik Mines Ltd.

GIGGENBACH, W. (1974); Equilibria involving polysulfide ions in aqueous solutions up to 240°C: *Inorganic Chem.*, vol. 13, p. 1724-1730

GIORDANO, T.H. and BARNES, H.L. (1981); Lead transport in Mississippi Valley type ore solutions: *Econ. Geol.*, vol. 76, p. 2200-2211

GIZE, A.P. and RIMMER, S.M. (1983); *Mesophase Development in a Bitumen from the Nanisivik Mississippi Valley – Type Deposit*: Report to Nanisivik Mines Ltd., 12 p

GRÖEPPER, H. (1978); *Geology and Mineralization of Nanisivik Main Orebody*: Interim Report to Nanisivik Mines Ltd. 12 p

GROGAN, R.M. and BRADBURY, J.C. (1981); Fluorite – zinc – lead deposits of the Illinois – Kentucky mining district: in *Ore Deposits of the United States, 1933 – 1967*; J.D. Ridge (ed.), A.I.M.E., p. 370-399

HANOR, J.S. (1980); Dissolved methane in sedimentary brines: potential effect on the PVT – properties of fluid inclusions: *Econ. Geol.*, vol. 75, p. 603-609

HARDY, J.L. (1979); *Stratigraphy, Brecciation and Mineralization: Gayna River, Northwest Territories*: Unpub. MSc thesis, Univ. of Toronto, 461 p

HOLLAND, H.D. and MALININ, S.D. (1979); The solubility and occurrence of non-ore minerals: in *Geochemistry of Hydrothermal Ore Deposits*; H.L. Barnes (ed.), John Wiley and Sons, p. 461-508

HOLLISTER, L.S., CRAWFORD, M.L., ROEDDER, E., BURRUSS, R.C., SPOONER, E.T.C. and TOURET, J. (1981); Practical aspects of microthermometry: in *Fluid Inclusions: Applications to Petrology*, Mineral. Assoc. Can. Short Course Notes, Calgary, p. 278-304

HUNSTBERGER, D.V. and BILLINGSLEY, P. (1977); *Elements of Statistical Inference* (4th ed.): Allyn and Bacon, Inc., Toronto, 385 p

JACKSON, G.D. and IANNELLI, T.R. (1981); Rift-related sedimentation in the Neohelikian Borden Basin, northern Baffin Island: in *Proterozoic Basins of Canada; Geol. Surv. Can. Pap. 81-10*, p. 269-302

JALONEN, M. (1982); *Fluid Inclusion Studies on the Nanisivik Zinc-Lead Deposit:* Unpub. BSc thesis, Univ. of Windsor, 44 p

JIAMO, F. (1979); Some characteristics of the evolution of organic matter in carbonate formations: in *Advances in Organic Geochemistry*, A.G. Douglas and J.R. Maxwell (eds.), Physics and Chemistry of the Earth, vol. 12, Pergamon Press, London, England, p. 39-50

JONASSEN, I.R. and SANGSTER, D.F. (1978); Cd ratios for sphalerites from Canadian sulphide ore samples: *Geol. Surv. Can. Pap. 78-1B*, p. 195-201

JOWET, E.C. (1975); Nature of the ore forming fluids of the Polaris lead-zinc deposit, Little Cornwallis Island, NWT: from fluid inclusion studies: *Can. Min. and Met. Bull.*, vol. 68, p. 124-129

KING, L.H., GOODSPEED, F.E. and MONTGOMERY, (1963); A study of sedimentated organic matter and its natural derivatives: *Mines Branch Research Report R114*, Dept. of Mines and Technical Surveys, Ottawa

KINNEY, C.R. and DOUCETTE, E.I. (1958); Infra-red spectra of a coalification series from cellulose and lignin to anthracite: *Nature*, vol. 128

KISSIN, S.A. (1983); Report on visit to Nanisivik Mines Ltd.: 3 p

KISSIN, S.A. and SCOTT, S.D. (1982); Phase relations involving pyrrhotite below 350°C: *Econ. Geol.*, vol. 77, p. 1739-1754

KROGER, F.A. and VINK, H.J. (1954); The origin of the fluorescence in self-activated ZnS, CdS and ZnO: *Jour. Chem. and Phys.*, vol. 22, p. 250-252

KULP, B.A. and KELLEY, R.H. (1960); Displacement of the sulfur atom in CdS by electron bombardment: *Jour. App. Phy.*, vol. 31, p. 1057-1061

KWIATKOWSKI, D. (1975); *Geology and Geochemistry of the Kakabeka Falls Anthraxolite:* Unpub. BSc thesis, Lakehead Univ., Thunder Bay, Ontario, 103 p

LAKEFIELD RESEARCH (1984); *Mineralogical Examination of Area 14:* Report to Nanisivik Mines Ltd., 6 p

LARGE, D.E. (1983); Sediment hosted massive sulphide lead-zinc deposits: in *Sediment-Hosted Stratiform Lead-Zinc Deposits;* Mineral. Assoc. Can. Short Course Notes, D.F. Sangster (ed.), Victoria, p 1-29

LARSON, L.T., MILLER, J.D., NADEAU, J.E. and ROEDDER, E. (1973); Two sources of error in low-temperature inclusion homogenization determinations and corrections on published temperatures for the East Tennessee and Laisvall deposits: *Econ. Geol.,* vol. 68, p. 113-116

LAWLER, J.P. and CRAWFORD, M.L. (1983); Stretching of fluid inclusions resulting from a low-temperature microthermometric technique: *Econ. Geol.,* vol. 78, p. 527-529

LEVIN, P. and AMSTUTZ, G.C. (1976); Kristalliation und bewegung in erzrhythmiten am beispiel Triassisch - Jurassischer Lagerstatten in Ostperu: *Münster, Forsch. Geol. Palaont.,* 38/39, p. 111-128

LYDON, J.W. (1983); Chemical parameters controlling the origin and deposition of sediment-hosted stratiform lead-zinc deposits: in *Sediment-Hosted Stratiform Lead-Zinc Deposits;* Mineral. Assoc. Can. Short Course Notes, D.F. Sangster (ed.), Victoria, p. 175-250

MacQUEEN, R.W. and POWELL, T.G. (1983); Organic geochemistry of the Pine Point Lead-zinc ore field and region, Northwest Territories, Canada: *Econ. Geol.,* vol. 78, p. 1-25

MacQUEEN, R.W. and THOMPSON, R.I. (1978); Carbonate hosted lead-zinc occurrences in northeastern British Columbia with emphasis on the Robb Lake deposit: *Can. Jour. Earth Sci.,* vol. 15, p. 1737-1762

McCONNEL, R.H. and ANDERSON, R.A. (1968); The Metaline District, Washington: in *Ore Deposits in the United States,* Graton - Sales vol. 2, A.I.M.E., p. 1460-1481

McKAY, D. (in prep.); *The Abundance and Distribution of Gallium in Upper Mantle - Derived Lherzolites and Related Rocks:* MSc thesis, Lakehead Univ., Thunder Bay, Ontario

McKIBBEN, M.A. and ELDERS, W.A. (1985); Fe-Zn-Cu-Pb Mineralization in the Salton sea geothermal system, Imperial Valley California: *Econ. Geol.,* vol. 80, p. 539-559

McLIMANS, R.K. (1977); *Geological, Fluid Inclusion, and Stable Isotope Studies of the Upper Mississippi Valley Zinc-Lead District, Southeast Wisconsin:* Unpub. PhD thesis, Penn.State Univ., 175 p

McNAUGHTON, K. (1983); *A Fluid Inclusion Study of the Nanisivik Lead-Zinc Deposit, Baffin Island, NWT:* Unpub. MSc thesis, Univ. of Windsor, Ontario, 94 p

MUROWCHICK, J.B. (1984); *The Formation and Growth of Pyrite, Marcasite and Cubic Ferrous Sulfide:* Unpub. PhD thesis, Penn. State Univ., 168 p

MUROWCHICK, J.B. and BARNES, H.L. (1984); The significance of porous pyrite (abs.): *Geol. Soc. of Am. Abstracts with Programs,* p. 604

NEUMANN, M. (1985); Monthly PhD thesis progress reports on mineralogy to Nanisivik Mines Ltd.

NEUMANN, M. (1984); Monthly PhD thesis progress reports on mineralogy to Nanisivik Mines Ltd.

NORMAN, D.I., WUPOA TING, B.R., PUTNAM, B.R. and SMITH, R.W. (1985); Mineralization of the Hansonburg Mississippi Valley - type deposit, New Mexico: Insight from composition of gases in fluid inclusions: *Can. Mineral.,* vol. 23, p. 353-368

OHMOTO, H. (1972); Systematics of sulfur and carbon isotopes in hydrothermal ore deposits: *Econ. Geol.,* vol. 67, p. 551-578

OHMOTO, H. and LASAGA, A.C. (1982); Kinetics of reactions between aqueous sulfates and sulfides in hydrothermal solutions: *Geochim. et Cosmochim. Acta.,* vol. 46, p. 1727-1745

OHMOTO, H. and RYE, R.O. (1979); Isotopes of sulfur and carbon: in *Geochemistry of Hydrothermal Ore Deposits;* H.L. Barnes (ed.), John Wiley and Sons, p. 509-567

OHMOTO, H. and RYE, R.O. (1970); The Bluebell Mine, British Columbia, I. mineralogy, paragenesis, fluid inclusions and the isotopes of oxygen and carbon: *Econ. Geol.,* vol. 65, p. 417-437

OLSON, R.A. (1984); Genesis of paleokarst and strata-bound zinc-lead sulfide deposits in a Proterozoic dolostone, northern Baffin Island, Canada: *Econ. Geol.* vol. 79, p. 1056-1103

OLSON, R.A. (1977); *Geology and Genesis of Zinc-Lead Deposits Within a Late Proterozoic Dolomite, Northern Baffin Island, NWT:* Unpub. PhD thesis. Univ. of British Columbia, Vancouver, 371 p

ORR, W.L. (1982); Rate and mechanism of non-microbial sulfate reduction (abs.): *Geol. Soc. of Am. Abstracts with Programs,* p. 580

ORR, W.L. (1975); Geological and geochemical controls on the distribution of hydrogen sulfide in natural gas (abs.): *Geol. Soc. of Am. Abstracts with Programs,* p. 1220

PERING, K.L. (1973); Bitumens associated with lead, zinc and fluorite ore minerals in North Derbyshire, England: *Geochim et Cosmochim. Acta.*, vol. 37, p. 401-419

POTTER, R.W. (1977); Pressure corrections for fluid inclusion homogenization temperatures based on the volumetric properties of the system $NaCl-H_2O$: *U.S. Geol. Surv. J. Res. 5*, p. 603-607

POTTER, R.W., CLYNNE, M.A. and BROWN, D.L. (1978); Freezing point depression of aqueous sodium chloride solutions: *Econ. Geol.*, vol. 73, p. 284-285

POWELL, T.G. (1978); An assessment of the hydrocarbon source rock potential of the Canadian Arctic Islands: *Geol. Surv. Can. Pap. 78-12*, 82 p

RADKE, B.M. and MATHIS, R.L. (1980); On the formation and occurrence of saddle dolomite: *Jour. Sed. Petrol.*, vol. 50, p. 1149-1168

RISING, B.A. (1973); *Phase Relations Among Pyrite, Marcasite and Pyrrhotite Below 300°C:* Unpub. PhD thesis. Penn. State Univ. 192 p

ROEDDER, E. (1984); Fluid Inclusions: Reviews in Mineralogy, *Mineral. Soc. Am.*, vol. 12, 644 p

ROEDDER, E. (1981); Origin of fluid inclusions and changes that occur after trapping: in *Fluid Inclusions: Applications to Petrology;* Mineral. Assoc. Can. Short Course Notes, Calgary, p. 101-135

ROEDDER, E. (1979); Fluid inclusions as samples of ore fluids: in *Geochemistry of Hydrothermal Ore Fluids*, H.L. Barnes (ed.), John Wiley and Sons, p. 684-737

ROEDDER, E. and DWORNIK, E.J. (1968); Sphalerite colour banding: lack of correlation with iron content, Pine Point, Northwest Territories, Canada: *Am. Mineral.*, vol. 53, p. 1523-1529

RYE, R.O. (1974); A comparison of sphalerite - galena sulfur isotope temperatures with filling temperatures of fluid inclusions: *Econ. Geol.*, vol. 69, p. 26-32

RYE, R.O. and OHMOTO, H. (1974); Sulfur and carbon isotopes and ore genesis: a review: *Econ. Geol.*, vol. 69, p. 826-842

SAMSON, I.M. and RUSSELL, M.J. (1983); Fluid inclusion data from the Silvermines base metal + baryte deposits, Ireland: *Inst. Min. Met. Trans.*, vol. 92, p. B67-B71

SASS-GUSTKIEWICZ, M., DZULYNSKI, S. and RIDGE, J.D. (1982); The emplacement of zinc-lead ores in the Upper Silesian district. A contribution to the understanding of Mississippi Valley type deposits: *Econ. Geol.*, vol. 77, p. 392-412

SAXBY, J.D. (1976); The significance of organic matter in ore
genesis: *Handbook of Strata-bound and Stratiform Ore Deposits;*
K. H. Wolf (ed.), vol. 2, Elsevier, New York, p. 111-134

SAXBY, J.D. (1970); Technique for the isolation of kerogen from
sulfide ores: *Geochim. et Cosmochim. Acts.,* vol. 34,
p. 1317-1326

SCOTT, S.D. (1974); Stocichiometry of sulfides: in *Sulfide
Mineralogy;* P.H. Ribbe (ed.), Mineral. Soc. Am. Short Course
Notes, vol. 1, p. CS 99 - CS 110

SCOTT, S.D. and KISSIN, S.A. (1973); Sphalerite composition in the
Zn-Fe-S system below 300°C: *Econ. Geol.,* vol. 68, p. 475-479

SCOTT, S.D. and BARNES, H.L. (1972); Sphalerite - wurtzite equi-
libria and stoichiometry: *Geochim. et Cosmochim. Acta.,*
vol. 36, p. 1275-1295

SCOTT, S.D. and BARNES, H.L. (1971); Sphalerite geothermometry
and geobarmetry: *Econ. Geol.,* vol. 66, p. 653-669

SEAL, R.R., COOPER, B.J. and CRAIG, J.R. (1985); Anisotropic
sphalerite of the Elmwood - Gordonsville deposits, Tennessee:
Can. Mineral., vol. 23, p. 83-88

SHAW, D. (1957); The geochemistry of gallium, indium, thallium -
A review: in *Physics and Chemistry of the Earth*, vol. 2,
L.H. Ahrens, F. Press, K. Rankama and S.K. Runcorn (eds.),
Pergamon Press, London, England, p. 164-211

SHIONOYA, S. (1966); Luminescence of lattices of the ZnS type:
in *Luminescence of Inorganic Solids;* P. Goldberg (ed.),
Academic Press, New York, N.Y. p. 205-286

SMITH, F.G. (1955); Structure of zinc sulfide minerals: *Am.
Mineral.,* vol. 40, p. 658-675

SPIRAKIS, C.S. (1983); A possible precipitation mechanism for
sulfide minerals in Mississippi Valley-type lead-zinc deposits:
in *International Conference on Mississippi Valley Type Lead-
Zinc Deposits, Proceedings Volume;* G. Kisvarsanyi, S.K. Grant,
W.P. Pratt and J.W. Koenig (eds.), Univ. of Missouri-Rolla,
p. 211-215

STRATHAM, P.J. (1976); A comparative study of techniques for
quantitative analysis of the X-ray spectra obtained with a Si
(Li) detector: *X-Ray Spectrometry,* vol. 5, p. 16-28

SVERJENSKY, D. (1984); Oil field brines as ore-forming solutions:
Econ. Geol., vol. 79, p. 23-37

SVERJENSKY, D. (1981); The origin of a Mississippi Valley – type deposit in the Viburnum Trend, Southeast Missouri: *Econ. Geol.*, vol. 76, p. 1848-1872

SVERJENSKY, D., RYE, D.M. and DOE, B.R. (1979); The lead and sulfur isotopic composition of galena from a Mississippi Valley – type deposit in the New Lead Belt, Southeast Missouri: *Econ. Geol.*, vol. 74, p. 149-153

TAYLOR, H.P. (1979); Oxygen and hydrogen isotope relationships in hydrothermal mineral deposits: in *Geochemistry of Hydrothermal Ore Deposits*; H.L. Barnes (ed.), John Wiley and Sons, p.236-277

TAYLOR, M., KESLER, S.E., CLOKE, P.L. and KELLY, W.C. (1983); Fluid inclusion evidence for fluid mixing, Mascot – Jefferson City Zinc District, Tennessee: *Econ. Geol.*, vol. 78, p. 1425-1439

THIEDE, D.S. (1984); *Organic and Related Volatile Compounds in Rock Samples from the Nanisivik Mine Area, Baffin Island, Northwest Territories:* Report to Nanisivik Mines Ltd., 13 p

TRUDINGER, P.A. (1976); Microbiological processes in relation to ore genesis: in *Handbook of Stratabound and Stratiform Ore Deposits*; vol. 2, Elsevier, New York, N.Y., p. 135-190

UCHIDA, I. (1964), Fluorescence of pure zinc sulfide in correlation with deviation from stoichiometry: *Jour. Phys. Soc. Japan*, vol. 19, p. 670-674

WILLAN, R. and COLEMAN, M. (1983); Sulfur isotope study of the Aberfeldy barite, zinc, lead deposit and minor sulfide mineralization in the Dalradian metamorphic terrain, Scotland: *Econ. Geol.*, vol. 78, p. 1619-1656

WILLIAMS, N. and RYE, D.M. (1974); Alternative interpretation of sulphur isotope ratios in the McArthur lead-zinc-silver deposit: *Nature*, vol. 247, p. 535-537

ZIMMERMAN, R.K. and KESLER, S.E. (1981); Fluid inclusion evidence for solution mixing, Sweetwater (Mississippi Valley – type) district, Tennessee: *Econ. Geol.*, vol. 76, p. 134-142

APPENDIX I : X - RAY DIFFRACTION DATA FOR SPHALERITE WITH CALCULATED UNIT CELL PARAMETERS

INDEX	Observed Diffraction Lines in Degrees 2θ									
	1	2	3	4	5	6	7	8	9	10
(111)	28.640	28.402 / 28.878	28.623	28.700	28.311 / 28.864	28.236 / 28.912	28.675	29.107	28.959	28.373 / 29.729
(200)	33.104	33.065	33.145	33.267	33.333	33.220	33.162	33.564	33.572	37.885 / 32.541 / 33.495
(220)	47.700	47.128 / 47.655	47.737	47.818	47.386 / 47.939	47.277 / 47.979	47.575	47.525	47.764	47.054 / 48.360
(311)	56.528	56.378	56.462	56.699	56.522	56.222 / 56.748	56.398	56.649	56.765	57.198
(222)	59.437	ND	58.868	59.509	ND	59.153	59.657	58.887	ND	59.207
(400)	67.719	69.322	69.549	69.645	69.749	69.601	ND	69.586	69.703	69.050 / 70.757
(331)	76.992	76.902	76.670	76.970	77.028	76.516 / 77.293	76.727	76.649	76.848	77.286
(420)	79.450	ND	79.127	79.160	ND	79.247	79.133	79.302	79.080	78.943
(422)	88.662	88.624	88.570	88.896	88.649	88.267	ND	ND	88.692	87.597
(511)	95.935	95.669	95.790	95.703	95.593	95.566	ND	95.796	95.278	94.929
(440)	107.722	107.752	107.692	107.795	107.590	107.442	107.333	107.503	107.238	106.836
(531)	115.196	115.172	114.913	114.921	114.844	114.557	114.878	114.659	114.609	114.263
(600)	117.654	ND	ND	117.480	ND	115.083	ND	117.300	ND	117.377
(620)	128.839	128.709	128.503	128.619	128.548	128.613	128.464	128.179	128.524	127.772
(533)	138.644	ND	138.230	138.253	ND	ND	138.048	137.985	137.977	137.314
(444)	ND	ND	ND	ND	ND	ND	ND	ND	ND	159.963
Unit cell (Å)	5.4009	5.4056	5.4077	5.4077	5.4071	5.4104	5.4120	5.4122	5.4125	5.4256
Error (±)	0.0012	0.0021	0.0015	0.0019	0.0017	0.0014	0.0019	0.0026	0.0033	0.0051

ND - Not determined; Unit cell parameters calculated using the averages of split diffraction lines.

PREPARATION OF DOUBLY POLISHED THIN SECTIONS WITH HEATING

D. Crothers, Department of Geology, Lakehead University

1. Take specimens provided and trim to fit the interior dimensions of a 1"
    Bakelite polished section mounting ring. Leave enough ease around
    specimen for some movement. Be careful that sample depth will not catch
    on Bakelite lug depressions.

2. Grind sample surface on 400 grit carborundum to give a smooth working
    surface. Clean well to remove all carborundum. Dry thoroughly. Never
    heat specimen above 100°C as this will denature the fluid inclusions
    rendering the specimen useless.

3. Take blank Bakelite mounts and lightly skim surface to insure a smooth
    inclusive surface. Clean rings.

4. Have ready for use, a clean teflon surface big enough to hold all
    specimens. Using vaseline or other suitable product, carefully apply
    a light coating to the outer rim of the mounting rings. This will help
    to make a seal between the ring and the teflon when mounting takes place.
    Place specimens, flat side down, far enough apart to allow for mounting
    rings. Be sure that markings are visible, or that a specific order is
    maintained.

5. Place rings down over specimens. Mix or have on hand a cool setting
    epoxy such as araldite. Fill rings up to the bottom of the lug
    depressions. Using a dissecting pin or other instrument slightly agitate
    specimens to help air bubbles trapped around specimen to release. Be
    careful not to move mount.

6. When epoxy has set, lift mounted specimens and grind on a 400 grit
    carborundum to remove epoxy leaving a free sample surface. Clean
    thoroughly, then examine each surface carefully for pits or holes using
    a binocular microscope. Holes will have to be roughed out and filled
    with more epoxy, reground and re-examined. It is important to maintain
    a clean uncontaminated surface for diamond polishing on a Düren polishing
    machine.

7. Prior to the final grind, slightly level the edge of the bakelite holder. This will help to reduce surface drag and allows the free passage of the specimen on the polishing medias.

8. When the surface of the specimen has a satisfactory bond it should be ground with a slurry of 5 micron alumina or a "fine grained" cast iron lap especially machined to fit the "Düren" machine. The samples should rotate until the surfaces are very smooth, almost to matte polish, and most importantly, free from as many cavities as possible. This stage of the polished surface is for the specimen in the bakelite ring ONLY not for a P.T.S. Remove samples and clean as previously stated. The surface will be smooth therefore there will be no need to use 6 or 3 micron diamond. If the lead lap is flat, 1 micron diam. will give a quick and satisfactory polish.

9. When the surface has reached a stage of clear areas the wanted mineral is showing 1 micron scratches - a hand polish using a slurry .03 micron alumina and distilled water with a soft tissue or pad; held in the hand will produce a clean satisfactory polish, - for P.S. and P.T.S. with NO surface relief.

10. When surface is satisfactory clean specimens and place on a cool hot plate (less than 100°C) to warm. Using 1" circular glass discs and a cool melting thermal plastic (eg. Crystalbond ND509. Lakeside 70 C) mount the polished surface on the glass discs being careful that the bond is flat. Mount the discs on regular petrographic slide by the same method.

11. Carefully offcut specimens being careful to maintain the identifying marking in some manner. Grind samples to transluscence as per thin section techniques. This varies from specimen to specimen.

12. Leaving specimens mounted on glass, apply polish to the second side as previously explained.

13. When the samples are ready for use, they can be floated from the glass discs by using a suitable solvent.

COLD MOUNTING MODIFICATION

To prepare doubly polished thin sections for the Area 14 Orebody without heating, Lepage's Miracle Mender was substituted for thermal plastic cement when bonding the first polished surface to the 1" glass disc. As Miracle Mender does not bond two glass surfaces very well, an aluminum template with a 1" diameter hole was used for cutting and grinding instead of cementing the glass disc to a rectangular glass slide. Sections prepared with Miracle Mender required submersion in acetone for up to 8 hours to separate the thin section from the glass disc.

APPENDIX III

DETAILED DOUBLY POLISHED THIN SECTION DESCRIPTIONS WITH INCLUSION DATA

Sample #	Unit, Zone	Section #	Incl. #	Incl. Type	Th (°C)	O.Q.	Host Dolomite	Mineral Sphalerite
37-11E #2	1	F30	A 1	PS	176	1		Complex zoning
			B 1	PS	153	3		Complex zoning
			2	"	150	"		" "
			3	"	150	"		" "
			4	"	145	"		" "
			5	"	147	"		" "
			6	"	147	"		" "
37-11E #3	1	F14	1	PS	98	3		Simple zoning
			2	"	94	"		" "
			3	"	91	"		" "
			4	"	98	3		" "
			5	"	97	"		" "
			6	"	95	"		" "
		F18	1	P	113	1	Interstitial	
35-11 #1	1	F26	1	P	162	2	Interstitial	
			2	"	133	"	"	
			3	"	165	"	"	
			4	"	136	"	"	
			5	"	137	"	"	
			6	"	138	"	"	
			7	"	132	"	"	
		F8	A 1	P	75	3	Vien center	
			2	"	90	1	" "	
			3	"	113	"	" "	
			4	"	95	"	" "	
			5	"	111	"	" "	
			6	"	99	"	" "	
			7	"	108	"	" "	
			8	"	94	"	" "	
			9	"	108	"	" "	
			B 1	P	189		Vien center	
			2	"	155	1	" "	
			3	"	176	3	" "	
			4	"	138	2	" "	
			5	P	176	3	" "	
			C 1	P	171	1	Vien center	
			2	"	106	3	" "	
			3	"	167	"	" "	
			4	"	121	2	" "	
35-11 #2	1	F28	A 1	P	117	1	Interstitial	
			2	"	117	"	"	
			3	"	145	"	"	

Sample #	Unit, Zone	Section #	Incl. #	Incl. Type	Th (°C)	O.Q.	Host Mineral Dolomite	Sphalerite
			B 1	S	103	1	Interstitial	
			2	"	95	"	"	
			3	"	96	"	"	
			C 1	PS	169			Simple zoning
			2	"	173			" "
			3	"	189			" "
			4	"	193			" "
			5	"	191			" "
35-11 #6	1	F4	A 1	P	167		Band center	
			2	"	169		" "	
			3	"	175		" "	
			4	"	184		" "	
			B 1	P	172		Band center	
			2	"	169		" "	
			3	"	172		" "	
			C 1	P	164		Band center	
			2	"	132		" "	
			3	"	155		" "	
			4	♥	168		" "	
			5	"	145		" "	
			6	"	148		" "	
			D 1	P	172		Band center	
			2	"	186		" "	
			3	"	161		" "	
			4	"	157		" "	
			5	"	130		" "	
			6	"	147		" "	
			7	"	138		" "	
			8	"	178		" "	
21-09cc #1	1	F33	A 1	P	74	1	Interstitial	
			2	"	102	"	"	
			3	P	106	3	"	
			B 1	S	96	1	Interstitial	
			2	"	187	3	"	
			3	"	182	1	"	
			4	P	144	1	"	
			5	"	161	"	"	
			6	"	183	"	"	
			C 1	P	196	1	Interstitial	
			2	"	196	"	"	
21-09N a		F66	A 1	P	124	2		Simple zoning
			2	"	124	"		" "
			3	"	124	"		" "
			B 1	PS?	77	1		Simple zoning
			2	"	94	"		" "
			3	"	95	"		" "
			4	"	95	"		" "

Sample #	Unit, Zone	Section #	Incl. #	Incl. Type	Th (°C)	O.Q.	Host Dolomite	Mineral Sphalerite
			5	PS?	76	1		Simple zoning
			6	"	99	"		" "
			7	"	96	"		" "
		C 1		P	95	3		Simple zoning
			2	"	86	"		" "
			3	"	86	"		" "
			4	"	86	"		" "
21-11W	1	F67	A 1	PS	115	3		Simple zoning
			2	"	147	2		" "
			B 1	PS	120	3		" "
			2	"	125	2		" "
			3	"	118	3		" "
			4	"	124	"		" "
			5	"	121	2		" "
13-09S a	1	F40	1	P	172	2	Interstitial	
			2	"	181	2	"	
			3	"	187	1	"	
			4	P	189	2	"	
			5	"	179	1	"	
			6	"	202	1	"	
			7	"	183	1	"	
			8	"	191	2	'	
			9	"	179	2	"	
			10	"	191	2	"	
			11	"	185		"	
			12	"	181	3	"	
37-11 #4	2	F19	A 1	PS	162	1		Simple zoning
			2	"	163	"		" "
			B 1	PS	124	3		" "
			2	"	143	3		" "
			3	"	145	"		" "
			4	"	152	1		" "
			5	"	144	2		" "
			6	"	149	"		" "
			7	"	152	"		" "
			8	"	152	"		" "
			9	"	119	"		" "
			10	"	145	2		" "
			11	"	145	"		" "
37-11 #4	2	F19	C 1	P	132	2		Simple zoning
			2	"	157	"		" "
			3	"	152	"		" "

Sample #	Unit, Zone	Section #	Incl. #	Incl. Type	Th (°C)	O.Q.	Host Mineral Dolomite	Sphalerite
37-11 #5	2	F10	A 1	P	200	1	Band center	
			2	PS	188	"	" "	
			3	"	186	"	" "	
			4	"	188	"	" "	
			5	P	168	2	" "	
			6	P	161	2	" "	
			B 1	PS	131	1	Band rim	
			2	"	106	"	" "	
			3	"	113	"	" "	
			4	P	168	"	" "	
			5	PS	143	"	" "	
			6	"	127	"	" "	
			C 1	P	125		Band center	
			2	"	171		" "	
			3	"	181	3	" "	
			4	"	176		" "	
35-11 #5	2	F9	A 1	PS	139	1		Single colour
			2	"	173	"		" "
			3	P	170	2		" "
21-09cc #2	2	F32	A 1	PS	171	2	Band center	
			2	"	177	"	" "	
			3	S	95	"	" "	
			4	PS	166	"	" "	
			5	P	142	"	" "	
			6	PS	186	"	" "	
			B 1	P	105	1	Band center	
			2	"	187	"	" "	
			3	P	132	"	" "	
			4	P	166	"	" "	
		F77	C 1	P	216	1	Interstitial	
			2	"	173	1	"	
			3	"	189	2	"	
			4	"	178	"	"	
			5	"	132	3	"	
			D 1	P	169	1	Interstitial	
			2	"	143	2	"	
			3	"	149	2	"	
			4	"	151	1	"	
			5	PS	168	1	"	
			6	P	184	1	"	
			7	"	148	"	"	
37-10W b	3	F87	A 1	P	139	1		Reverse zoning
			2	PS	182	2		" "
			3	P	165	1		" "
			4	"	169	1		" "
			5	PS	172	2		" "
			6	PS	179	2		" "
			7	"	179	2		" "

Sample #	Unit, Zone	Section #	Incl. #	Incl. Type	Th (°C)	O.Q.	Host Mineral Dolomite	Sphalerite
			B 1	PS	208	1		Reverse zoning
			2	"	179	"		" "
			3	"	185	"		" "
			4	"	174	"		" "
37-11 #6	3	F73	A 1	P	104	1	Interstitial	
			2	P	99	"	"	
			3	P	71	"	"	
			4	P	93	"	"	
			5	P	92	"	"	
			6	P	99	"	"	
37-11 #4	3	F34	A 1	PS?	89	2		Simple zoning
			2	"	76	"		" "
			3	"	89	"		" "
			4	"	88	"		" "
		F78	B 1	P	145	1	Interstitial	
			2	P	155	"	"	
			3	P	148	"	"	
			4	P	163	2	"	
21-09S #3	3	F21	A 1	P	95	1	Interstitial	
			2	P	94	"	"	
			3	P	98	"	"	
			4	P	94	"	"	
			5	P	91	"	"	
			6	P	99	"	"	
			B 1	P	108	1	Interstitial	
			2	P	99	"	"	
			3	P	86	"	"	
21-09cc #3	3	F3	A 1	P	167	3		Zoning N.D.
			2	P	165	2		"
21-09N b	3	F68	A 1	PS	131	1	Interstitial	
			2	"	111	"	"	
			3	"	129	"	"	
			4	"	98	"	"	
			5	"	129	"	"	
			6	"	128	"	"	
			7	"	111	"	"	
			B 1	P	93	3	Interstitial	
			2	PS	85	1	"	
			3	"	88	1	"	
			4	"	95	1	"	
			C 1	P	89	1	Band rim	
			2	P	89	1	" "	
			3	P	90	1	" "	
			4	P	94	1	" "	
			5	P	92	1	" "	
			6	P	91	1	" '	

Sample #	Unit, Zone	Section #	Incl. #	Incl. Type	Th (°C)	O.Q.	Host Mineral Dolomite	Host Mineral Sphalerite
35-11 #3	4	F23	A 1	P	148	2	Interstial	
			2	P	164	3	"	
			B 1	P	98	1	Interstitial	
			2	P	100	1	"	
			3	P	90	2	"	
			4	P	102	2	"	
			5	P	105	1	"	
			C 1	P	77	1		Simple zoning
			2	P	93	2		" "
			3	P	74	2		" "
			4	P	90	3		" "
			5	P	93	3		" "
21-09S #5	4	F31	A 1	P	101	1	Interstitial	
			2	PS	100	1	"	
			3	P	119	2	"	
			4	P	100	1	"	
			5	P	85	1	"	
			B 1	PS	90	2	Interstitial	
			2	P	90	2	"	
		F17a	1	P	190	1	Interstitial	
			2	P	253	1	"	
			3	P	236	1	"	
			4	P	237	1	"	
21-09S #6	4	F16	A 1	PS	165	1		Simple zoning
			2	"	166	1		" "
			3	"	154	1		" "
			4	"	150	1		" "
			5	"	152	1		" "
			6	"	104	1		" "
			7	"	160	1		" "
			8	"	109	1		" "
			B 1	PS	171	1		Simple zoning
			2	"	181	1		" "
			3	"	158	1		" "
			4	"	206	2		" "
			5	"	159	2		" "
		F71	A 1	PS	101	1		Simple zoning
			B 1	PS	155	3		" "
			2	"	150	2		" "
			3	"	156	3		" "
			C 1	P	84	3		" "
			2	PS	115	3		" "
			D 1	PS	122	1		" "
			2	"	133	1		" "
21-09cc #4	4	F24a	A 1	PS	89	3		Zoning N.D.
			B 1	P	157	3		"
			2	P	172	3		"
			3	P	161	2		"

Sample #	Unit, Zone	Section #	Incl. #	Incl. Type	Th (°C)	O.Q.	Host Dolomite	Mineral Sphalerite
		F24b	A 1	P	93	1	Interstitial	
			2	P	92	1	"	
			3	P	95	1	"	
			B 1	P	109	1	Interstitial	
			2	PS	102	1	"	
			C 1	P	128	1	"	
			2	P	110	2	"	
			3	P	109	1	"	
			4	P	115	3	"	
13-09S d	4	F43	A 1	PS	136	1		Simple zoning
			2	"	135	2		" "
			3	"	148	2		" "
			B 1	P	151	2		" "
21-09S #7	5	F72	1	PS	140	2		Zoning N.D.
			2	"	150	2		"
			3	"	153	2		"
			4	"	154	2		'
			5	"	176	1		"
37-11 #6	5	F73	A 1	P	104	1	Interstitial	
			2	P	104	1	"	
			3	P	108	1	"	
			4	P	105	1	"	
37-11 #8	6	F29	A 1	P	163	1	Interstitial	
			2	P	166	1	"	
			3	P	185	1	"	
			B 1	P	166	1	"	
			2	P	161	1	"	
			3	P	172	1	"	
			4	P	176	1	"	
			5	P	180	1	"	
22-10W	6	F75	A 1	S	87	3		Simple zoning
			2	S	80	3		" "
			3	S	90	3		" "
			B 1	p	91	2	Interstitial	
			2	p	142	2	"	
			3	P	163	2	"	
			C 1	P	159	1	Band rim	
			2	P	169	1	" "	
			3	P	169	1	" '	
			4	P	185	1	" "	
		F69	A 1	P	86	2	Interstitial	
			2	P	86	2	"	
			3	P	117	1	"	
			4	P	96	1	"	
			5	P	132	1	"	
			6	P	114	2	"	

Sample #	Unit, Zone	Section #	Incl. #	Incl. Type	Th (°C)	O.Q.	Host Mineral Dolomite	Sphalerite
			B 1	P	167	2	Interstitial	
			2	P	150	2	"	
			3	P	138	2	"	
			4	P	83	2	"	
			5	P	152	2	"	
			C 1	S	113	3		Zoning N.D.
			2	S	116	3		"
			3	S	102	3		"
13-09S f	6	F45	A 1	PS	103	2		Simple zoning
			2	"	90	3		" "
13-09S e	6	F44	A 1	PS	118	1		Simple zoning
			2	"	123	1		" "
			3	"	130	1		" "
			4	"	130	1		" "
			5	"	133	1		" "
			6	"	132	1		" "
09-07 S	Shale Zone	F61	A 1	P	313	1		Simple zoning
			2	P	293	2		" "
			3	P	238	3		" "
			4	P	303	2		" "
			5	P	255	1		" "
			6	P	305	2		" "
			7	P	282	3		" "
			8	P	304	3		" "
07-08S	Shale Zone	F58	A 1	P	217	1	Interstitial	
			2	P	184	2	"	
			3	PS	197	1	"	
			4	PS	159	1	"	
			B 1	P	230	1	"	
			2	P	231	1	"	
			3	P	213	1	"	
			C 1	P	200	3		Reverse zoning
08-08N	Shale Zone	F62	A 1	PS	281	1		Zoning N.D.
			2	"	232	2		"
			3	"	102	1		"
			4	PS	294	1		"
			5	"	278	1		"
			6	"	181	3		"
			7	PS	255	2		"
			8	"	182	2		"
			9	"	289	3		"
			B 1	PS	294	1		"
			2	"	294	1		"
			3	"	295	1		"

Sample #	Unit, Zone	Section #	Incl. #	Incl. Type	Th (°C)	O.Q.	Host Dolomite	Mineral Sphalerite
			B 4	PS	291	1		Zoning N.D.
			5	"	295	1		"
			6	"	259	1		"
			7	"	257	1		"
			8	"	262	1		"
			9	"	270	1		"
			10	"	279	1		"
			11	"	279	1		"
			12	"	289	1		"
6.5-08S b	West Zone	F36	A 1	PS	90	3		Simple zoning
			2	"	91	3		" "
			3	"	91	3		" "
			B 1	"	113	2		" "
			2	"	124	2		" "
			3	"	126	2		" "
			4	"	129	3		" "
5.5-08S b	West Zone	F38	1	P	93	1	Interstitial	
			2	P	102	1	"	
			3	P	98	1	"	
			4	P	103	1	"	
5.5-08S c	West Zone	F39	1	P	118	1	Interstitial	
			2	P	95	2	"	
			3	P	79	2	"	
			4	P	80	2	"	
			5	P	81	2	"	
			6	P	80	2	"	
			7	P	96	2	"	
LD 54S	Lower Lens	F56	A 1	P	129	2	Vien center	
			2	P	142	2	" "	
			3	P	137	3	" "	
			4	P	123	2	" "	
			5	P	138	1	" "	
			6	P	138	1	" "	
			7	P	122	1	" "	
			8	P	122	1	" "	
			B 1	P	129	3	Interstitial	
			2	P	129	3	"	
			3	P	133	1	"	
			4	P	127	3	"	
			5	P	132	3	"	
			6	P	146	1	"	
			7	P	143	1	"	
			8	P	139	1	"	
			9	P	147	1	"	
			10	P	148	1	"	

Sample #	Unit, Zone	Section #	Incl. #	Incl. Type	Th (°C)	O.Q.	Host Mineral Dolomite	Sphalerite
LD 60N b	Lower Lens	F55	A 1	P	164	1	Vien center	
			2	P	152	1	" "	
			3	P	159	1	" "	
			4	P	131	1	" "	
			5	P	132	3	" "	
			6	P	132	1	" "	
			B 1	P	181	2	Vien center	
			2	P	161	2	" "	
			3	P	162	1	" "	
			4	P	150	1	" "	
			5	P	151	1	" "	
			6	P	161	1	" "	
2-10N	Area 14	F46	A 1	P	76	1	Interstitial	
			B 1	P	174	2	"	
			2	P	142	2	"	
			C 1	P	131	3	"	
			2	P	130	2	"	
			3	P	120	2	"	
			D 1	P	109	1	"	
3-10N b	Area 14	F48	A 1	P	89	3		Zoning N.D.
			2	P	86	3		"
			B 1	P	81	2		"
			2	P	83	2		"
			3	P	134	1		"
			4	P	141	1		"
			5	P	150	1		"
3-11 a	Area 14	F49	A 1	P	147	1	Vien rim	
			2	P	144	1	" "	
			3	P	145	1	" "	
			4	P	105	3	" "	
			5	P	148	1	" "	
			6	P	138	1	" "	
			7	P	122	3	" "	
			B 1	P	124	1	Vien rim	
			2	P	119	1	" "	
			3	P	117	1	" "	
			4	P	118	1	" "	
			5	P	118	1	" "	
5-SW a	Area 14	F51	A 1	PS	90	2		Zoning N.D.
			2	"	112	1		"
			3	"	81	2		"
			4	"	117	1		"
			5	"	111	2		"
			B 1	PS	94	2		"
			C 1	P	132	2	Interstitial	
			2	P	132	1	"	
			3	P	142	3	"	
			4	P	122	3	"	
			5	P	97	1	"	
			6	P	146	2	"	

194.

Sample #	Unit, Zone	Section #	Incl. #	Incl. Type	Th (°C)	O.Q.	Host Mineral Dolomite	Sphalerite
4-11S	Area 14	F52	A 1	P	135	2	Interstitial	
			2	P	129	1	"	
			3	P	129	1	"	
			4	P	129	1	"	
			5	P	135	1	"	
			6	P	148	1	"	
			B 1	P	131	1	"	
			2	P	129	2	"	
			3	P	126	1	"	
			4	P	134	2	"	

Incl. # - Inclusion number may be preceded by a letter identifying the
        heating run.
Incl. Type - P; Primary inclusion, PS - Pseudo-secondary inclusion
        S; Secondary inclusion.
Th - Homogenization temperature uncorrected for pressure.
O.Q. - Observation quality; 1 - good, 2 - fair, 3 - poor.
ND - Not determined.